"Optimization of Glucose oxidase towards oxygen independency and high mediator activity for amperometric glucose determination in diabetes analytics"

Von der Fakultät für Mathematik, Informatik und Naturwissenschaften der RWTH Aachen University zur Erlangung des akademischen Grades eines Doktors der Naturwissenschaften genehmigte Dissertation

vorgelegt von

Master of Science (M. Sc.)
Biotechnologie

Erik Uwe Arango Gutierrez
(geb. Zeithammel)

aus Plauen

Berichter: Universitätsprofessor Dr. Ulrich Schwaneberg
Universitätsprofessor Dr. Lothar Elling

Tag der mündlichen Prüfung: 19.12.2014

Sworn statement

I hereby assure that this doctoral thesis („Optimization of Glucose oxidase towards oxygen independency and high mediator activity for amperometric glucose determination in diabetes analytics”) represents my original work and that I have used no other sources for text, data or contents and no additional help other than stated by citation.

Erik Uwe Arango Gutierrez

Parts of this thesis have been published previously:

Erik Arango Gutierrez, Hemanshu Mundhada, Thomas Meier, Hartmut Duefel, Marco Bocola and Ulrich Schwaneberg (2013). Reengineered Glucose Oxidase for Amperometric Glucose Determination in Diabetes Analytics. Biosensors and Bioelectronics *50*, 84–90

Parts of his thesis will be published:

Erik Arango Gutierrez, Alexandra Balaceanu, Marco Bocola, Thomas Meier, Hartmut Duefel and Ulrich Schwaneberg (2015). Reengineered Glucose Oxidase towards Optimized Enzyme-Mediator Couples and Computational Assessment of a Mediated Electron Transfer Model. In preparation

Other publications:

Erik U. Zeithammel, Hemanshu Mundhada and Ulrich Schwaneberg (2012) “Directed evolution of Glucose oxidase for their application in biofuel-cells”, *Biosensors & Bioelectronics 2012*, Las Vegas, Nevada, *Poster presentation*

Erik U. Zeithammel, Hemanshu Mundhada and Ulrich Schwaneberg (2011) “Directed evolution of Glucose oxidase for their application in biofuel-cells”, *Biotrans 2011*, Giardini Naxos, Italien, *Poster presentation*

Jager, G., Wulfhorst, H., **Zeithammel, E.U.**, Elinidou, E., Spiess, A.C., and Buchs, J. (2011). Screening of cellulases for biofuel production: online monitoring of the enzymatic hydrolysis of insoluble cellulose using high-throughput scattered light detection. Biotechnol J *6*, 74-85.

I Acknowledgments

First of all I want to express my special thanks to Prof. Dr. Schwaneberg who not only gave me the opportunity to be part of the research team and made the project possible but rather supported me during my entire PhD-study and inspired me by his incredible way to develop and manage a powerful research group of significant scientific and industrial importance. I also would like to thank Prof. Dr. Lothar Elling and Prof. Dr. Marc Spehr for being part of my evaluation and PhD-defense committee.

I want to thank my supervisors Hemanshu and Marco for their support during my time as a PhD student. Thank you Hemanshu for the important support during my start period. Special thank goes to Marco for his supervision after Hemanshu left, for the fruitful discussions and of course for all the computational impact on the project. At this point I also want to thank my undergraduate students Shohana, Meena and Markus who did a great job and gave a high input to my work and of course I want to thank Alexandra for her impressive Master Thesis and her contribution to the computational assessment of the GOx.

I also would like to thank the whole Schwaneberg Group for the warm and friendly working atmosphere, for the help and the support. It was a great experience and a pleasure to work in such a dynamic and international researcher group.

I also like to thank Julia, Nina, Christian and Christian for our awesome “cooking circle”. I really enjoyed the delicious food every day and the time with you as friends.

Special thanks also go to Josiane, Paula, Christina and Alex who are great colleagues and friends.

The most special thank goes to my family who always supports me not only during my time as a PhD-student but during my entire life. I want to dedicate this dissertation to my wife Isabel and my daughter Valentina. Without you Isabel my life wouldn’t be as awesome as it is and without all your support I couldn’t have managed the last months.

II Figures

III Tables

1. Background of the study and problem statement

366 million people were affected by the metabolic disease diabetes mellitus in 2011 and there is an expected increase to 552 million until 2030 [1]. A precise and a easy control of the blood glucose level are prerequisites for diabetes patients to avoid long term effects through hyperglycemia or life threatening hypoglycemia during insulin application.

The most common glucose determination systems patient self-monitoring follow the principle of electrochemical biosensors (see chapter 1.4). Different sensors have been developed for glucose sensing based on enzymatic (e.g. through oxidireductases) and non-enzymatic recognition systems (e.g. platinum or non-catalytic binding proteins) [2-8]. The most common systems in diabetes care are amperometric measurement setups employing either Glucose oxidases (GOx's) or Glucose dehydrogenases (GDH's) for biological recognition [3, 9].

One major challenge in diabetes care is the development of specific systems which show no interferences by components of the investigated blood sample or the measurement environment. On one hand the GOx's are highly specific for β-D-glucose [10, 11] but naturally accept molecular oxygen as an electron acceptor. This leads to competitive electron shuttling between the employed mediators in electrochemical sensors and the molecular oxygen in the blood sample [12-15]. This oxygen activity of GOx might lead to an underestimation of the glucose level [16, 17] what is crucial for pO_2 levels > 100 Torr. Oxygen effects, caused by the oxygen dependency of GOx, can be relevant for critically ill patients [18-20].

On the other hand GDHs do not accept molecular oxygen as an electron acceptor but can convert different clinical relevant sugars like galactose, maltose and xylose to an analytical relevant extent [21, 22]. This for instance plays an important role for dialysis patients during Icodextrin administration. Icodextrin is a corn starch derived high molecular polymer which is used as an osmotic agent during peritoneal dialysis [23]. The polymer is metabolized after absorption from the peritoneal cavity yielding in an average serum concentration of 300 mg/dL (concentration of maltose, maltotriose and maltotetraose) [24-29].

Both, the GOx and the GDH, have been extensively reengineered in order to design enzymes which meet the desired properties for specific applications in β-D-glucose sensing. In terms of high β-D-glucose specificity, pyrrolochinolinchinon depending

GDH (GDH-PQQ) were engineered for less maltose activity (50-times reduced maltose activity) [30, 31]. Alternatively, flavin adenine dinucleotide (FAD) dependent GDH's were introduced for their application in glucose sensing which exhibit a residual activity for maltose of about 0.3 % [32-35].

GOx was mainly engineered to increase activity and / or stability [36-40]. Two reports describe reengineered GOx's for mediated electron transfer. In report one ferrocenemethanol was used as a mediator component in a directed evolution campaign resulting variant T30V-I94V which exhibits a two-fold increased k_{cat}-value (69.5/s WT; 137.7/s T30V-I94V) as well as a slightly increased thermal resistance and a shifted pH-activity profile [40]. In report two Horaguchi et al. employed phenazine methosulfate as an electron acceptor in a rational protein engineering approach. This approach delivered a variant of the GOx from *Penicillium amagasakiense* with a 11-fold higher dehydrogenase/oxidase ratio and a GOx variant of the GOx from *Aspergillus niger* with a 6-fold higher dehydrogenase / oxidase ratio [41]. None of the latter two reports describe a system in which a diabetes care relevant mediator system was used.

1.2 Objectives and project overview

The aim of the present work was to reengineer Glucose oxidase (GOx) from *Aspergillus niger* for less oxygen dependency and for improved acceptance of artificial mediators for applications in diabetes care. Thereby, the focus was to develop a GOx, suitable for oxygen inference free β-D-glucose sensing while maintaining the high β-D-glucose specificity and thermal stability. Furthermore, the electron transfer mechanism from the active site via oxygen and artificial mediator systems was investigated and described.

The project was divided in three parts. In the first part (chapter 3) a suitable screening system for GOx engineering was established for the selection of GOx variants with the desired properties. The screening compounded of two different assays. The ABTS-assay was employed to detect reduced oxygen dependent variants and a quinone diimine mediator assay (QDM-1 assay) was employed to detect improved mediator activity. The quinone diimine mediator system was selected due to its low interferences with blood components and its high importance in diabetes care [3]. In the following, the aim was the identification of amino acid residues which contribute to the reduction of the oxygen dependency and the

increase of the mediator activity applying random mutagenesis. Moreover, identified “hot-spots” were investigated by focused site saturation to assess their impact on the change of the GOx properties and to identify the ideal occupation for each amino acid residue. Cooperative effects along the identified amino acid positions were addressed by simultaneous site saturation. A final variant was subjected to characterization studies regarding oxygen independency, mediator activity, specificity and stability. The first part was finalized by the implementation of computational studies (by the subgroup for computational biology) for an assessment of the experimental results and to describe a model for an oxygen independent GOx.

The results of the first project part were taken as a basis for studies of the mediator mechanism in part two (chapter 4). Therefore, the binding of two different quinone diimine mediator systems and ferrocenemethanol was assessed by site directed mutagenesis, variant characterization and computational analysis.

In order to ensure a reproductive supply of purified GOx for the characterization studies of selected variants from thesis part one and two, an establishment of a GOx production process was implemented within the third project part (chapter 5). The up-stream process development was based on the hypo-glycosylating *Saccharomyces cerevisiae ngd29* strain [42]. The *Sc ngd29* generates a homogeneous hypo-glycosylation pattern what ensures comparability between different experiments and between different variants. The development of the down-stream process was based on reported protocols from Ziwei Zhu [39, 40, 43] including ion-exchange chromatography, hydrophobic interaction chromatography as well as gel filtration. The development focused on the performance optimization of the liquid-chromatography steps, the up-scaling and the establishment of tangential-flow filtration in order to achieve a quick and simple protocol with the possibility for large volume handling at pilot scale.

1.3 Glucose oxidase (GOx)

1.3.1 Structural insights / reaction mechanism

Glucose oxidase (β-D-glucose: oxygen 1-oxidoreductase) is a flavoprotein which has mainly been isolated from the genus *Aspergillus* and *Penicillium* whereby the best in literature described GOx is from *Aspergillus. niger* [44-49]. GOx from *A. niger* is a homodimeric glycoprotein with an average molecular weight of 186 kDa, depending on the carbohydrate content [49]. The carbohydrate content varies from 10 -16 % [50, 51]. The force for dimer formation is provided by strong hydrogen bonds and salt bridges within a narrow but long contact area [52, 53]. Each monomer carries one molecule of the noncovalently bound redox cofactor flavin adenine dinucleotide (FAD) [54]. The dimer formation and FAD binding are coupled by the formation of a lid structure in the dimer interface (Fig. 1-1-a). This lid structure covers a FAD binding channel and is partially buried within the formed dimer preventing the opening of lid [52, 53].

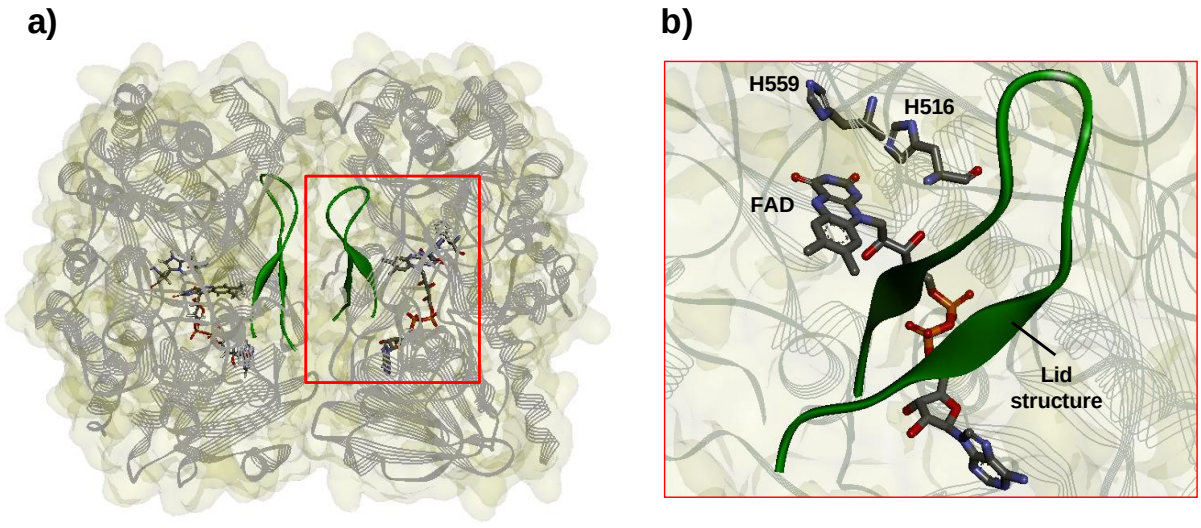

Figure 1-1: Representation of GOx from *A. niger* based on the x-ray structure 1cf3 [53]. a): GOx-dimer; b): Active site enlargement. H516 and H559 are highlighted as catalytic active residues along with FAD in the active site. Green solid ribbon: surface lid structure in the dimer interface. Ribbon representation was prepared using the Discovery Studio software package [55].

The reaction kinetics of GOx follows the Ping Pong Bi Bi mechanism [56] and the catalysis may be divided in two steps. In step one the enzyme catalyzes the oxidation of β-D-glucose to D-glucono-δ-lactone whereby the cofactor FAD is reduced to $FADH^-$ [57]. To step one of the reaction is often referred as reductive half reaction of

the enzyme. In step two molecular oxygen acts as an electron acceptor and the reduced cofactor is re-oxidized resulting in hydrogen peroxide formation, often referred to as oxidative half reaction [14] (Fig. 1-2).

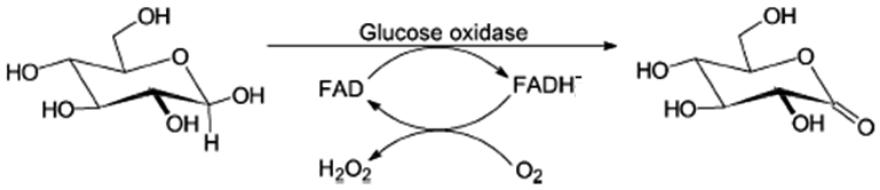

Figure 1-2: Representation of the GOx reaction cycle. Reductive half reaction: oxidation of glucose to gluconolactone, reduction of FAD to $FADH^-$. Oxidative half reaction: oxidation of $FADH^-$ to FAD by oxygen, formation of H_2O_2 [57].

The N5 of the isoalloxazine ring of the FAD represents the catalytic center of the Enzyme [14] which is accessible through a funnel shaped pocket that is formed from the surface lid structure (residues 75 to 98) into the active site [52]. The catalytic active residues His 516 and His 559 are located in close vicinity to the active center (Fig. 1-1-a).

The GOx reaction mechanism was studied intensively [56, 58-60] and reviewed by Leskovac et al. [57]. A hydride abstraction mechanism has been proposed to be most likely for the reductive half reaction of GOx [57]. In the oxidative half reaction the re-oxidation of the $FADH^-$ to FAD takes place by the reduction of dioxygen to hydrogen peroxide via two single electron transfer steps [57]. Not all terms of the oxidative half reaction are well understood yet.

1.3.2 Substrates of Glucose oxidase

The substrates of GOx can be divided into two groups, the electron donor substrates of the reductive half reaction and the electron acceptor substrates of the oxidative half reaction. Table 1-1 shows an overview of possible substrates for the reductive half reaction.

Table1-1: Electron-donor substrates of GOx. Modified after Lescovac et al., 2005 [57].

Substrate	Relative to glucose (%)[a]	Source	Substrate	Relative to glucose (%)[a]	Source
β-D-Glucose	100	[14, 15, 56, 61-63]	3-Deoxy-D-glucose	1	[15]
2-Deoxy-D-glucose	25-30	[15, 61, 62]	6-O-methyl-D-glucose	1	[15]
4-O-methyl-D-glucose	15	[15]	α-D-Glucose	0.64	[15, 61]
6-Deoxy-D-glucose	10	[15]	Mannose	0.2; 1	[15, 61, 62]
4-Deoxy-D-glucose	2	[15]	Altrose	0.16	[15, 61]
2-Deoxy-6-fluoro-D-glucose	1.85	[61]	Galactose	0.08	[15, 61, 62]
3,6-Methyl-D-glucose	1.85	[61]	Xylose	0.03	[15, 61, 62]
4,6-Methyl-D-glucose	1.22	[61]	Idose	0.02	[15, 61]

[a] Activity relative to β-D-Glucose in percentage.

Table 1-1 shows that GOx accepts next to β-D-glucose a variety of substrates, but β-D-glucose is by far the best. Even though GOx utilizes molecular oxygen as a natural electron acceptor the electron transfer from the enzyme to electrodes or redox indicators is described for several mediator compounds which incorporate GOx as examples given in Table 1-2.

Table1-2: Overview of mediator compounds which can incorporate GOx. Table modified after Harper et al., 2010 [64].

Mediator / Mediator system	Reference
Benzyl viologen	[65]
Indigo disulfonate	[65]
Methylene blue	[66]
2,5-dihydroxybenzoquinone	[66]
Phenazine methosulfate	[41]
Ferrocenemethanol	[39, 43]
Quinone diimine / phenylenediamine	[3, 67-69]

The high specificity of GOx for β-D-glucose and the acceptance of artificial electron acceptors is a prerequisite to employ GOx for accurate diabetes analytics.

1.4 Enzymes in blood glucose meters

Easy to handle self-measurement devices, which work reliably at all live situations and deliver a real time blood-glucose value are crucial for keeping diabetes patients close to a high quality of living. The development of pocket suitable devices, which work highly accurate and provide the blood-glucose concentration directly in a digital form was the main challenge in the last 40 years [3]. Self-measurement of blood-glucose started around 1970. The Chemstrip bG® from Boehringer Mannheim was a typical system produced in 1975. This system worked with a test stripe designed for visual determination of glucose by the patient. A large drop of blood (25 µL) had to be placed on the test stripe by the patient. After a defined measurement interval of 1 min, the blood was manually wiped off, and after a further minute, the color of the chemistry pad hat to be compared with a printed color scale [3]. Modern systems need around 1 µL per measurement.

Most of current glucose determination systems for the patient self-monitoring are based on the principle of electrochemical biosensors [3] [9, 70, 71]. Typical biosensors consist of two main components. Component one is the biological recognition system which translates information from a biochemical event into a measurable output signal depending on the concentration of the analyte. This output signal can be of chemical or physical nature [71]. The main purpose of the biological recognition is the generation of an analyte-specific signal. The recognition can either be specific for a single analyte or an analyte group. The second component is the transducer. The transducer transfers the output signal from the recognition system to the electrical domain; thereby a non-electrical signal is transduced to an electrical signal [71].

Different sensors have been developed for glucose sensing based on enzymatic- (e.g. through oxidireductases) and non-enzymatic recognition systems (e.g. platinum or non-catalytic binding proteins) [2-8]. The most common systems in diabetes care are amperometric measurement setups employing either Glucose oxidases (GOx's) or Glucose dehydrogenases (GDH's) for the biological recognition [3, 9]. In the latter system electrons are transferred from the redox center of the GOx or the GDH to a

counter electrode employing mediator compounds or mediator cascade systems. The resulting electron flux is thereby proportional to the glucose concentration in the investigated blood sample [70]. Table 1.3 shows a selection of enzymes -mediator couples which are employed in blood-glucose sensors.

Table1- 3: Enzyme / mediator systems employed in blood-glucose sensors [3]. GOD: Glucose oxidase; GDH: Glucose dehydrogenase; PQQ: pyrrolo quinoline quinone; POD: peroxidase; FAD: flavin adenine dinucleotide; NAD: nicotinamide adenine dinucleotide; GucDOR: glucose dye oxidoreductase.

Enzyme	*Coenzyme*	*Additional enzyme*	*Mediator system*	*Indicator*	*Product examples*
GOD	FAD	POD	Air oxygen/hydrogen peroxide	Leuco dye	Chemstrip bG, One Touch
GOD	FAD	None	Hexacyanoferrate III/hexacyanoferrate II	Palladium electrode	Accu-Chek Advantage
GOD	FAD	None	Hexacyanoferrate III/Hexacyanoferrate II	Carbon electrode	One Touch Ultra
GDH (GlucDOR)	PQQ	None	Hexacyanoferrate III/hexacyanoferrate II	Palladium electrode	Accu-Chek Advantage (Comfort Curve strip)
GDH (GlucDOR)	PQQ	None	Quinoneimine/ phenylendiamine	Phosphomolybdic acid	Accu-Chek Active, Accu-Chek Compact, Accu-Chek Go
GDH (GlucDOR)	PQQ	None	Quinoneimine/ phenylendiamine	Gold electrode	Accu-Chek Aviva
GDH (GlucDOR)	PQQ	None	Osmium	Electrode	FreeStyle
GDH	NAD	None	Phenanthroline quinone	Electrode	Precision Xtra
GDH	FAD	None	Hexacyanoferrate III/hexacyanoferrate II	Palladium electrode	Ascensia Microfill

A common system in diabetes care is the Accu-Chek Aviva system from Roche, which applies a PQQ dependent Glucose dehydrogenase (GlucDOR) in combination with a Quinone diimine / phenylenediamine mediator system for mediated electron transfer [3, 68, 72].

1.4.1 Quinone diimine / phenylenediamine mediator systems

Requirements of mediator systems for blood glucose monitoring are efficient electron transfer rates, low unspecific interactions with blood components and high storage stabilities when immobilized on glucose test stripes. These properties are given for quinone diimine / phenylenediamine mediator systems which are employed in blood-glucose meters [3]. Low unspecific interactions of this system can be attributed to low redox potentials and to a specific mediator chemistry. Additionally, quinone diimines feature a high stability when immobilized in form of N-substituted *p*-nitrosoanilin, a storage stable precompound of the corresponding quinone diimine [3, 68, 69]. Figure 1-3 shows the structure of two N-substituted *p*-nitrosoanilines which are Roche

internally used for glucose determination assays and which were also selected as mediator systems for the present investigations.

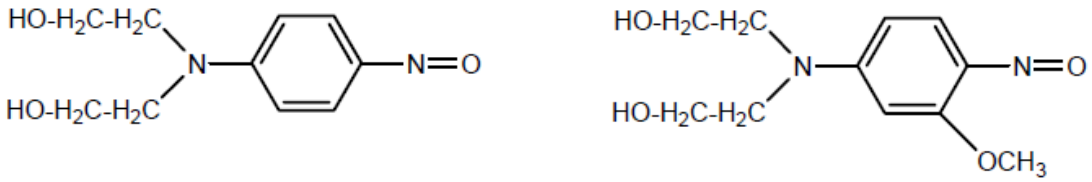

BM 31.1008 BM 31.1144

Figure 1-3: N-substituted *p*-nitrosoanilines BM 31.1008 and BM 31.1144. Nitrosoanilines are storage stable precompounds of the quinone diimines which are used as electron mediators in glucose sensing. BM 31.1008: N,N-bis(2-hydroxyethyl)-4-nitrosoaniline; BM 31.1144: N,N-bis(2-hydroxyethyl)-2-methoxy-4-nitrosoaniline.

BM 31.1008 is a Roche internal designation for N,N-bis(2-hydroxyethyl)-4-nitrosoaniline and BM 31.1144 for N,N-bis(2-hydroxyethyl)-2-methoxy-4-nitrosoaniline. BM 31.1144 carries an additional methoxy group which makes the mediator more polar and more soluble in aqueous solutions.

A commonly used blood glucose determination system is the Accu-Chek Aviva from Roche, which applies a quinone diimine / phenylenediamine mediator system in combination with a PQQ dependent Glucose dehydrogenase (GlucDOR) [3]. Fig. 1-4 shows the reaction principle for the latter system. Like for the GOx, the reaction mechanism of the GlucDOR can be divided in two half reactions, the reductive half reaction and the oxidative half reaction. In this system the GlucDOR oxidize β-D-glucose to gluconolactone by simultaneous reduction of the cofactor PQQ (reductive half reaction). The N-substituted *p*-nitrosoaniline is reduced to the corresponding chinondiimine via hydroxylamine in the oxidative half reaction of GlucDOR. The chinondiimine act as the actual mediator for the electron transfer and it is converted in the oxidative half reaction of enzyme to phenylendiamine. Two electrons come out of the spontaneous nonenzymatic back reaction of phenylendiamine to chinondiimine. Those two electrons get indicated amperometric using an electrode system, or photometric using a redox indicator dye [3, 68, 69].

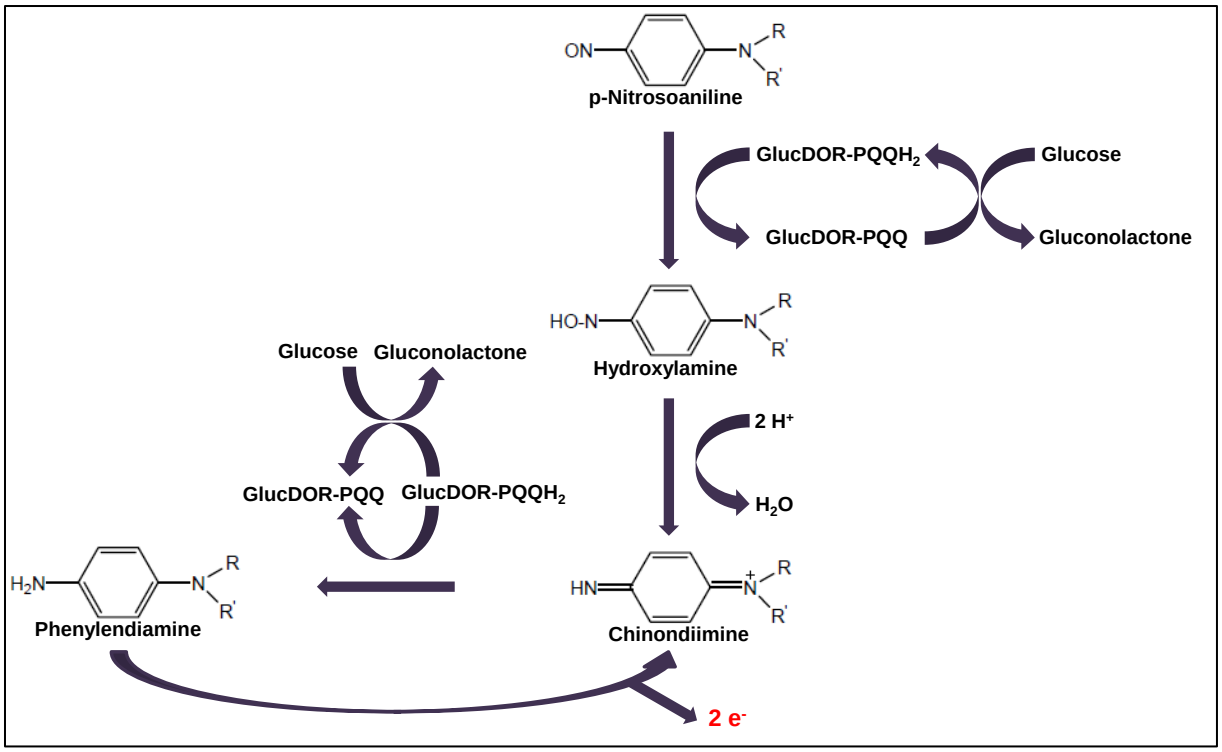

Figure 1-4: principle of mediated electron transfer employing a quinone diimine / phenylenediamine mediator system. Two enzymatic conversions are involved in the mediuated electron transfer. In the first conversion the N-substituted nitrosoaniline is converted to chinondiimine (the actual mediator compound) via hydroxylamine. Subsequently the chinonediimine is is converted to phenylendiamine. Two electrons than are donated during the spontaneous back reaction to chinondiimine. The recycled chinondiimine is than available for the next conversion. GlucDOR: Glucose-Dye-Oxidoreduktase; PQQ: pyrrolo quinolone quinone.

The described mechanism is also applicable for GOx, but in contrast to the oxygen independent GlucDOR, GOx will simultaneously use molecular oxygen as an electron acceptor as described in chapter 1.3.1. The reaction principle for the GOx - Quinone diimine / phenylenediamine mediator assay for mutant library screening is shown in chapter 3.3.1.1.

1.5 Directed protein evolution

Proteins are bio molecules which are of great interest for industrial applications, for instance as drug substances in medicine, as chemical reagents, for molecular recognition in diagnostics or as food additive. Thereby the protein can act as structural molecule (e.g. as antibody, antigen or nutrient) or the protein is able to catalyze biochemical reactions as an Enzyme which feature a high substrate specificity and high conversion rates under moderate conditions. Enzymes are usually isolated from natural sources where they work under specific conditions with

respect to temperature, pH-value, ionic strength and they mostly work in aqueous environment. For industrial applications enzymes often need to be optimized to fulfill the requirements for a specific application. The optimization may affect the enzymatic activity under selected conditions, the biochemical reaction itself (e.g. selectivity) or enzyme stability. Protein engineering gives the opportunity to adapt proteins to specific requirements and to design high effective processes, analytical tools and drug products based on renewable molecules. The most common strategies for protein engineering are rational design and directed evolution [73].

Rational design is based on fundamental knowledge of the protein structure and function and the relationship between the sequence the structure and the function. Furthermore, a certain computational power is necessary for the experimental design and the assessment of results by molecular modeling. However, rational design requires a less intensive laboratory setup since preferred engineering methods are site-directed mutagenesis and site-saturation mutagenesis.

In contrast, directed evolution does not require as much pre-knowledge and computational power as a rational design approach, but requires an enormous laboratory effort. Directed evolution is based on the selection of proteins with the best properties out of a diverse population, but it significant differs from the natural Darwinian evolution since it requires a laboratory screening- or selection system to direct the evolution in terms of the desired conditions [74]. In the last years an increasing number of success stories were observed for improved proteins for industrial applications by directed evolution ranging from biotransformation in chemical synthesis, hydrolysis in detergents, molecular recognitions in biosensors to medical applications [67, 75-79]. A classical experiment combines methods of molecular biology, biochemistry and bio-processing and can be divided in three major steps: gene diversity generation, screening for improved variants and gene isolation (Figure 1-5).

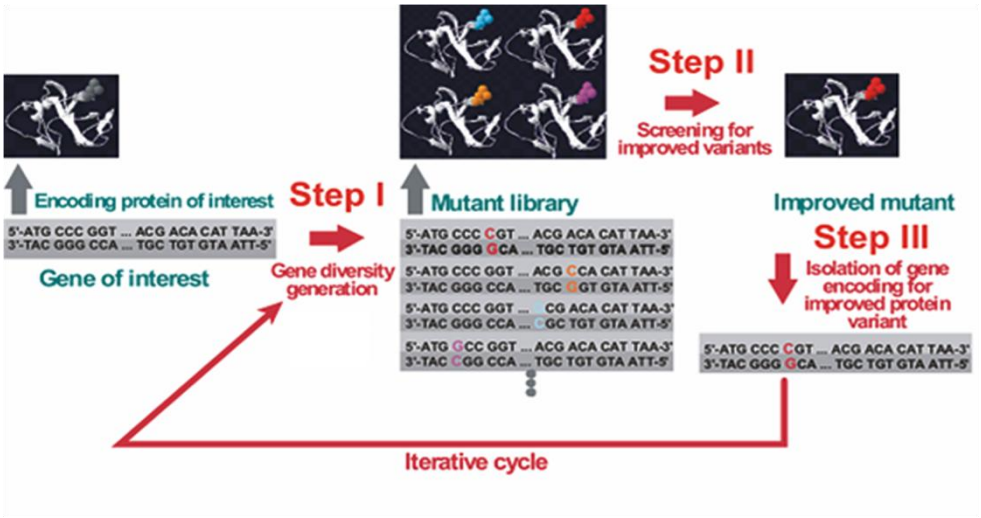

Figure 1-5: Scheme of a directed evolution experiment with iterative cycles. The experimental setup consist of three major steps: 1. Gene diversity generation; 2. Screening for improved variants; 3. Gene isolation [80].

Fundamental challenges in directed evolution are the unbiased generation of diversity and the screening of gene libraries of a statistical relevant size under conditions close to those of the final application. Both aspects will be discussed in the following paragraphs. Furthermore, it is important to notice that the success of a directed evolution campaign also depends on a suitable and detailed characterization of selected protein variants, wherefore the development of up- and down-stream protocols are often necessary.

1.5.1 Diversity generation

The success of a directed evolution campaign strongly depends on the ability to generate gene libraries of a sufficient size and more important a sufficient diversity. Gene recombination and random mutagenesis are two general principles which have been established [81]. In gene recombination beneficial mutations can be accumulated and unfavorable ones eliminated. Therefore, recombination techniques find their application if several related proteins are known or in late states of directed evolution campaigns. Common recombination methods are DNA shuffling and the staggered extension process [82, 83].

“The estimative goal for any random mutagenesis method is to replace any amino acid of a polypeptide chain by the other 19 amino acids in a statistical manner without limiting protein expression in the host organism” [84]. Different methods for random

mutagenesis have been developed [85, 86] whereby the generation of unbiased mutational spectra, consecutive nucleotide substitutions and independency of gene lengths outline the biggest challenges in the method development [84]. Wong et al. 2006 give an detailed overview about the diversity challenge in directed protein evolution including a classification and summary of random mutagenesis methods [84]. Two frequently used methods are the error prone polymerase chain reaction (epPCR) [87] and the sequence saturation mutagenesis (SeSaM) [88]. The epPCR is a rapid, simple and robust low fidelity method which is usually based on the polymerase from *Thermus aquatcus* (*Taq* polymerase). The *Taq* DNA polymerase misses a 3'-5' proofreading exonuclease function [89] and shows a substitution error rate of around 10^{-5} mutation/bp/duplication depending on the PCR conditions and the amplified gene [90]. To reach mutations rates high enough to perform an efficient directed evolution experiment the PCR-fidelity can be modified for instance by adding $MnCl_2$, unbalanced nucleotide concentrations or number of PCR-cycles [87]. Alternatively, the mutation frequency can be increased by use of engineered polymerases with increased inaccuracy [91]. However, the mutational spectra of polymerases are highly biased and especially transversions ((A→C, T→G); (G→C, C→G)) are highly underrepresented and subsequent mutations are rarely observed (reviewed by Wong et al. 2006) [84]. SeSaM was introduced in 2004 [88] and overcomes the main limitations of epPCR by an un-biased mutational spectra, a homogenous distribution of mutations over the gene and the ability to introduce subsequent mutations. A SeSaM-protocol comprises four steps: 1) generation of a DNA-fragment pool with random size distribution; 2) enzymatic fragment elongation with universal bases; 3) full-length gene synthesis; 4) universal base replacement [88]. The SeSaM-technology was continuously improved towards a transversion-enriched bias and the introduction of consecutive mutations [85, 92] and was successfully applied in several directed evolution campaigns [67, 78, 93].

1.5.2 Screening of mutant libraries

The selection of desirable proteins out of a diverse mutant library is another challenging step in directed protein evolution. The screening system needs to be designed in a way that the screening conditions are very close to the conditions of the intended application in order to identify variants that exhibit all necessary

properties. The screening of the mutant library takes place on the level of mature protein after in-vivo or in-vitro expression. Available technologies to identify beneficial variants can be divided into selection and screening [94]. The selection is based on the advantage a host cell achieves during expression of the protein of interest, so that only cells producing an improved protein will be selected. Prerequisite for the selection is the ability to detect an improved protein, most easily by a change in growth through a change in the phenotype. The screening might be divided in agar plate screening, microtiter plate screening, cell-in-droplet screen, cell as microreactor, cell surface display, in-vitro compartementalization [94]. Agar plate screening is based on the change of the host cell phenotype caused by the expression of the protein of interest, like for selection methods. This change of the phenotype can be used to detect whether the host cell expresses the protein of interest after cell transformation, or it can be used to screen for host cells which express already an improved variant. Prerequisite for agar plate screening is also the ability to detect the change in phenotype. A prominent example is the skim milk detection system to detect proteolytic activity of proteases on agar plates, where a clearance around colonies is observed [78, 95]. The most common used screening systems are indeed the microtiter plate (MTP) based systems. In MTP based screenings the cell clones are usually cultivated in MTP's after transformation and subsequently the cell supernatants or cell lysates are transferred to a second plate for the performance of the screening assay. A great variety of analytical methods (like UV/VIS or fluorescence spectroscopy) can be applied in MTP's and they show the least limitation in the dynamic range compared to the mentioned screening platforms. Challenges are the homogeneous cultivation over a whole plate to achieve acceptable standard deviations and also the accurate handling of the liquids. Screening capacities of MTP based systems are limited to few thousand variants a day, what outlines the biggest limitation of MTP based screening systems. In compare, cell-in-droplet screenings, cell as microreactor, cell surface display and in vitro compatimentalization show screening capacities of around 10^{10} variants but all require the availability of fluorescence detection systems [94].

Several screening systems are described for the engineering of GOx, based on microtiter plates as well as on fluorescence activated flow cytometric sorting [36-41, 67, 96]. Most of the GOx-systems rely on the reduction of molecular oxygen to hydrogen peroxide. Only two reports refer to the use of electron mediator systems

[40, 41]. Zuh et al. 2007 employed ferrocnemethanol as a mediator to evolve GOx for bio-fuel cells and Horaguchi et al. 2012 employed phenazine methosulfate as a mediator to develop a GOx with reduced oxidase activity. Within the present dissertation the well-known 2,2′-azino-bis(3-ethylbenz-thiazoline-6-sulfonic acid) (ABTS) –assay [39, 97] was employed to detect the oxidase activity of GOx and a phenylendiamine/chinonediimine based assay was employed for the specific detection of the mediated electron transfer. The phenylendiamine/chinonediimine based mediators are introduced in chapter 1.4.1 and the establishment of the mediator assay in chapter 3.3.1.

1.6 The *Saccharomyces cerevisiae* strain *ngd29*

The selection of a suitable host organism is a crucial step in the planning of a heterologous gene expression experiment. A large variety of host organisms are described for the production of recombinant proteins with *Escherichia coli* as the most prominent example [98]. For a directed protein evolution campaign the selection of the host organism depends on the ability to cultivate the organism in multi-well plates, the desired cultivation time, the expression level, the ability of protein secretion, but it may also depends on post-translational modifications. A. Pourmir and T. W. Johannes 2012 give a detailed overview of the employment of different host organism in directed protein evolution [99]. GOx from *A. niger* is a homodimeric glycoprotein whose N-glycosylation structures are involved in the stabilization of the protein-dimer [52, 53] (see chapter 1.3). *Saccharomyces cerevisiae* is one organism which is described to be a suitable host for GOx expression and was already successfully employed in directed evolution of GOx [39, 40, 42]. Outer chain glycosylation in *S. cerevisiae* leads to a heterogeneous hyper-glycosylation pattern of the type $[Man]_n[GlcNac]_2$ on secreted glycoproteins [100]. Lehle et al. published in 1995 the glycol-engineered *S. cerevisiae strain ngd29* which is not able to transfer mannose from GDPmannose to the asparagine linked core-structure $[Man_8][GlcNAC_2]$ leading to a uniform N-glycosylation of the structure $[Man_8][GlcNAC_2]$ of secreted glycoproteins [42]. The *ngd29* mutant was chosen for the directed evolution of GOx for diabetes analytics in order to achieve GOx-molecules with a homogenous hypo-glycosylation pattern.

2 Materials and Methods

2.1 Materials

All chemicals were of analytical grade and purchased from Sigma-Aldrich (Taufkirchen, Germany), Applichem (Darmstadt, Germany) or Carl Roth (Karlsruhe, Germany). All enzymes were purchased from New England Biolabs (UK) and Sigma-Aldrich (Taufkirchen, Germany). The pYES2 shuttle vector, the *Saccharomyces cerevisiae* INV and *Escherichia coli strain DH5α* were purchased from Invitrogen (Karlsruhe, Germany). The *Saccharomyces cerevisiae* strain *ngd29* was provided by Roche diagnostics [42]. Nucleotide analogues dPTPαS and dGTPαS and polymerases along with respective buffers (SeSaM-Taq and 3D1) were obtained from SeSaM Biotech GmbH (Aachen, Germany). All other nucleotides were purchased from Fermentas (St. Leon-Rot, Germany). DNA was quantified using a NanoDrop photometer (NanoDrop Technologies, Wilmington, DE, USA). Sequencing and Oligonucleotide synthesis was done by Eurofins MWG Operon, Ebersberg, Germany. The two quinone diimine based mediators QDM-1 and QDM-2 were provided by the collaboration partner Roche (Roche Diagnostics, Penzberg).

2.2 Methods

2.2.1 Individual site saturation mutagenesis

For individual site saturation mutagenesis (SSM) a two-step PCR protocol has been followed [101]. In step one, two extension reactions are performed in separate tubes; one containing the forward primer and the other containing the reverse primer. In step two, the two reactions are mixed and a standard PRC procedure is carried out. The mutations were introduced through the mutagenesis primer. For the site saturation degenerate primers of the form NNK were used. Tab 2-1 summarizes the primers used for the site saturation of position 173, 332, 414 and 560.

Table 2-1: Primer used for individual site saturation mutagenesis.

Position	Sequence (5` → 3`)

173	GGT ACT GTC CAT NNK GGA CCC CGC GAC AC
173	GTG TCG CGG GGT CCM NNA TGG ACA GTA CC
332	GAC CAG ACC ACC NNK ACC GTC CGC TCC C
332	GGG AGC GGA CGG TMN NGG TGG TCT GGT C
414	TAC TCG GAA CTC NNK CTC GAC ACT GCC
414	GGC AGT GTC GAG MNN GAG TTC CGA GTA
560	ATG TCG TCC CAT NNK ATG ACG GTG TTC TA
560	TAG AAC ACC GTC ATM NNA TGG GAC GAC AT

50 µl PCR reaction mixtures were prepared containing 1 ng/µl of plasmid template, 1x Phusion buffer (New England Biolabs, Frankfurt, Germany), 1 U of Phusion polymerase and 300 µM dNTP's. The reaction mixture was divided in two equal volumes and forward primer and reverse primer of the targeted site were added (reaction mixture 1: 400 nM forward primer; rection mixture 2: 400 nM reverse primer). The following PCR program was carried out (Tab. 2-2):

Table 2-2: PCR program for individual site saturation mutagenesis.

Step	Temperature	Time	Cycles
Initial denaturation	98 ˚C	45 sec	5
Denaturation	98 ˚C	15 sec	
Annealing	60 ˚C	30 sec	
Extension	72 ˚C	4 min	
Hold	72 ˚C	--	--
The reaction mixture of the forward primer was mixed with the mixture of the respective reverse primer and the following program was started			
Denaturation	98 ˚C	15 sec	13
Annealing	60 ˚C	30 sec	
Extension	72 ˚C	4 min	
Hold	8 ˚C	--	--

4 µl of the PCR product of each reaction was loaded on the 0.8 % agarose gel. The residual PCR-product was purified using the NucleoSpin® Extract II – kit (MACHERY-NAGEL, Germany) and subjected to *Dpn*I digestion.

2.2.2 Multiple site saturation

For multiple site saturation mutagenesis the OmniChange protocol was applied [102]. The method is based on the amplification of multiple fragments employing primer with phosphorthioated region. The first 12 nucleotides of primers are phosphorothioated and the phosphorthioated region of the forward primer of one fragment is always complementary to the phosphorthioated region of reverse primer of the previous fragment. The resultant PCR product is subjected to cleavage in presence of iodine and ethanol under alkaline conditions. This treatment leads to the removal of phoshphorthioate region of the PCR product and generates complementary overhangs of 12 bp. After hybridization of all fragments to the full circular plasmid nick-repair in a suitable host organism is necessary [102]. Tab 2-3 summarizes the primers used for the simultaneous site saturation of position 173, 332, 414 and 560.

Table 2-3: Primer used for the multiple site saturation of the GOx gen. Lower case letters indicate phosphorothioated bonds.

Primer	Sequence (5` → 3`)
P1	ggtactgtccatRYTGGACCCCGCGACAC
P2	ggtggtctggtcCTGCAGGTTCAAG
P3	gaccagaccaccARTACCGTCCGCTCCC
P4	gagttccgagtaCGCGACGTTGTGG
P5	tactcggaactcNDTCTCGACACTGCC
P6	atgggacgacatTTGCGTAGGAGG
P7	atgtcgtcccatVYKATGACGGTGTTCTA
P8	atggacagtaccATTAACACCATG

The PCR reaction mixture was prepared as a recently reported [102]. For Fragment 1 amplification, targeting A173, primers P1 and P2 were added in the master mix. While for A332 saturation, P3 and P4 were used. F414 site was targeted by using P5 and P6. The V560 site was included in vector backbone as it was amplified by P7 and P8. The following PCR program was carried out (Tab. 2-4):

Table 2-4: PCR program of simultaneous site saturation mutagenesis.

Step	Temperature	Time	Cycles
Initial denaturation	98 ˚C	45 sec	1
Denaturation	98 ˚C	15 sec	20

Annealing	65 ˚C	30 sec	
Extension	72 ˚C	30 sec	
Final extension	72 ˚C	5 min	--
Hold	8 ˚C	--	--

The fragments were digested and ligated as previously reported before transformation of chemical competent *E. coli* DH5α for library amplification [102]. For yeast transformation the gene library was isolated from *E. coli* DH5α using the plasmid isolation kit "NucleoSpin Plasmid MACHERY-NAGEL GmbH & Co. KG Düren".

2.2.3 Diversity generation by epPCR

Error prone PCR is the low fidelity method for the generation of random mutagenesis libraries. epPCR is usally based on the *Taq*-polymerase which misses a 3'-5' proofreading exonuclease function [89]. More details about the method background are given in chapter 1.5.1. Tab 2-5 summarizes the primers used for the random mutagenesis of the GOx-gen.

Table 2-5: Primer used for the random mutagenesis by epPCR.

Primer	Sequence (5` → 3`)
P1	GTGGTCTCCCTCGCTGCGGCCCTGCCACACTACATCAGGAGCAATG GCATTGAAGCCAG
P2	ATTACATGATGCGGCCCTCTAGATGCATGCTCGAGCGGCCGCCAGTG TGATGGATATCTG

The PCR-mix had a total volume of 50 µL and was composed as follows: 3 ng/µL pDNA template, 0.2 mM dNTP mix, 0.1 mM $MnCl_2$ for adjusting the mutation frequency, 10 pmol of each primer (P1 and P2) and 5 U Taq polymerase. Tab 2-6 summarizes the PCR program which was carried out.

Table 2-6: PCR program epPCR library generation.

Step	Temperature	Time	Cycles
Initial denaturation	94 ˚C	2 min	1
Denaturation	94 ˚C	1 min	30

Annealing	65 ˚C	1 min	
Extension	72 ˚C	2 min 25 sec	
Final extension	72 ˚C	10 min	1
Hold	8 ˚C	--	--

4 µl of the PCR product was loaded on the 0.8 % agarose gel. The residual PCR-product was purified using the NucleoSpin® Extract II – kit (MACHERY-NAGEL, Germany) and subjected to *Dpn*I digestion before cloning.

2.2.4 Diversity generation by SeSaM

SeSaM is an advanced PCR based mutagenesis method for the construction of libraries with a homogeneous mutation distribution over the gen, with the ability to generate subsequent mutations without a mutational bias. A SeSaM-protocol comprises four steps: 1) generation of a DNA-fragment pool with random size distribution; 2) enzymatic fragment elongation with universal bases; 3) full-length gene synthesis; 4) universal base replacement [88]. More details about the method background are given in chapter 1.5.1. Tab 2-7 summarizes the primers used for the SeSaM-library generation.

Table 2-7: Primer used for the multiple site saturation of the GOx gen. Lower case letters indicate phosphorothioated bonds.

Primer	SeSaM step	Sequence (5` → 3`)
P1	1	GGC GTG AAT GTA AGC GTG ACA TA
P2	1	CACACTACCGCACTCCGTCG CCG GAT CGG ACT ACT AGC AG
P3	3	CCG GAT CGG ACT ACT AGC AG
P4	3	GTGTGATGGCGTGAGGCAGC GGC GTG AAT GTA AGC GTG ACA TA
P5	final amplification	GTGGTCTCCCTCGCTGCGGCCCTGCCACACTACA TCAGGAGCAATGGCATTGAAGCCAG
P6	final amplification	ATTACATGATGCGGCCCTCTAGATGCATGCTCGAG CGGCCGCCAGTGTGATGGATATCTG

SeSaM library generation was carried out as previously described [85]. DNA templates for SeSaM-TV-II-step 1 and step 2 were prepared by PCR. The 50 µL PCR mixture contained: 1x Phusion HF Buffer; (New England Biolabs); 0.2 mM of each dNTP; 12.5 pmol of each primer (forward and reverse); 2.5 U of Phusion polymerase

(New England Biolabs) and 50 ng of plasmid as template. Tab 2-8 summarizes the PCR program which was carried out.

Table 2-8: PCR program for SeSaM template generation.

Step	Temperature	Time	Cycles
Initial denaturation	98 ˚C	30 sec	1
Denaturation	98˚C	10 sec	
Annealing	60 ˚C	30 sec	20
Extension	72 ˚C	1 min 20 sec	
Final extension	72 ˚C	5 min	1
Hold	8 ˚C	--	--

The primers P1 and P2 were used for step 1 template generation and the primer P3 and P4 for the step 3 template generation. The PCR-product of step-4 was subjected to a final PCR-amplification applying identical PCR-conditions as used for the SeSaM-Tv-II template preparation employing the primers P5 and P6.

2.2.5 Gene cloning

A ligation free Method was selected for the cloning of mutant libraries in the vector pYES2 [103]. The method is based on homologous recombination by the yeast cell itself. Figure 2-1 shows the principle of the cloning strategy.

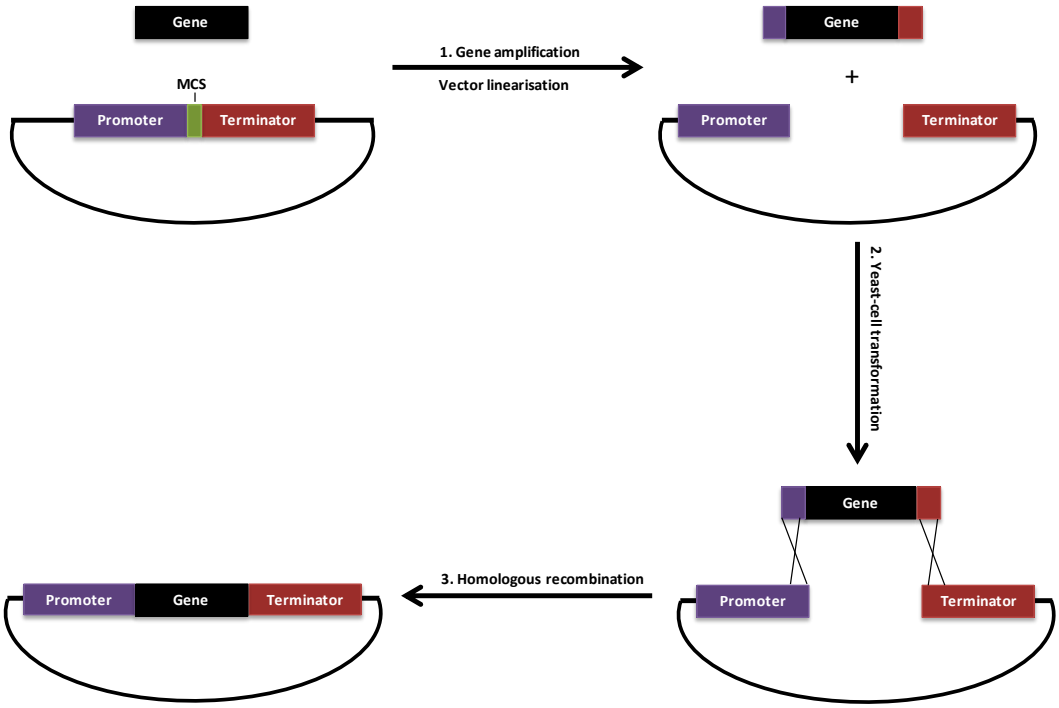

Figure 2-1: Cloning strategy fort he directed GOx evolution based on homologous recombionation. The strategy consists of four steps: 1. Gene amplification and vector linearization; 2. Yeast cell transformation; 3. Homologous recombination.

The cloning method comprises three steps: 1. the gene amplification with special recombination primer and the vector linearization; 2. yeast cell transformation and 3. homologous recombination by the yeast cell. The primers for the amplification of the gene of interest are designed in a way, that the primers have an at least 30 bp overhang complementary to the vector backbone (forward primer to the promoter, reverse primer to the terminator). For the transformation of the SeSaM-1 library a transformation efficiency of $2x10^4$ cfu/µg has been obtained.

The cloning of mutated *GOxs* into the pYES2 vector backbone was performed according to a recombination method [103]. Tab. 2-9 summarizes the primers used for the insert amplification.

Table 2-9: Primer used for the insert amplification within the cloning by homologous recombination.

Primer	Sequence (5` → 3`)
FWD	GTGGTCTCCCTCGCTGCGGCCCTGCCACACTACA TCAGGAGCAATGGCATTGAAGCCAG
REV	ATTACATGATGCGGCCCTCTAGATGCATGCTCGAG CGGCCGCCAGTGTGATGGATATCTG

The 50 µL PCR mixture contained: 1x Phusion HF Buffer; (New England Biolabs); 0.2 mM of each dNTP; 12.5 pmol of each primer (FWD and REV); 2.5 U of Phusion polymerase (New England Biolabs) and 3 ng of plasmid as template. Tab 2-10 summarizes the PCR program which was carried out.

Table 2-10: PCR program for insert amplification

Step	Temperature	Time	Cycles
Initial denaturation	98 ˚C	40 sec	1
Denaturation	98˚C	20 sec	
Annealing	68 ˚C	30 sec	29
Extension	72 ˚C	1 min 20 sec	
Final extension	72 ˚C	5 min	1
Hold	8 ˚C	--	--

2 µg of pYES2-GOx T30V I94V were linearized by SalI/BamHI digestion (10 U/µg DNA, 6 h, 37°C) and subsequently purified by gel-extraction employing the NucleoSpin® Extract II – kit (MACHERY-NAGEL, Düren, Germany). The linearized pYES2-vector and the amplified gene library were mixed in a ratio of 1:3 (250 ng / 750 ng). This DNA-mix was used for the transformation employing a lithium acetate method [104]. Transformants were grown on SC-U selective plates containing 2 % glucose. For the transformation of closed plasmids 300 ng DNA was used. To obtain GOx-molecules with a reduced glycosylation level the glyco-engineered *S. cerevisiae* strain ngd29 was chosen as expression host [42].

2.2.6 Cultivation in microtiter plates

Single colonies were grown on SC-U selective agar plates containing 2 % glucose at 30°C for 48 – 72 h. Subsequently, single colonies were transferred into 96-well microtiter plates (100 µL SC-U media; 1 % glucose; PS-F-bottom, Greiner Bio-One). The cultivation of the pre-culture took place in a microtiter plate shaker (900 rpm; 30°C; 70 % humidity; 24 h; Infors GmbH, Eisenach, Germany). A certain amount of pre-culture was transferred to each well of a deep well plate (500 µL SC-U media; 0.5 % glucose; 2 % galactose; riplate-rectangular, ritter). The main-culture was cultivated as the pre-culture with an elongated cultivation step (72 h). Cell supernatants were

harvested after centrifugation (3300 g; RT; 20 min) and used for activity determinations. For library conservation, 50 µL of the pre-cultures were transferred in a new microtiter-plate(PS-F-bottom, Greiner Bio-One) and 100 µL glycerol (50 % w/w) was added. After homogenizing of the cell-culture / glycerol mixtures the plates were stored at ≤-60°C.

2.2.7 QDM detection system

The mediators selected for the GOx evolution are based on quinone diimine sytems. Quinone diimines attribute efficient electron transfer rates and low unspecific interactions with blood components. Furthermore, they are storage stable if they are immobilized in form of the respective N-substituted *p*-nitrosoanilin, a storage stable precompound. The mediator system was introduced in chapter 1.4.1 and the mediator reaction in the QDM detection system is described in chapter 3.3.1.1. The term QDM-q refers to the usage of the *p*-nitrosoaniline (N,N-bis(2-hydroxyethyl)-4-nitosoaniline) and the term QDM-2 to the usage of N,N-bis(2-hydroxyethyl)-2-methoxy-4-nitrosoaniline.

For the liquid handling multi-channel pipettes from Brand (Transferpette S-8) and Eppendorf (Research pro) were used. 75 µL of supernatant (see cultivation and expression in 96-well plates) or purified enzyme were transferred into a 96-well flat-bottom microtiter plate (Greiner Bio-One). 100 µL of mediator solution (19.05 mM N,N-bis(2-hydroxyethyl)-4-nitrosoaniline [68], Roche - Material No. 100088314; 5% (w/w) polyvinylpyrrolidone, Roche - Material No. 10003476964; pH 7) and 20 µL of 25 g/L phosphomolybdic acid (Roche, Genisys-nr.: 11889893001) were supplemented. Reactions were initiated by supplementing 25 µl substrate solution. The kinetic of phosphomolybdic acid reduction was monitored at 700 nm in microtiter plate reader (Tecan Sunrise; Tecan Trading AG, Switzerland). The amount of GOx that converts 1 µmol of substrate in 1 min was defined as 1 U of that enzyme.

2.2.8 Thermal resistance

100 µL of the enzyme solution were incubated at the corresponding temperature for 15 min and subsequently chilled on ice for 5 min. 75 µL were used for the activity

determinations employing the QDM detection system. The following temperatures were investigated: 30-, 35-, 40-, 45-, 50-, 55-, 60-, and 65°C.

2.2.9 ABTS assay

The ABTS [2,2′-azino-bis(3-ethylbenz-thiazoline-6-sulfonic acid)]-assay is a coupled enzyme assay which can be applied for the activity determination of GOx. The assay is based on the β-D-Glucose oxidation by GOx in the present of oxygen to β-D-Glucono-δ-lactone and H_2O_2. In a subsequently reaction the H_2O_2 and Horseradish peroxidase (HRP) are used to oxidize the chromogenic substrate ABTS, resulting in a color change of the chromogenic substrate (Fig. 3-1) [105].
For liquid handling multi-channel pipettes from Brand (Transferpette S-8) and Eppendorf (Research pro) were used. 75 µL of supernatant (see cultivation and expression in 96-well plates) or purified enzyme transferred to a 96-well flat-bottom microplate (Greiner Bio-One) containing 100 µL of phosphate buffer (0.2 M; pH 7). 20 µL of reaction mixture were supplemented to each well resulting in final concentrations of 0.91 U/mL HRP and 2.3 mM ABTS. Reactions were initiated by supplementing 25 µl substrate solution. The oxidation of ABTS was kinetically determined at 414 nm using the microplate reader FLUOstar Omega (BMG LABTECH). The amount of GOx that converts 1 µmol of substrate in 1 min was defined as 1 U of that enzyme.

2.2.10 Oxygen consumption assay

For the direct determination of the oxygen consumption the optical oxygen probe “Fibox3 – Minisensor Oxygen Meter” (Precision Sensing GmbH Regensburg) was used. The 1540 µL reaction mixture consisted of 840 µL phosphate buffer (0.2 M / pH 7), 175 µL Substrate solution and 525 µL GOx-solution. The oxygen consumption (%/min) was kinetically determined.

2.2.11 Normalization of GOx concentrations employing an enzyme-linked immunosorbent assay (ELISA)

An enzyme-linked immunosorbent assay (ELISA) was used for specific determination of GOx concentrations, employing two GOx specific polyclonal antibodies. The principle of the ELISA is shown in Figure 2-2.

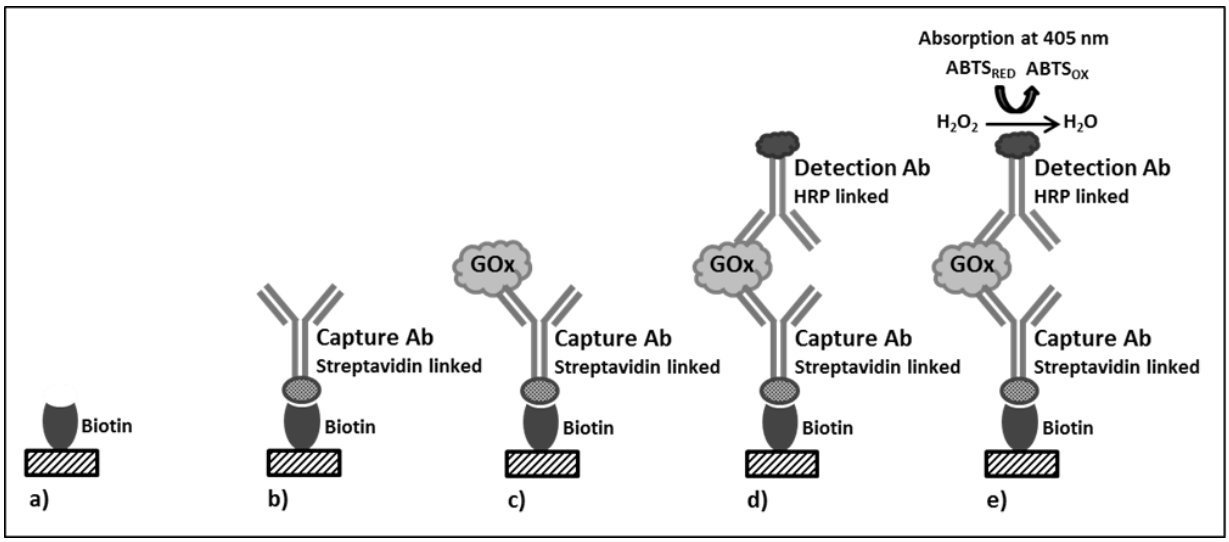

Figure 2-2: Principle of specific GOx determination employing two polyclonal antibodies. a) The assay starts from a streptavidin coated microtiter plate. b) A polyclonal capture antibody binds specific to the streptavidin through covalent linked biotin. c) GOx molecules of the applied sample are recognized and bound by the capture antibody. d) A polyclonal detection antibody which carries a covalent linked horseradish peroxidase (HRP) binds specific the captured GOx. e) In the last step a H_2O_2/ABTS solution is applied. The H_2O_2 enzymatically converted by the HRP by simultaneous (2,2'-azino-bis(3-ethylbenzothiazoline-6-sulphonic acid) (ABTS) -oxidation. The color change of the ABTS is photometric detected at 405 nm. For implementation and material information see material and methods section of the main article. Ab: Antibody.

Each well of a streptavidin coated microtiter plate (Roche 11643673 001) was filled with 100 µL of a primary antibody solution (2 µg/mL; Rabbit PAK GOD-Biotin Acris R1083B; 1 h; RT; 400 rpm). After a subsequent washing step (4 times 350 µL 9 g/L NaCl_0.1 % Tween 20) 100 µL of GOx sample was transferred into each 96-well of a microtiter plate (1 h; RT; 400 rpm). The washing step was repeated and the 96-well plate was filled with 100 µL of a secondary antibody solution (10 µg/mL; Rabbit PAK GOD-HRP Acris R1083HRP; 1 h; RT; 400 rpm). After a third washing step the 96-well plate was filled with 100 µL of a ABTS/H_2O_2 solution (11684302001 Roche Diagnostics GmbH Mannheim; 30 min; RT; 400 rpm), subsequently the absorption at 405 nm was determined. Glucose oxidase from *A. niger* was used as internal standard (0.075-20 ng/mL; G7141-50KU Sigma-Aldrich).

2.2.12 SDS-PAGE

For the protein analysis by reducing and denaturizing gel electrophoresis the following gel was prepared. *Separating gel:* 25% (v/v) acylamid (40%), 25% (v/v) 1.5 M Tris-HCL (pH 8), 1% (v/v) sodiumdodecylsulfate (10%), 1% (v/v) Ammoniumpersulfate (10%), 0.04% (v/v) Temed, 48% deionized water. *Stacking gel:* 12.5% (v/v) acylamid (40%), 12.5% (v/v) 1.5 M Tris-HCL (pH 6.8), 1% (v/v) sodiumdodecylsulfate (10%), 1% (v/v) Ammoniumpersulfate (10%), 0.1% (v/v) Temed, 72% deionized water. The protein samples were mixed with sample buffer (25 % (v/v) and subsequently boiled at 99°C for 10 min (sample buffer: 2% (w/v) sodiumdodecylsulfate, 0.1 % (w/v) bromphenol blue, 100 mM dithiothreitol). The following electrode buffer was used: 25 mM Tris, 250 mM glycin, 0.1% sodiumdodecylsulfate. After the prepared samples were loaded on the SDS-gel, the electrophoreses was performed (1 h / 150 V). For each run 5 µL of the PageRuler™Prestained Protein Ladder was employed. After the electrophoreses the gel was stained for 1 h and subsequently destained for at least 2 h (staining solution: 0.1% coomassie brilliant blue G-250, 50% ethanol, 10% acetic acid; de-staining solution: 50% ethanol, 10% acetic acid).

2.2.13 Cultivation of *Sc* ngd29 at pilot scale

Pre-cultivation: 500 mL SynY media (2 % glucose) were inoculated to an OD_{600}=0.2 using an overnight-culture of *S. cerevisiae* ngd29/pYES2-GOx (overnight culture: 10 mL YPD media, 30°C, 250 rpm, 20h); pre-cultivations took place in 5L shaking flasks (12 h; 30°C; 250 rpm).
Main-cultivation: 9.5 L SynY media (1 % glucose) was inoculated with 500 mL pre-culture. For the cultivation a 10 L fermenter was used (30°C; 400 rpm; 1 vvm; 48 h, pH 5).For the pH conditioning during the fermentation 30% phosphoric acid and 15% ammonia was used.

2.2.14 Tangential flow filtration

For the primary separation a tangential flow filtration setup was selected employing the SartoJet-slice system (Sartorius Stedim Biotech GmbH Göttingen). The process

included two steps, the cell-separation (micro-filtration) and the concentration / buffer exchange (ultra-filtration). For the microfiltration a trans-membrane pressure of 1.5 was applied using a Hydrosart 0.45 µm membrane (Sartorius Stedim Biotech GmbH Göttingen). The filtration took place until the 10 L cell broth was reduced to 0.5 L, the cleared supernatant was collected in the permeate. A diafiltration setup was employed for the ultra-filtration using a Hydrosart 10 kDa membrane (Sartorius Stedim Biotech GmbH Göttingen). The cell supernatant was concentrated to 0.5 – 1 L and seven diafiltration volumes were applied for buffer exchange. A trans-membrane pressure of 1.5 was applied also for the ultra-filtration

2.2.15 Anion-exchange chromatography (AEC)

For the purification of GOx an AEC step was performed at pH 6. The applied conditions are described in the following.

Table 2-11: Equipment for AEC

Equipment	
FPLC system	ÄKTApilot (GE Healthcare)
Column	FineLine Pilot 35 (GE Healthcare)
Resin	Fractogel TSK DEAE-650 (s)
Bed volume	220 mL

Table 2-12: Chromatography sequence of AEC

Step	**Step length [mL]**	**Flow rate [cm/h]**	**Buffer**
Equilibration	660	62.5	sodium phosphate (50 mM, pH 6)
Load	500- 1000	62.5	---
Wash-1	440	62.5	99% sodium phosphate (50 mM, pH 6) / 1% sodium chloride (1M)

Wash-2	440		95% sodium phosphate (50 mM, pH 6) / 5% sodium chloride (1M)
Elution (10 mL fractions were collected)	220	62.5	92.5% sodium phosphate (50 mM, pH 6) / 7.5% sodium chloride (1M)
Regeneration	440	62.5	sodium chloride (1M)
Sanitization	660	62.5	Sodium hydroxide (0.5 M)
Equilibration-2	Until stable pH at column exit	62.5	Water
Storage	440	62.5	Ethanol (20%)

3. Reengineered Glucose oxidase for oxygen independent glucose sensing

3.1 Purpose

Oxygen sensitivity, substrate specificity and good electrochemical communication (via mediators) are three enzymatic properties which are crucial for accurate enzymatic glucose sensing. GOx exhibits excellent β-D-glucose specificities, but lacks a specific and efficient electron transfer by artificial mediators due to its high oxygen dependency. In order to develop a GOx which meets the requirements for accurate β-D-glucose sensing in biological samples, a directed evolution campaign was implemented employing a diabetes relevant quinone diimine/ phenylendiamine mediator system [3, 68, 69]. The focus of the study was thereby the engineering of GOx towards oxygen independency and the adoption of GOx to the quinone diimine/ phenylendiamine mediator system by maintaining the high β-D-glucose specificity and thermal stability.
The background of the study and the overall objectives are described in detail in chapter 1 and 1.2.

3.2. Strategy

For the identification of relevant residues a specific directed evolution platform needed to be established, beforehand of the mutant-library screening. Identified residues were investigated individual and cooperatively. The directed evolution campaign included the following activities:

- Establishment of a suitable screening system comprising two assays, one for oxygen- and one for mediator activity
- Diversity generation by different random mutagenesis methods
- Screening the gene diversity for oxygen independency and mediator activity
- Investigation of identified residues individually and cooperatively by site saturation mutagenesis
- Characterization of selected variants with respect to the desired properties

- Computational investigations to construct a GOx model for oxygen independency and improved mediator activity

3.3 Results

3.3.1 Establishment of a screening platform

3.3.1.1 The activity assays

Two activity assays had to be established to screen for reduced oxygen dependency and for improved mediator activity. The ABTS detection system was employed to detect the electron acceptance by oxygen and to screen for variants with reduced oxygen dependency. The performance of ABTS assay with respect to directed GOx evolution is described elsewhere [39]. Figure 3-1 shows the principle of the activity determination employing the ABTS assay.

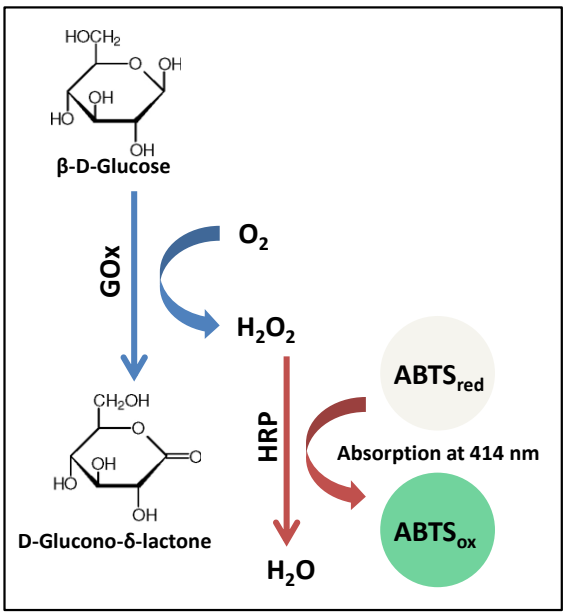

Figure 3-1: Principal of GOx-activity determination by oxidation of ABTS. The in the GOx oxidative half reaction produced H_2O_2 and the added HRP are used to oxidize the chromogenic substrate ABTS. The color change of ABTS is monitored by absorption at 414 nm and is proportional to the reduction of O_2.

A quinone diimine mediator detection system (QDM-1 assay) was established to detect variants with increased mediator activity. The system is based on storage stable *p*-nitrosoaniline (N,N-bis(2-hydroxyethyl)-4-nitosoaniline) [3, 68, 69]. Figure 3-2 shows the principle of the QDM-1 assay.

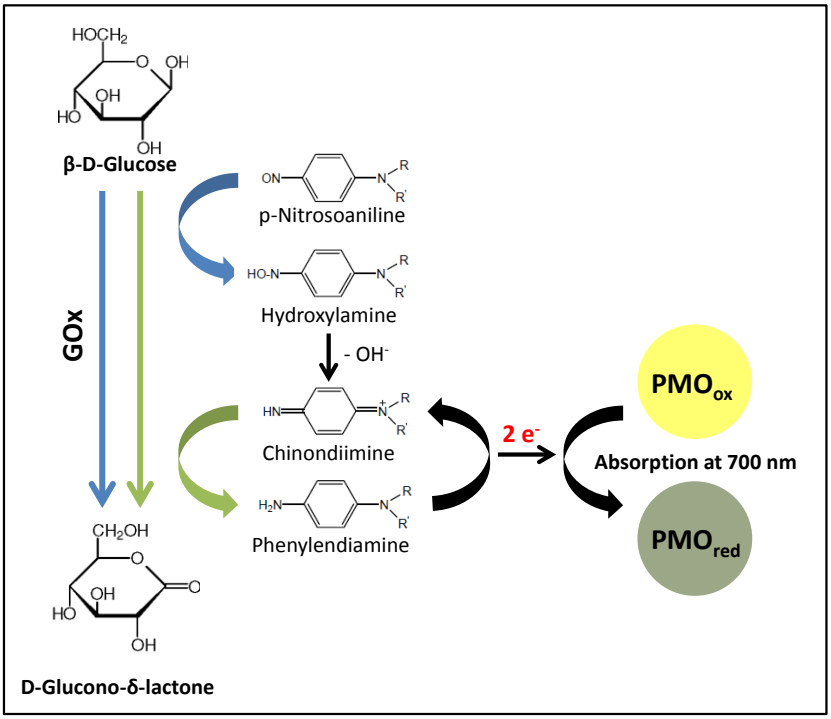

Figure 3-2: QDM-1 detection system. The *p*-nitrosoaniline gets reduced to hydroxylamine. The mediator quinone diimine occurs after spontaneous water elimination and is further reduced by GOx to phenylendiamine. Phenylendiamine is reoxidzed (two electron process) with PMO_{ox} which is reduced to the blue PMO_{red} (recorded at 700 nm). PMO: phosphomolybdic acid [3, 67-69, 106, 107].

The mediator reaction starts from the *p*-nitrosoaniline which is converted to the corresponding quinone diimine, the actual electron mediator. The quinone diimine is further reduced to phenylendiamine, which is deoxidized to the quinone diimine (two electron process) [3, 68, 69]. Phosphomolybdic acid (PMO) serves as final electron acceptor and indicates the GOx mediator activity [106, 107]. The sceening system is based on the activity determination of GOx which is expressed in *Saccharomyces cerevisiae ngd 29* (*Sc ngd29*) and secreted to the cell supernatant. The standard deviation of the QDM-1 assay in cell supernatants was detected to be 10.2% with a linear detection range from 1 to 25 U/L. Screening systems with standard deviations below 20 % have often successfully been employed in directed enzyme evolution experiments [93, 108, 109].

3.3.1.2 Comparison of two different *Saccharomyces cerevisiae* expression strains

The *S. cerevisiae strains Sc*. INV (INVITROGEN) and *Sc*. *ngd29* (ROCHE) have been tested for the recombinant expression of GOx from *Aspergillus niger* [42]. Both are able to secrete recombinant GOx into the culture medium by employing an N-terminal MFα-signal peptide [42, 43].

The *S. cerevisiae strains Sc*. INV (INVITROGEN) hyper-glycosylates recombinant proteins with an N-glycosylation structure of the type $Man_nGlcNac_2$. However, a uniform glycosylation pattern may play an important role in the industrial production of analytical enzymes where a stable product homogeneity has to be ensured. Therefore we investigated a hypo-gylcosylation strain *Sc.* 7087 which provides GOx-molecules with a uniform asparagine-linked $Man_8GlcNac_2$ glycosylation pattern [42]. To compare the two expression systems in regard to an assay establishment on medium high-throughput level, the GOx expressing strains were cultivated in a 96-well format. The GOx-activity of the resulted supernatants was analyzed using the QDM-1 detection system (see 3.3.1.1). Figure 3-3 shows the activity profiles of the two different strains always compared to the respective mock-strain.

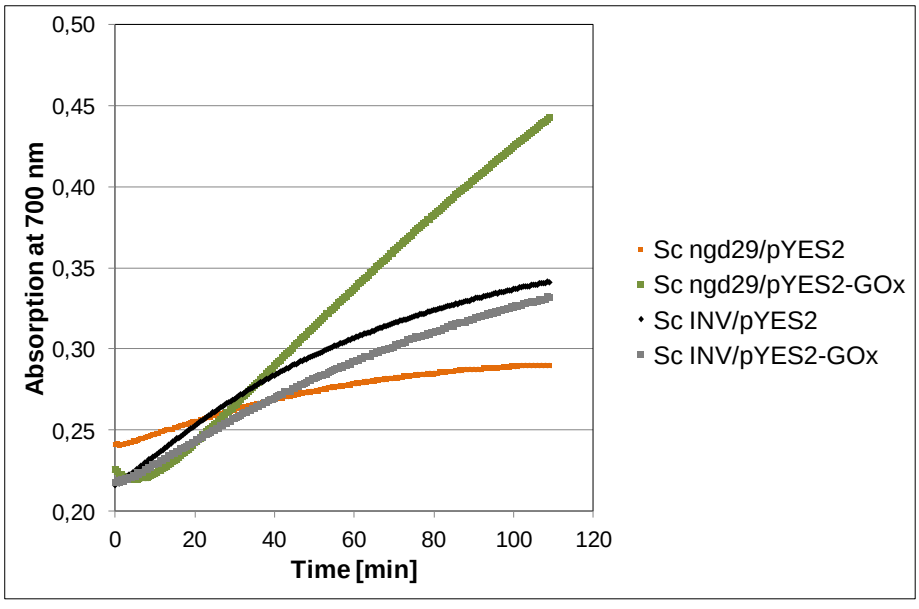

Figure 3-3: determination of GOx-activity in supernatants of two different *S. cerevisiae* expression strains. The cultivation was carried out in microtiter plates. For the activity determination the QDM-1 detection system was performed in in a 96-well format and absorption at 700 nm was observed for 115 min. The activities of the two different expression strains were compared to the respective mock-strains.

Figure 3-3 Shows that the initial reaction rate in the supernatant of the GOx expression strain *Sc ngd29*/pYES2-GOx is characterized by a linear slope and it is clearly distinguishable from that of the negative control strain (background). However, the GOx-activity in the supernatant of the expression strain *Sc* INV is not detectable using the QDM-1 detection system, since it cannot be distinguished between the expression strain and the negative control strain. Therefore, the *Sc ngd29*/pYES2-GOx strain is more suitable for the expression of GOx in the desired directed evolution experiments. The higher GOx-activity in the supernatant of the hypo-glycosylation strain can be caused either by a higher expression and secretion rate or higher enzymatic activity due to the altered glycosylation pattern. The cause of the difference between both *S. cerevisiae* strains will not be investigated within the present thesis and further experiments are focusing on the implementation of the *Sc ngd29* based GOx-screening system.

3.3.1.3 Implementation of an auto-induction media

In 2005 Zhu et al. published a two-step strategy to cultivate *S. cerevisiae* in microtiter-plates [110]. Step one is a cell growth step in which the cells utilize glucose as a carbon source. In step two the galactose inducible promoter gets induced by galactose in the media. The method provides that the glucose containing media is exchanged by a galactose containing media after a certain growth phase, which ensures a growth-uncoupled expression of the recombinant protein. Apart from a high working effort, the media exchange leads to a long lag-phase, which may result in less formation of the recombinant protein.

Since the galactose inducible promoter is repressed by glucose and glucose is the preferred carbon source for *S. cerevisiae*, a growth-uncoupled recombinant protein expression should also be possible using an auto-induction approach. Figure 3-4 shows the initial reaction rates of Glucose oxidase in cell-supernatants under different cultivation conditions applying the QDM-1 detection system in microtier-plates (see chapter 3.1.3.1). To establish a suitable auto-induction media the cultivation was performed for 48- and 72 h using different concentrations of glucose for cell growth and galactose as well as maltose for induction (based on SC-U media). Three different expression strains were selected for the experimental setup;

the *Sc ngd29* negative control strain, the *Sc ngd29* strain expressing GOx wild type and the *Sc ngd29* strain expressing a variant of GOx (GOx T30VI94V) [43].

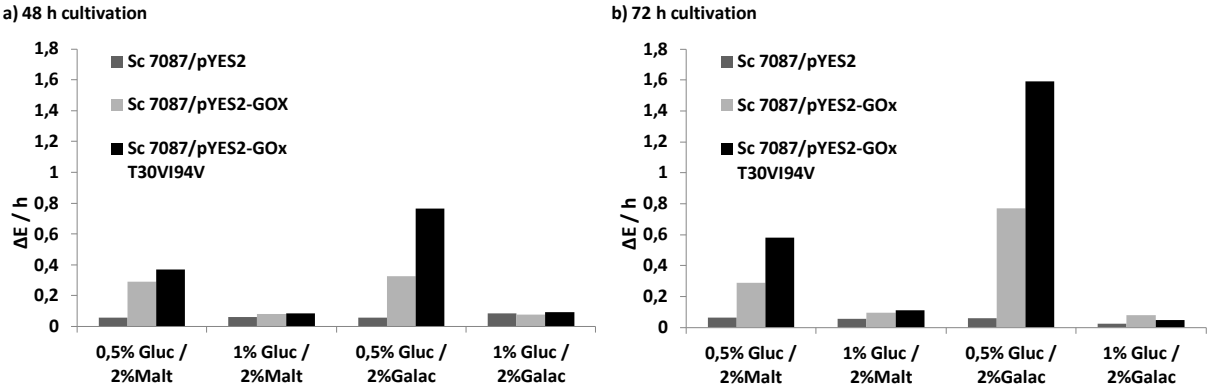

Figure 3-4: GOx-activity in cell-supernatants after 48 h (a) and 72 h (b) cultivation using different Glucose concentrations for cell-growth and different galactose/maltose concentrations for induction.

Figure 3-4 shows clearly higher activities in the media with 0.5 % glucose compared to 1 % glucose for all approaches. Furthermore, there is a preference for galctose over maltose as an inductor. Cultivations for 72 h clearly deliver higher activities than those over 48 h. The best result was obtained using 0.5 % glucose in combination with 2 % galactose and a cultivation time of 72 h. The detailed cultivation conditions are described in the material and methods section.

3.3.2 Gene mutagenesis and screening of mutant libraries

Figure 3-5 shows a scheme of directed GOx evolution for reduced oxygen dependency and improved mediator activity. The campaign started from the parent variant GOx-T30VI94V, a variant that exhibits a increased thermal stability (from 58°C to 62°), a increased pH stability (at alkaline pH, 8-11) as well as a increased catalytic efficiency (k_{cat}: 69.5/s to 137.7/s) [40]. After diversity generation on gene level the host stain *Sc ngd29* was transformed and isolated cell clones were cultivated in 96-well plates. Cell supernatants were investigated employing the ABTS- and the QDM-1 detection system in parallel in order to indentify variants with reduced oxygen dependency and improved mediator activity. In the pre-screening each clone was investigated once and promising candidates were selected. The candidates were analyzed 12-times in a re-screening approach for statistical assessments. Subsequently, DNA-sequence analysis of selected variants took place. Mutated

genes from improved variants were subjected to a further round of directed evolution (iterative cycles).

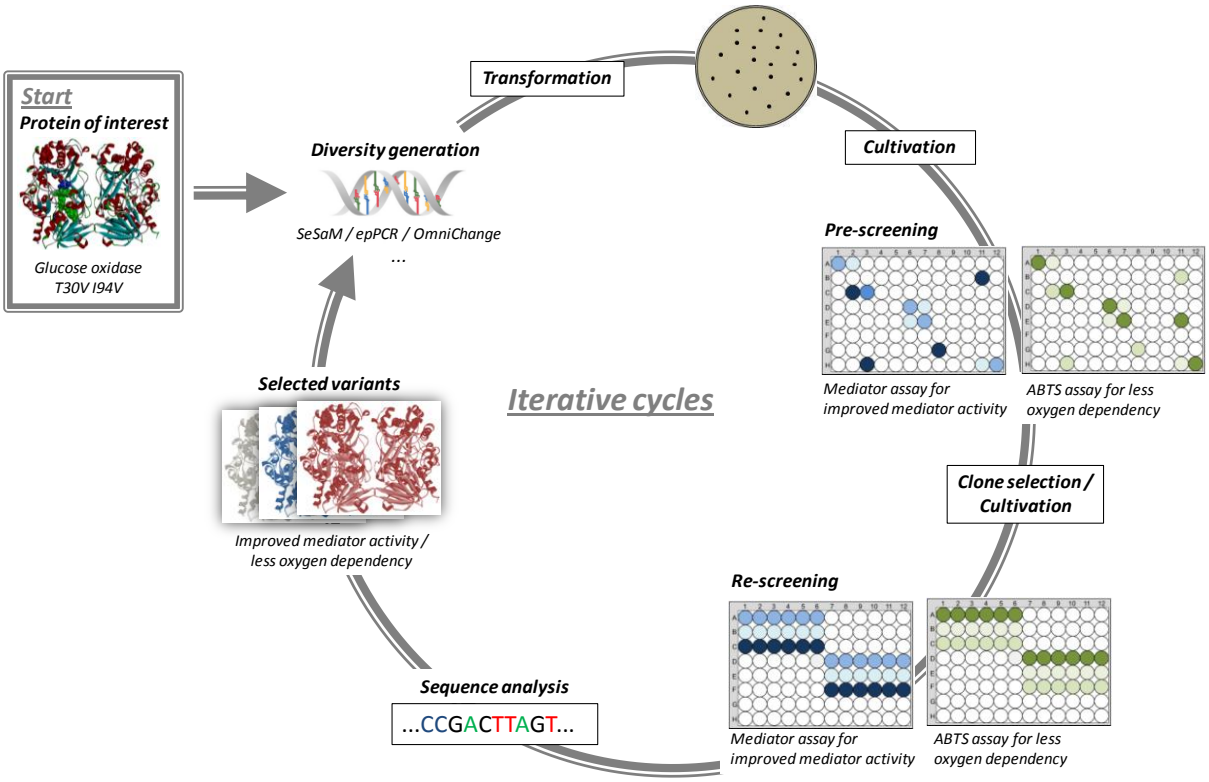

Figure 3-5: Directed evolution platform for Glucose oxidase. The experiment includes the steps; diversity generation on gene level, transformation of *Saccharomyces cerevisiae ngd 29*, cultivating and screening for desired properties (pre-screening/re-screening), gene isolation and sequence analysis. Genes of selected variants serve as parents for the next evolution round (iterative cycles).

Two iterative cycles of directed evolution were performed to identify GOx residues or regions which either modulated oxygen activity or mediator activity (Fig. 3-6). In the first cycle the mutant library was generated by the SeSaM technology [85] based on the parent GOx-T30V I94V. The two best variants from the SeSaM library (A173T, A332S) were used as parents for the second cycle in which an error-prone-PCR mutant library (epPCR; 0.1 mM $MnCl_2$) was screened.

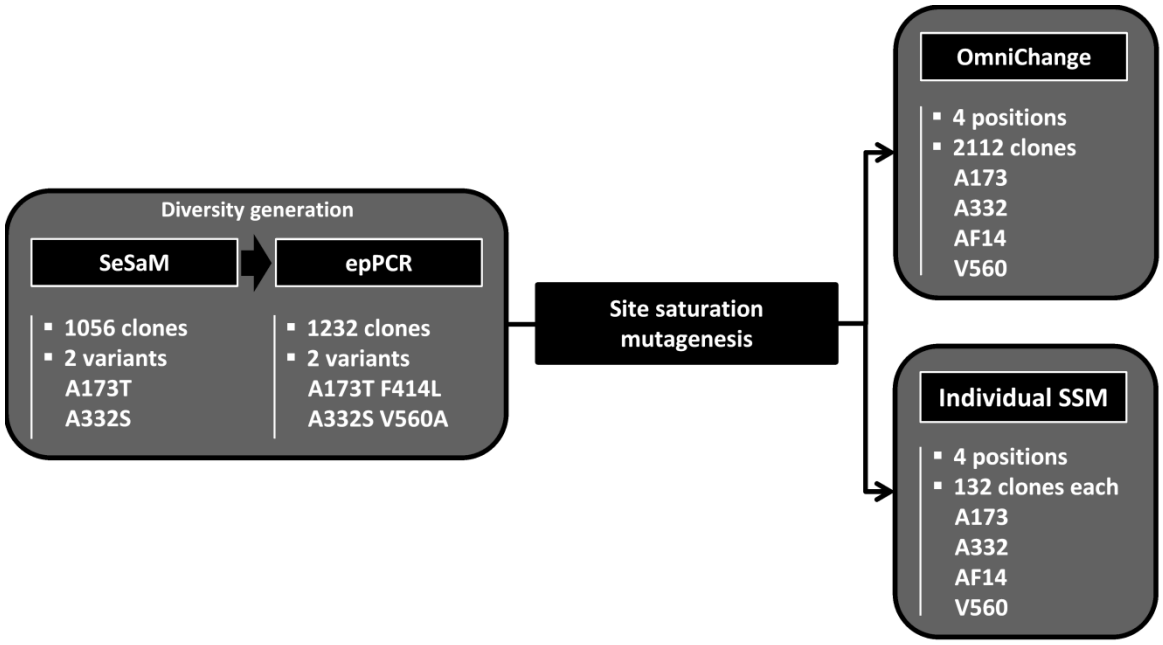

Figure 3-6: Overview of the directed GOx evolution campaign. The campaign was performed to decrease the oxygen dependency and to increase the mediator activity. Two iterative cycles of random mutagenesis were performed yielding four beneficial positions (A173, A332, F414, and V560). All four positions were mutagenized either individually (QuikChange; -NNK) or simultaneously (OmniChange; reduced amino acid subsets) [67].

The random mutagenesis yielded four beneficial substitutions (A173T, A332S, F414L, V560A). V1 (A173T) and V2 (A332S) showed increased oxygen and mediator activity in the ABTS and in the QDM-1 assay (V01: 170% QDM-1 assay, 165% ABTS assay; V2: 175% QDM assay, 135% ABTS assay - residual activity of reference GOx-T30V I94V). In contrast, V3 (A173T F414L) and V5 (A332S V560A) showed significantly decreased oxygen activity (< 30% than GOx reference) in combination with a slightly increased mediator activity (V3: 200%; V5 160% - residual activity of GOx reference).

All four identified positions were further investigated by individual site saturation mutagenesis to elucidate their functions (with respect to oxygen independency and mediator activity) and to assess the most beneficial substitution for each residue. Table 3-1 summarizes the sequencing results of the individual site saturation approach and the properties of each residue.

Table 3-1: Sequence analysis of individual saturated positions in GOx variants and influence of identified positions (A173, A332, F414, V560) on mediator and oxygen activity. Clones from the mutant libraries were selected based on increased mediator activity and / or decreased oxygen activity. Substitutions and the number of occurrence in 11 to 18 sequenced clones are given [67].

Residue wild type	No. seq. clones	Found substitution (No. of occurrence)	Property
A173	12	V (5); A (4); I (2); T (1)	Improved oxygen and mediator activity
A332	14	V (5); T (4); M (2); S (2); P (1)	Improved oxygen and mediator activity
F414	11	F (4); M (3); V (3); L (1)	Improved mediator activity / reduced oxygen activity (M)
V560	18	L (8); P (6); T (2); W (1); Q (1)	Significantly reduced oxygen activity

Residue 173 and 332 contribute to the increased oxygen and mediator activity. Substitutions of residue 414 resulted mostly in improved mediator activity but also in reduced oxygen activity (F414M). Residue 560 is crucial for the reduced oxygen dependency of GOx; substitutions to L, P, T, W or Q led to a substantial decreased oxygen activity while maintaining the mediator activity (Tab. 3-1).
Results of the individual site saturation experiments prove that the identified residues allow to modulate individual or jointly (V3, V5) the oxygen sensitivity and mediator activity. An overview of the location of all identified residues in the GOx-WT is given in Fig. 3-13.

For the assessment of cooperative effects an OmniChange multi-site site saturation experiment [102] was performed including all four residues (A273, A332, F414, V560). Since a screening of the full diversity with 20 aa / 32 codons (NNK) at 4 positions would generate 1.05 mio. gene variants, a reduced subsets of amino acids were selected for each position, according to the most frequent amino acids in a multiple sequence alignment of Gox and oxygen independent glucose dehydrogenases (Tab. 3-2).

Table 3-2: Selected amino acid set for simultaneous site saturation of identified positions using the OmniChange method [67].

Residue	Subset of amino acids	Degenerated codons
173	AITV	RYT
332	SN	ART
414	CDFGHILNRSVY	NDT
560	AILMPTV	VYK

The reduced OmniChange library consisted of 1152 codon variants and 2112 clones were screened (theoretically 94% coverage) [111]. The OmniChange library was screened with respect to reduced oxygen independency and improved mediator activity yielding five variants (V6-8; V10-11) exhibiting significantly improved properties (less oxygen sensitivity; higher mediator activity) compared to those of the individual site saturation experiment. Tab. 3-3 summarizes the sequencing results and the residual activities of the five selected OmniChange variants. The residual activities are based on the comparison of the specific activities (oxygen and mediator activity at 34 mM β-D-glucose) of the GOx reference (GOx T30V I94V) and the respective variant.

Table 3-3: Results of the OmniChange multi-site saturation library of the GOx reference variant (GOx-T30V I94V). GOx variants were selected according to mediator and / or lower oxygen activity. Sequencing results are reported for the positions 173, 332, 414, and 560 with improvements in mediator and/or oxygen sensitivity. 34 mM ß-D-glucose was used in all activity determinations. Calculations are given in % as ratios of specific activities (U/mg) compared to the GOx reference variant (RV; T30V I94V). n.d.: not detected [67].

Variant	Substitutions				Residual activity (%)	
	A 173	A 332	F 414	V 560	Mediator activity	Oxygen activity
V6	I	S	L	*V*	160	30
V7	V	S	I	T	440	n.d.
V8	V	N	*F*	P	100	n.d.
V10	V	N	V	L	243	n.d.
V11	*A*	S	*F*	P	120	n.d.

All values in Tab. 3-3 were calculated using GOx containing cell supernatants without any protein purification steps; recorded values have therefore to be considered as apparent values which were used for the selection of the most beneficial variants V7 and V10.

V7 and V10 exhibit increased mediator activity (reference variant: 3.2 U/mg; V7: 14.1 U/mg; V10: 7.8 U/mg) by simultaneously reduced oxygen activity (reference variant: 296 U/mg; not detected for V7 and V10 under selected conditions).

To select a final variant, substrate specificity and thermal stability was determined for all variants (V6-8; V10-11; data not shown) in order to ensure that the high β-D-glucose specificity and thermal stability of GOx was maintained during directed evolution. V7 showed for the latter two properties a comparable performance to the GOx reference (specificity: Tab. 3-5; thermal stability: Fig. 3-7). In essence, V7 exhibited after pre-characterization (in yeast cell supernatants) all required properties and was selected for detailed characterization.

3.3.3 Characterization of V7, reference variant (RV) and WT

V7, RV (GOx-T30V I94V) and WT were produced in *Sc ng29* in 10L scale and subsequently purified according to the material and method section. The establishment of the GOx production process is described in chapter 5. Purified GOx and variants (content > 90%) were subjected to kinetic investigations employing the QDM-1 assay and the ABTS assay. Michaelis-menten kinetics were recorded and the enzymatic parameters (Vmax; K_M) were obtained by non-linear regression. Table 3-4 summarizes the kinetic parameters and the residual activities of V7, RV and WT.

Table 3-4: Kinetic parameters and residual activities of WT, RV, and V7. Kinetic parameters (v_{max}; K_M) were obtained by non-linear regression based on the Michaelis-Menten model using GraphPad Prism software package.

	Mediator assay			ABTS assay		
	V_{max} [U/mg]	Residual activity	K_M [mM]	V_{max} [U/mg]	Residual activity	K_M [mM]
WT	7.4±0.1	100 %	13.2±1.0	172.3±4.2	100 %	14.2±1.3
RV (T30V-I94V)	13.7±0.2	184 %	11.9±0.9	221.6±6.0	128 %	8.7±1.0
V7	47.5±1.0	638 %	28.2±1.9	30.1±0.2	17 %	1.3±0.1

V7 has 638 % residual activity in the QDM assay (WT: 7.4 U/mg; V7: 47.5 U/mg) and 17 % residual activity in the ABTS assay (WT: 172.3 U/mg; V7: 30.12 U/mg), resulting in a 37.5 times reduced oxygen dependency (Residual activity QDM assay / residual activity ABTS assay - OI-ratio) when compared to WT and RV (OI-ratio WT: 1; OI-ratio T30V I94V: 1.4).

Oxygen activity was determined indirectly by applying the coupled ABTS-assay. For final characterization and in order to validate the ABTS results an oxygen probe (Oxygen Meter - Precision Sensing GmbH Regensburg) was used to directly measure the oxygen consumption [%-/min]. The direct oxygen consumption measurements yielded comparable results, for instance in case of V7 (17 % ABTS assay; 22 % oxygen probe). In detail, a rate of 3.9 %/min was observed for V7, 17.4 %/min for WT and 24.2 %/min for RV.

V7 is attractive for amperometric ß-D-glucose determination if the specificity for ß-D-glucose is kept during directed GOx evolution in order to avoid cross-reactivity with clinical relevant sugars (β-D-maltose, maltotriose, β-D-galactose, and D-xylose). Table 3-5 summarizes residual activities of GOx, WT, RV, and V7 for β-D-maltose, maltotriose, β-D-galactose, and D-xylose. WT, RV, and V7 activity for ß-D-glucose were set to 100 % as reference value and the QDM assay was employed in specificity studies.

Table 3-5: Residual activities of WT, RV, and V07 on ß-D-maltose, maltotriose, ß-D-galactose and D-xylose. Activity was determined using the QDM-assay and 182 mM of each sugar was employed in activity measurements. WT, RV, and V7 activity for ß-D-glucose were set to 100% as reference value. n.d.: not detected.

	Residual activity [%]		
	WT	RV	V7
ß-D-Glucose	100.0±1.10	100.0±2.10	100.0±0.30
β-D Maltose	n.d.	n.d.	n.d.
Maltotriose	0.2±0.01	0.8±0.03	0.3±0.01
β-D-Galactose	1.1±0.08	1.0±0.02	0.4±0.02
D-Xylose	0.4±0.04	0.3±0.02	1.7±0.01

Overall, the activities for β-D-maltose, maltotriose, β-D-galactose and D-xylose are less than 2 % of the glucose activity in WT, RV and V7 and differ less than 1.3 % among all investigated sugars. Therefore the specificities of WT, RV and V7 can be regarded as nearly unaltered for diabetes relevant sugars. V7 has a neglectable increased activity for D-xylose (from 0.38 % to 1.66 % residual activity) and interestingly the β-D-galactose activity is slightly reduced from 1.08 % to 0.42 %. Additionally none of the three GOx enzymes has a detectable activity on maltose (for experimental setup see material and methods section).

Furthermore the thermal resistance of GOX-WT and variants was investigated to ensure no stability loss during GOx evolution (Fig. 3-7).

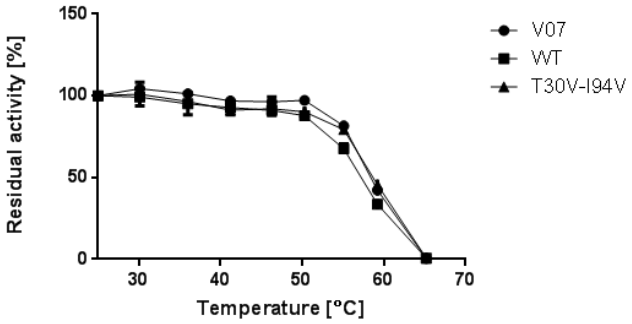

Figure 3-7: Thermal resistance of WT, RV, and V7 determined after thermal incubation (15 min; 25-65°C) and subsequent cooling on ice. Activities were determined with the QDM-1 detection system employing 182 mM ß-D-Glucose. Figure was prepared using the GraphPad Prism software package (La Jolla California USA)

Thermal resistance of GOx WT, RV, and V7 was determined after 15 min incubation at varied temperatures (25-65°C in 5°C steps) as shown in Figure 3-7. The activity after incubation at 25°C was set to 100 %. GOx WT and variants exhibit a high thermal resistance up to 50°C, no significant difference between WT, RV and V7 could be observed.

3.3.4 Further optimization of GOx

Two further residues of GOx from *A. niger* were investigated with respect to improved GOx activity. A137 was identified within the second round of directed GOx-evolution (epPCR – see chapter 3.1.4) and S53 within an additional third cycle (Fig.-3.8).

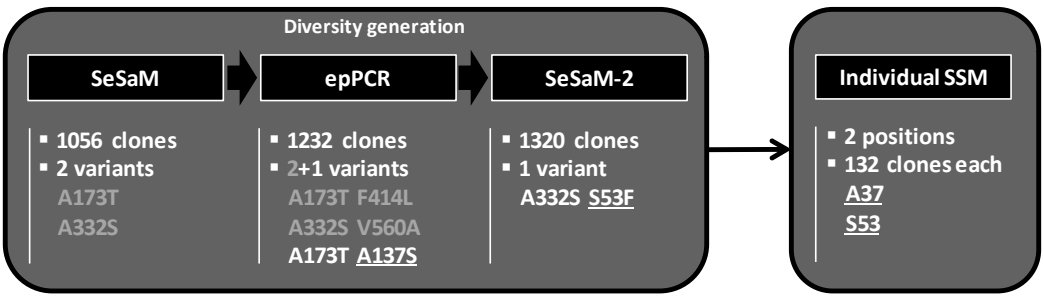

Figure 3-8: Overview of the directed GOx evolution campaign. The campaign was performed to decrease the oxygen dependency and to increase the mediator activity. Two iterative cycles of random mutagenesis (SeSaM; epPCR) were performed yielding four beneficial positions (A173, A332, F414, and V560) for oxygen dependency and mediator activity, which were further investigated (see chapter 3.1.4). The additional residues A137 from cycle two and S53F from an additional

SeSaM library (SeSaM-2, iterative cycle 3) were considered as independent overall-activity residues and were further investigated by site saturation mutagenesis (QuikChange; -NNK).

Fig. 3-8 shows a modified directed evolution scheme for GOx (see also chapter 3.1.4). The additional Variant A173T A137S (in the following named as V4) was identified in the second cycle during the epPCR screening. V4 showed an approximately 1.7-fold improvement in the GOx activity, for the ABTS-assay as well as for the QDM-1 detection system. The gens of all so far identified variants (cycle 1+2) were used as parents for the construction of the mutant library of the third cycle of directed GOx evolution. Only the variant A332S S53F (in the following named as V12) was identified as a 3rd generation variant with improved properties. This variant showed similar properties as V4, with slightly less activity in the oxygen activity compared to the mediator activity. None of the two variants showed a significant alternation in the oxygen to mediator activity ratio. Both new identified residues (A137 and S53) were considered as overall activity improving residues and were not included in investigations towards an oxygen independent GOx (see chapter 3.14 / 3.15). Nevertheless both residues were subjected for individual site saturation mutagenesis in order to investigate the whole diversity for each position. Site saturation studies revealed leucine as the best substitution for residue 137 with an activity improvement of around 5-fold in compare to GOx- T30VI94V. The substitution from serine to phenylalanine was the best for residue 53 with an activity improvement of approximately 2-fold compared to GOx T30VI94V.

Since the substitutions of the residues 52 and 137 were considered as independent activity positions, an incorporation of the substitutions into V7 were investigated with the objective to raise the activity of V7 without altering the oxygen independency.

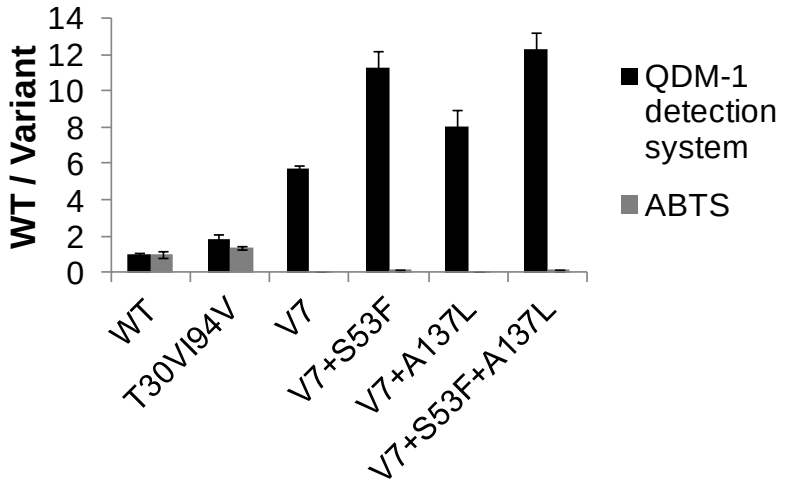

Figure 3-9: Incorporation of S53F and A137L into V7. The substitutions were incorporated in the GOx gen employing the QuikChange method. After transformation of *Sc*. *ngd29* the respective cell clones were cultivated in 96-well plates and clarified cell supernatants were subjected to activity determinations employing the QDM-1 detection system (mediator activity) and the ABTS-assay (oxygen activity).

Figure 3-9 shows the relative activities of the WT to respective variants including the combinations of V7 with the substitutions S53F and A137L. The combination of V7 with S53F as well as with A137L leads to improved activities in the QDM-1 detection system without altering the oxygen activity of V7 under the selected conditions. Also the combination of V7 with both substitutions improves the activity of V7, whereby no clear distinction is possible between V7 + S53F + A137L and V7 + S53F. It needs to be stated that these investigations were implemented with not purified enzymes in yeast cell supernatants and needs to be considered as preliminary results. For a clear assessment of the combinations a characterization in more detail would be necessary.

3.3.5 Computational assessment of V7 and residue A137

Computational investigations were implemented by the sub-group for computational biology of the chair for biotechnology (Dr. Marco Bocola, RWTH Aachen University). The results of the entire computational study are summarized and published within the master thesis of Alexandra Bălăceanu [112].

The scope of this chapter is the theoretical investigation of the oxygen activity for WT, V7, V8 and an external reference (GOx T110A [41]).

3.3.5.1 Selected variants and model preparation

The X-ray crystal structure of Glucose oxidase from *Aspergillus niger* was obtained from the Protein Data Bank entry 1CF3 [53] and prepared for molecular modeling activities [112]. In order to assess the oxidative half reaction a dimeric GOx model with bound substrate and product was constructed and validated with respect to the reduction state of the cofactor (semi-reduced $FADH^{\cdot}$ form) and the protonation state of the active site histidines (His 516 and His 559 fully protonated). The model construction and validation is described in detail in Bălăceanu 2013 [112].

The three additional model structures V7, V8 and T110A were created. The experimental characterization of V7 was shown in chapter 3.1.5. V8 was introduced in chapter 3.1.4 and showed excellent properties with respect to oxygen independency, but was not further analyzed due to low mediator activity and residual activity on xylose. T110A was published by Horaguchi et al. and exhibits a 6-fold higher dehydrogenase/osidase ratio [41], this variant was selected as a comparison to V7 and V8. Table 3-6 summarizes the substitutions of the respective variants.

Table 3-6: GOx variants and respective amino acid substitutions.

Variant	T110	A173	A332	F414	V560
V7	-	Val	Ser	Ile	Thr
V8	-	Val	Asn	-	Pro
T110A	Ala	-	-	-	-

Substitutions in the GOx structure were introduced using FoldX considering stability changes upon the substitution and by allowing all residues within a 6 Å radius around the substitution to be moved, obtained structures were energy minimized in water [112].

3.3.5.2 Oxygen placement and MD-simulations

Solvent accessible molecular surfaces were studied and it has been found that WT exhibits an oxygen stabilizing pocket close to the active site [112] (Fig. 3-10).

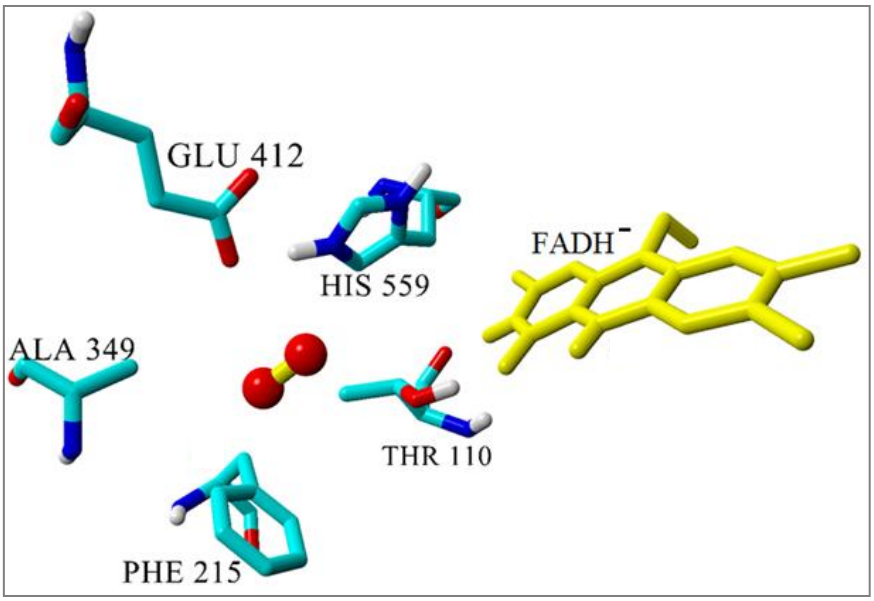

Figure 3-10: Oxygen stabilizing pocket in GOx WT. The pocked has been discovered by the comparison of solvent accessible surfaces. Oxygen was placed in this pocked and the respective complex was energy minimized [112].

For the WT the oxygen was placed in the oxygen stabilizing binding pocket. For V7, V8 and T110A this binding pocket could not be observed and the oxygen molecule was initially placed as close to the cofactor as possible. Obtained protein-oxygen complexes were subsequent energy minimized [112].

Two different rotamers were found for V7 during model preparation and each rotamer showed a different behavior towards oxygen. In one rotamer of V7 a new pocket is formed in which oxygen can be stabilized (Rotamer 2). This pocket cannot be observed in the second rotamer (Rotamer 1) (data provided from the subgroup of computational biology, Marco Bocola).

The received structures were used as a starting point for molecular dynamic simulations over 5 ns with the active site H516 in a protonated state. The trajectory analysis was implemented to assess the GOx-oxygen models whereby the distance from oxygen to the N5 atom of the FDH^- and the distance F215 were followed (Tab 3-7). F215 is a residue of the observed oxygen pocket in GOx WT.

Table 3-7: Recorded average distances of the oxygen radical to the N5 atom and to F215 during molecular dynamic simulations. Data provided by the subgroup for computational biology.

Oxygen	WT	V7 – Rot 1	V7 – Rot 2	V8	T110A
Dist FAD [Å]	9.3	12.1	7.8	20.4	18.4
Dist F215 [Å]	4.0	14.1	5.5	24.2	19.3

Figure 3-11 shows the time evolution of the distance of the oxygen radical to the N5 atom of the $FDH^{-\cdot}$

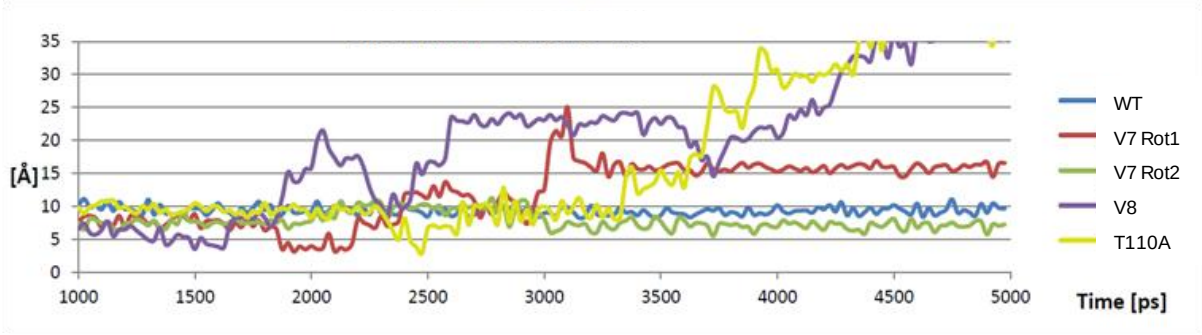

Figure 3-11: Time evolution of the oxygen radical to the N5 atom of the FAD over 5 nS. Data provided by the subgroup for computational biology, Marco Bocola.

Figure 3-10 shows that the distance of the oxygen to the cofactor is increasing drastically for V8 and T110A after 3.5 ns and that the oxygen is leaving the active site. The oxygen is also leaving the active site for V7 rotamer 1, but for rotamer 2 the oxygen remains in a close vicinity to the FAD similar to what is observed for the WT. The reduced capability to stabilize oxygen might explain the experimental data received for V7 and V8.

3.3.5.3 The surface residues A137 and A173

Additional to the two active site residues F414 and V560 the three surface residues A137, A173 and A332S were identified as “hot spots”. Substitutions in all three surface residues resulted in an increase in the activity of GOx for oxygen and for the mediator activity (see chapter 3.1.4 and 3.1.6), whereby only A332 is located close to substrate entrance channel. Analysis of the internal cavities of GOx in the published X-ray structure [53] proposed an additional channel from active site towards the residues A137 and A173 on the surface as an alternative entry / exit route for oxygen, hydrogen peroxide and water (Fig. 3-12) [112].

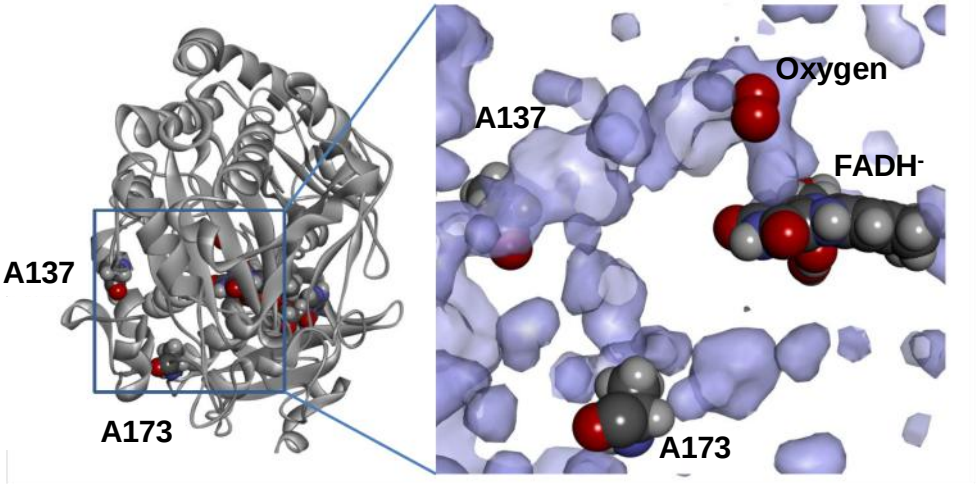

Figure 3-12: Solvent accessible surface representation of GOx. The representation proposes a channel from the active site towards the identified "hot spots" A137 and A173. A137 and A173 were identified during directed evolution of GOx (see chapter 3.1.4 / 3.1.5). Figure modified after A. Bălăceanu 2013 [112].

3.4 Discussion

In enzymatic biosensors, the performance of the enzyme, regarding the biochemical reaction as well as the enzyme stability, are directly linked to the performance of the sensor. Oxygen independency and substrate specificity are two major aspects for the improvement of enzymatic glucose sensors in diabetes care with respect to accuracy and robustness. Furthermore, in test stripe analytics the employed electron mediator needs to meet certain requirements such as storage stability, high electron transfer rates and low unspecific interactions. The goal of the present work was to design an "optimal" GOx for diabetes analytics regarding oxygen independency electron transfer, but also to get a deeper understanding of the enzymatic mechanism. To the best of my knowledge there is to date only one report in which GOx was improved towards reduced oxygen activity employing phenazine methosulfate as electron mediator [41]. Phenazine methosulfate is not employed in diabetes care applications. In this study a quinone diimine/phenylendiamine (QDM) mediator system was used which is successfully employed in diabetes care systems [3].

The present dissertation comprises the establishment of a suitable screening platform to select GOx variants with the desired properties, the directed evolution of the GOx from *A. niger*, the presentation of an enzyme model and the development of a pilot scale GOx production process. The results of each topic will be discussed individually.

3.4.1 Establishment of a screening platform and comparison of two suitable host organisms.

The ultimate goal of the present work was to reduce the oxygen activity of the *A. niger* GOx by simultaneous improvement of the mediator activity. In order to select such variant libraries needed to be screened for both properties, the oxygen activity and the mediator activity. To assess the oxygen activity the well kwon ABTS-assay was employed, the assay served as a control method to rather monitor the oxygen activity than to assess the enzyme performance. The ABTS-assay was already successfully employed in directed evolution campaigns and will not be discussed within this chapter [39].

To select variants which are well suited for the desired application it is important to design a screening assay which works under conditions that are as similar as possible to those of the desired application. Therefore, a quinone diimine/phenylendiamine (QDM) mediator system was selected to screen for variants that exhibit excellent electron transfer rates independent of the presence of oxygen. Quinone diimine/phenylendiamine systems are attributed by low unspecific interactions and a high storage stability in the applied *p*-nitrosoaniline form [3, 68, 69]. The assay conditions were adopted from a protocol provided by the cooperation partner (Roche) to a 220 µL scale in 96-well plates. The initial concentration of the mediator pre-compound N,N-bis(2-hydroxyethyl)-4-nitrosoaniline was set to 8.7 mM in the assay, a concentration which is close to the concentration that is needed for the test stripe application.

The comparison of the two different *S. cerevisiae* strains *Sc*. INV and *Sc*. *ngd29* showed that only the mediator activity of GOx expressed in *Sc*. *ng29* can be detected employing the QDM-1 detection system. A clear and linear reaction rate was observed after an initial lag-phase and the reaction rate was significantly different to the assay background detected with the negative control strain (Fig. 3-3). The initial lag phase of the QDM-1 assay might be attributed to the conversion of the *p*-nitrosoaniline to the active mediator component (chinondiimine). This initial activation of the *p*-nitrosoaniline by GOx is always necessary at the beginning of the reaction since the corresponding chinondiimine is not storage stable – no electrons can be transferred from the redox centre of the GOx during the mediator activation. It was

not possible to distinguish between the negative control strain and GOx expressing strain of the commercial available *Sc*. INV. This can be traced back to a higher assay background produced by the *Sc*. INV itself and also to lower detectable activities compared to the *Sc*. *ngd29* (Fig 3-3). The lower GOx activity in the supernatants of the *Sc*. INV can be attributed to lower expressions rates and also to a sterically blocked substrate availability due to the a high occupation of the GOx surface with carbohydrates since the carbohydrate content can be 10 -16 % for GOx's expressed in organisms providing a N-glycosylation structure of $[Man_n][GlcNAC_2]$.

In order to establish a reliable and easy screening system an auto-induction cultivation strategy was developed by testing different cultivation times in combination with either different glucose/galactose - or different glucose/maltose concentrations (Fig. 3-4). The figure shows that 72 h is the preferable cultivation time for all tested combinations. This result comes from the balance between the initial cell growth on glucose and subsequent expression of the recombinant GOx. The expression of the GOx is in the selected expression system controlled by the *Gal1*-promoter for which it is assumed that the gene transcription is induced in case of β-D-glucose limitation and the presence of D(+)-galactose [113, 114]. The better GOx activity after the longer cultivation indicates that either residual glucose was available after 48 h, attributing a lower cell density combined with a weak expression, or that a longer expression phase leads to the formation of more GOx over the time. The fact that also the approaches with less glucose (0.5 % instead of 1 %) lead to a better result supports the hypothesis that after 48 h of cultivation the residual concentration of glucose in the cultivation media was still too high. It can be concluded from the results that the ratio of glucose concentration to cultivation time is a crucial aspect in the development of an auto-induction media employing the selected expression system. The comparison of galactose and maltose as inducers showed the expected results with a clear preference to galactose. The best conditions with respect to the GOx activity in the screening assay was 0.5 % glucose in combination with 2 % galactose over the cultivation time of 72 h.

The final QDM-1 screening system was assessed with respect to the standard deviation over a whole 96-well screening plate in order to state the accuracy and suitability of the assay. The determined standard deviation of the mediator assay of 10.2 % with a linear detection range from 1 to 25 U/L makes the QDM-1 detection system to an excellent assy in 96-well plate format. Screening systems with standard

deviations below 20 % have often successfully been employed in directed enzyme evolution experiments [93, 108, 109].

3.4.2 Reduction of the oxygen sensitivity and improvement of mediator activity

A measure for the oxygen independency of GOx variants is the ratio mediator to oxygen activity termed as OI-ratio (Oxygen-Independent GOx ratio) in the whole thesis.

Two iterative cycles of directed evolution were executed, one with SeSaM (cycle 1) and one with epPCR (cycle 2). Two beneficial positions were identified in cycle one (A173, A332) and two in cycle two (F414, V560), substitutions in those positions affect either oxygen sensitivity, mediator activity or even both. Figure 3-13 shows an overview of the location of all four residues in the GOx (1cf3) x-ray structure [53, 67].

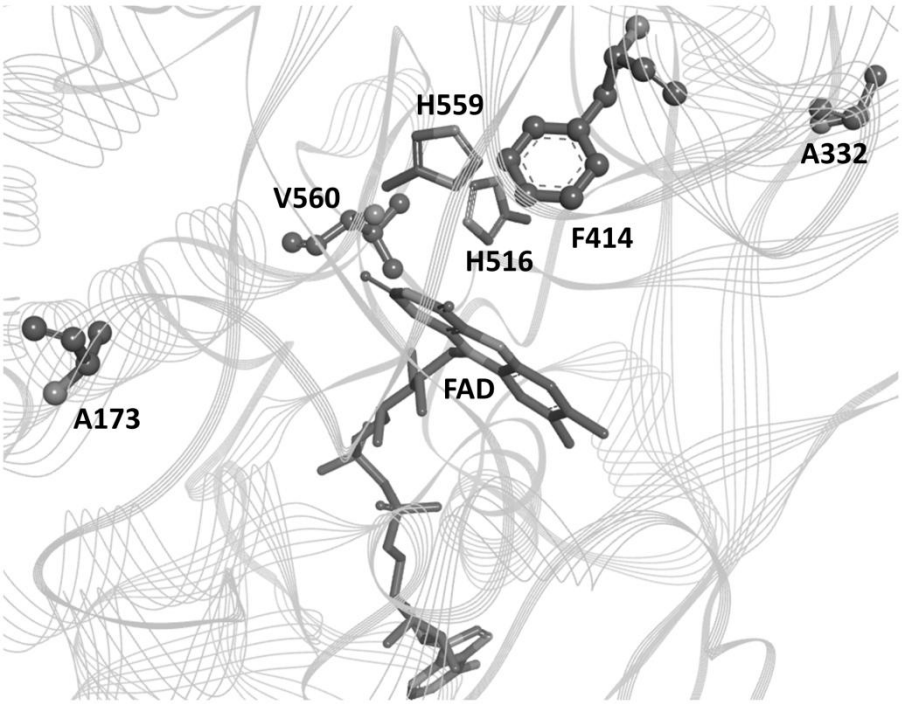

Figure 3-13: Ribbon representation of GOx from *A. niger* based on the x-ray structure 1cf3 [53]. F414, V560, A173, and A332 are identified “Hot-spots” for high mediator activity and reduced oxygen activity after two rounds of directed GOx evolution. H516 and H559 are highlighted as catalytic active residues along with FAD in the active site. Ribbon representation was prepared using the Discovery Studio software package [55]. Figure after E. Arango et al., 2013 [67].

A173 is located at the surface of the GOx, 14.8 Å away from the FAD and catalytic histidines. A332 is also a surface residue, located close to the substrate entrance

channel with a distance of 14.6 Å to the flavin isoalloxazine. F414 it is located 8.2 Å above the FAD in the substrate binding pocket and V560 neighbors the active site residues H516 and H559 [57].

Two focused site saturation approaches (individual site saturation with QuikChange; simultaneous site saturation with OmniChange) were implemented to asses each of the identified hot spots and in order to create an “ideal” GOx.

Since two of the identified residues are in close vicinity of the active site (414, 560) and two within 14.8 Å of the FAD (173, 332) cooperative effects seemed to be likely. Therefore, the simultaneous site saturation mutagenesis with OmniChange was performed including all four positions (137, 332, 414, 560). The simultaneous site saturation approach delivered V7, a variant which exhibits an approximately 2.5 times higher OI-ratio than the best variant obtained from the random mutagenesis libraries (data not shown). V7 shows a 6.4-fold increase in specific activity with the quinone diimine mediator (WT: 7.4 U/mg; EZ07: 47.5 U/mg) and a 5.7-fold reduced activity with oxygen (WT: 172.3 U/mg; EZ07: 30.12 U/mg) resulting in a 37-fold reduced oxygen dependency (OI-ratio). The only reported GOx from *A. niger* which was engineered for reduced oxygen sensitivity was the GOx-T110A with a 6-fold reduced oxygen dependency [41].

The goal of the individual site saturation experiment was to elucidate the specific impact of each identified residue on the oxygen sensitivity and the mediator activity. Substitutions of the two surface positions A173 and A332 showed to increase the mediator- as well as the oxygen activity (up to 3-fold; Tab 3-1). A substitution to the aliphatic and non polar alanine was the most favorable for both positions. The substitutions to threonine, a polar and hydrophilic residue, showed the similar effect for position 332. A173 is located at the surface of the GOx and 14.8 Å away from the FAD, a computational analysis of the inner cavity of the GOx suggest the existence of a channel from the active site towards this residue (see chapter 3.1.7.3). This channel maybe provides an alternative entry / exit route for oxygen and hydrogen peroxide as one possible explanation of the influence by residue 173. A332 is located at the substrate entrance channel with a distance of 14.6 Å to the flavin isoalloxazine. Substitutions from alanine to more polar residues such as serine (V7) or asparagine might support an easier entering of channel by the oxygen molecule. The exact contributions of the individual substitutions and how the best performing variants (A173V and A332V, individual site saturation) improve mediator activity and oxygen

activity remains to be studied by in-depth computational and structural analysis. Position F414 is responsible for increased mediator activity by substitutions from F to M, V, L or I. F414 it is located 8.2 Å above the FAD (Figure 2) in the substrate binding pocket and involved in the β-D-glucose binding [57]. After gluconolactone formation and dissociation from the active site [57], an oxygen molecule or a mediator acts as electron acceptor from the reduced cofactor $FADH_2$. The substitutions from F to aliphatic M, V, L or I indicate that a change in flexibility and size of the side chain is mainly contributing to an increased mediator activity. The location of the position 414 suggests the hypothesis that the QDM (quinone diimine mediator) can directly bind in the binding pocket to reoxidize $FADH_2$ efficiently. The latter hypothesis is supported by molecular docking results (4.3.3) in which the quinone diimine mediator compound binds directly in the active site, in close vicinity to residue F414 and the FAD. The binding efficiency (mediator affinity) and the associated electron transfer rate is thereby very likely depending on the mediator chemistry, the mediator size and the amino acid side chains surrounding the binding pocket. The latter renders it likely that improved mediator activities are dependent on the identified amino acid substitutions and specific for the employed mediator system. The further studies with the QDM are discussed in chapter 4.

The position V560 is most important for “oxygen sensitivity” and substitutions to L, P or T drastically reduce oxygen activity. V560 neighbors the active site residues H516 and H559 which are involved in shuttling of protons from $FADH_2$ to oxygen. Replacement of V by T can perturb the catalytic hydrogen-bond network (FAD, H559, H516, E412) due to an additional hydroxyl group (V560T). Replacement of V560 by L or P might alter the orientation of the neighboring catalytic residue H559. Therefore the oxygen activation and binding between FAD and His 559 is perturbed by substitutions in position 560.

A Computational analysis was investigated in order to assess the function of V7 and built a model for oxygen independent GOx. Comparison of the molecular surfaces revealed that only the WT has an opening to a pocket close to the active site which stabilizes oxygen in a reactive conformation close to the cofactor FAD. This pocket was not accessible in any of the studied variants (see chapter 3.3.5.2). A first conclusion was drawn in which the reduced oxygen activity of the variants V7, V8 and T110A is traced back to e reduced capability to bind oxygen in a reactive position. Furthermore, two different rotamers were found for V7. One of those opens

a new pocket which is able to stabilize oxygen, while the other doesn't. The existence of two rotamers might explain the residual oxygen activity of V7. The latter two results were proven by molecular dynamic simulations. The time evolution of the distance of the oxygen radical to the N5 atom of the FAD showed that in case of V7 rotamer one (without oxygen binding pocket) , V8 and T110A the oxygen is not only leaving the reactive position within the active site, but the enzyme completely (Fig 3-11). A. Bălăceanu [112] showed in a structural comparison of WT and V8 that the accessibility of the oxygen stabilizing pocket in the WT can be controlled by changing the orientation of the H559 in the active site. The computational analysis clearly demonstrated that substitutions of V560 change the capability of GOx to stabilize oxygen in the active site what leads, like in case of V7 and V8, to drastically reduced oxygen activity without altering the enzyme stability or specificity.

3.4.3 Further improvement of GOx towards increased catalytic activity

Two further residues, A137 and S53, were investigated with respect to GOx activity. A137 was identified in the first two rounds of directed evolution in the combination A137S + A173T and S53 was identified in the third round of directed evolution as the combination S53F+ A332S (see chapter 3.4). Individual site saturation experiments of both residues resulted in the two single substitutions A137L and S53F as the best variants (A137L: 5-fold activity improvement compared to T30VI94V; S53F: 2-fold activity improvement compared to T30VI94V). None of the two substitutions altered the oxygen sensitivity of GOx. Furthermore, it was shown that the addition of the two substitutions to V7 increase the mediator activity without changing the oxygen activity of V7 what leads to a further increase of the OI-ratio of V7 (a detailed characterization was not executed).

Position 137 is a surface position and is located at the exit of a channel which is formed from the active site (Figure 3-11). As it was already described for A173 (see chapter 4.2) this channel might offer an alternative entry / exit route for oxygen and hydrogen peroxide. The mechanism of influence of substitutions from alanine to leucine still needs to be investigated in further studies. S53 is also a surface position, but is located on the dimer interface and might be involved in the stabilization of the dimer.

3.4.4. Oxygen independent GOx's in industry – The Impact on diabetes analytics

Common glucose meters in diabetes analytics are based on electrochemical biosensors employing GDH's or GOx's for molecular glucose recognition (see chapter 1 and 1.4). Certain requirements need to be fulfilled in order to ensure a specific, accurate and stable glucose monitoring:

- High glucose specificity
- Oxygen independency
- Interference free electron shuttling
- Enzyme and mediator stability.

High glucose specificity can be ensured by the use of GOx's whereby for oxygen independent systems GDH's are used (see also chapter 1) [3, 9]. However, both enzymes exhibit good stability properties. Quinone diimine electron mediator (QDM) systems are often employed in diabetes analytics and ensure a specific electron shuttling between the enzyme and a counter electrode. QDM systems attribute low unspecific interactions with blood components and an excellent storage stability in form of N-substituted *p*-nitrosoanilins (see chapter 1.4.1).

The main challenge in glucose monitoring is the development of sensors which combine a high β-D-glucose specificity with an oxygen independent electron transfer. On one hand, GDH's are oxygen independent but exhibit residual activities on various sugars. On the other hand, GOx's are highly specific for β-D-glucose but naturally accept oxygen as electron acceptor substrate. Therefore, the right enzyme system needs to be selected in specific clinical application like during icodextrin application or during intensive care (see also chapter 1).

The reengineered GOx V7 offers an oxygen independent alternative to WT GOx. V7 is able to specifically detect β-D-glucose and to transfer electrons to a counter electrode without significant oxygen interference. Furthermore, V7 interacts on a high level with quinone diimine based mediators. With V7 it is first time possible to develop a glucose sensor which is absolutely specific for glucose, insensitive to blood components and can be applied at high oxygen levels. This allows accurate glucose monitoring under all the clinical conditions. Furthermore, V7 based sensors can also be applied in bio-engineering for the glucose determination in cell cultures,

independent from the oxygen contentment and the presence of other sugars. These insights will inspire researchers to reengineer GOx's and other oxidoreductases for diagnostics and to develop implantable bio-fuel cells.

4. Investigation of mediator binding and further GOx optimization

4.1 Purpose

An intensive research on enzymatic glucose sensors took place with focus on the direct electrochemical communication between the enzyme and a signal transducer, ever since the first enzyme entrapped biosensor was introduced by Clark and Lyons in 1962 [115]. A great number of research reports are available to improve the electro chemical communication between the enzyme and the transducer component which can be divided in material science and protein engineering. The material science is focused on the modification of the enzyme-electrode interface and it has been shown that electrode modifications with for instance multi-walled carbon nanotubes or conductive polymers can significantly improve the electron transfer kinetics [116, 117] [118]. Protein engineering aims to optimize the enzyme towards specific needs and to gain knowledge about the involved mechanisms on a molecular level. GOx was mostly engineered to improve catalytic activity or enzyme stability [36, 39]. Engineering reports involving mediator compounds to improve the electrochemical communication comprises three reports. The GOx T30V I94V was found in a directed evolution campaign and attributes an increased k_{cat}-value (from 69.5/s to 137.7/s) employing ferrocenemethanol as mediator component [40]. Horaguchi et al. (2012) reported a GOx with an 11-fold decreased oxygen activity found in a rational protein engineering approach [41]. Arango et al. (2013) employed a diabetes care relevant quinone diimine mediator system (N,N-bis[2-hydroxyethyl]-4-nitrosoaniline based) in a directed evolution campaign resulting in GOx-V7 which operates efficiently with the mediator component and exhibits a 37-fold decreased oxygen dependency [67]. The latter report of Arango et al. (2013) is described in detail in the chapter 3 of the present thesis.

A challenge in the improvement of the electrochemical communication of GOx is the deep in the enzyme buried redox center. The mechanism of the electron transfer to the in the enzyme buried redox center is not known to date [57]. Since the enzyme operates naturally in aqueous solution, water soluble low molecular weight compounds such as quinone diimines or hexacyanoferrates are most commonly used in commercial available glucose sensors. GOX V7 was successfully improved for the

N,N-bis[2-hydroxyethyl]-4-nitrosoaniline based mediator system (QDM-1). An alternative quinone diimine mediator system is based on the nitrosoaniline N,N-bis(2-hydroxyethyl)-2-methoxy-4-nitrosoaniline, which features a better solubility in aqueous solutions due to a higher polarity (named as QDM-2 in the whole thesis). The mediators were introduced in chapter 1.4.1. Both mediator systems are employed in diabetes care, whereby the higher solubility of QDM-2 is required for certain test stripe applications. Interestingly, GOx-V7 showed a much higher specific activity for QDM-1 compared with QDM-2.

In order to assess the mediator binding mechanism and in order to further develop V7 towards an efficient use of QDM-2, computational studies as well as focused mutagenesis experiments were implemented. The results of the computational analysis were provided by the sub-group for computational biology of the chair for biotechnology (RWTH Aachen University, Dr. Marco Bocola).

4.2 Strategy

In chapter 3.3.2 it was shown that the mediator activity was improved by substitutions in position 414 and was discussed that it is very likely that the mediator binds in close vicinity to residue 414. The results were generated employing the QDM-1 system. The QDM-2 only differs from the QDM-1 by an additional methoxy group in position 3, which leads to a more polar and sterically more demanding mediator component. The difference in the polarity and size between QDM-1 and QDM-2 makes this two mediator systems excellent candidates for the investigation of the mediator activity depending on the side chain chemistry of position 414. Ferrocenemethanol, a further example of a small water soluble mediator was included in the experimental studies as an additional control.

The study for the investigation of the mediator binding and the further GOx optimization included the following activities:

- Side directed mutagenesis of residue 414 to deduce a subset of amino acid residues which improve mediator activity.
- Characterization of a selected GOx variant.
- Molecular docking experiments to obtain a mediator binding model and to investigate the role of residue 414.

- Determination of theoretical electron transfer rates to obtain a quantitative mediator model and to support experimental data.

4.3 Results

4.3.1. Site directed mutagenesis and library screening

The basis for the site directed mutagenesis study was V7 of which residue I414 was identified to play a major role in the mediator binding (see chapter 3.3.2). The QuikChange mutagenesis method was employed for the saturation of position 414. 176 clones were screened employing the three mediator systems QDM-1, QDM-2 and ferrocenemethanol (FM), yielding the four beneficial substitutions I414Y, I414M, I414V, I414L (Table 4-1).

Table 4-1: Residual activities of variants after site saturation of position 414 in V7. Residue 414 was saturated using the QuikChange site directed mutagenesis method. The specific activities for four variants and references were determined in the respective mediator assays (2 M β-D-glucose; 8.9 mM QDM-1 / QDM-2 / FM). QDM-1/2: quinone diimine mediator 1/2; FM: ferrocenemethanol.

	Residual activity [%]		
	QDM-1	QDM-2	FM
V7	100.0±1.4	100.0±12.7	100.0±2.3
WT	21.3±0.5	n.d	72.0±0.7
V7-I141Y	52.4±1.6	813.9±54.2	108.8±7.2
V7-I414M	9.8±0.5	627.6±39.3	53.1±10.7
V7-I414L	15.3±0.5	230.6±15.1	40.1±3.1
V7-I414V	9.7±0.4	328.8±24.2	24.5±2.5

V7-I414Y showed a significant improvement for the more polar mediator QDM-2 (814 % residual activity compared to V7) whereas the activity for QDM-1 decreased by almost 50% (V7: 49 U/mg; V7-I414Y: 26 U/mg). The FM activity for V7-I414Y remained close to V7 activity. V7-I414M was also improved for QDM-2 (628 % compared to V7) but showed only 9.8 % residual activity for QDM-1 and an around 50% decreased activity for FM (compared to V7). A similar behavior was shown for V7-I414L and V7-I414V which are moderate improved for QDM-2 and decreased for QDM-1 and FM. V7-I414Y showed the highest improvement for the QDM-2 and

retains activity for FM. Therefore, V7-I414Y was selected for a detailed kinetic characterization.

4.3.2 Kinetic characterization of V7-I414Y, V7 and WT

GOx WT, V7 and V7-I414Y were expressed in *S. cerevsiae* ngd29 and subsequently purified. Purification and specific GOx quantification (employing ELISA) were executed as described in the material and method section. Enzyme reaction kinetics were recorded employing the QDM and FM assay (227.3 mM β-d-glucose) for 0-16.6 mM QDM-1/2 and 0-10.9 mM FM. The enzymatic QDM-1 and QDM-2 conversions do not follow typical enzymatic Michaelis-Menten kinetics but showed an individual lag phase at low mediator concentrations due to the enzymatic pre-activation of the quinone diimine (from the corresponding *p*-nitrosoaniline) and the complex mediator chemistry. Furthermore, a saturation of GOx with the mediator compound could not be reached in some cases due to a limited solubility of the mediator in aqueous environment. Therefore, the kinetics were not analyzed according to a kinetic model, but the kinetic progressions were discussed qualitatively and the specific activities at certain mediator concentrations were compared.

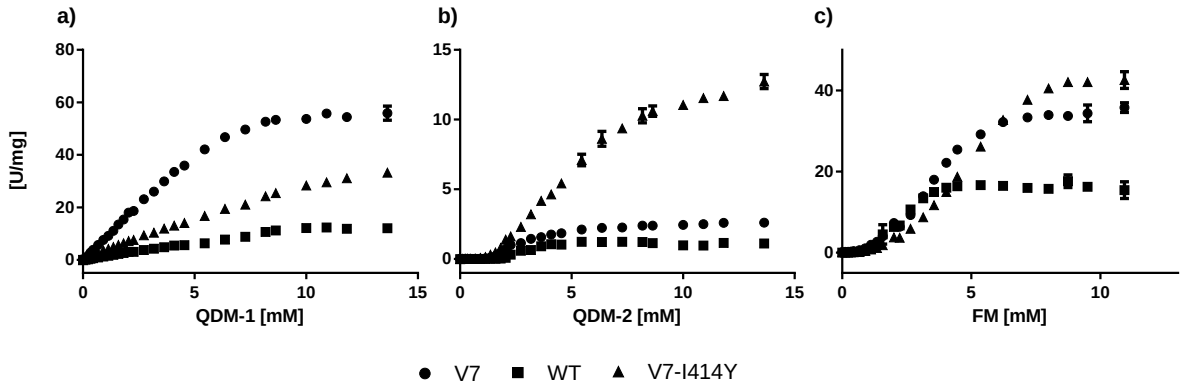

Figure 4-1: Kinetic progressions of V7, WT and V7-I414Y for the mediators QDM-1 (a), QDM-2 (b) and FM (c). The enzymatic kinetics were recorded at a fixed β-D-glucose concentration of 227 mM and for different mediator concentrations (QDM-1/2: 0 – 13.6 mM; FM: 0 – 10.9 mM).

Figure 4-1-a) shows that V7 (for QDM-1 evolved) reaches the highest activity for QDM-1. At 13.6 mM QDM-1 the activity of V7 is 1.7 fold higher than of V7-I414Y and 4.7 fold higher than of WT (V7: 55.9±1.6 U/mg; V7-I414Y: 33.2±0.4 U/mg; WT: 12.0±0.1 U/mg). The saturation of V7-I414Y was not reached at 13.6 mM QDM-1 and

the progression of the kinetic indicates a low affinity of QDM-1 to V7-I414Y in compare to V7. The best performance for QDM-2 shows, with respect to activity and mediator affinity, V7-I414Y. The activity of V7-I414Y is at 13.6 mM QDM-2 4.8 fold higher than of V7 and 11.7 fold higher than of WT (V7: 2.7±0.1 U/mg; V7-I414Y: 12.9±0.3 U/mg; WT: 1.1±0.6 U/mg). V7 and V7-I414Y show a similar behavior for FM, a slight difference can only detected in the saturation phase. GOx-WT seems to reach an inhibition after 3.6 mM FM. Nevertheless, V7-I414Y reached the highest activity for FM with 41.2±0.5 U/mg in compare to V7 with 35.8±0.2 U/mg and WT with 13.5±0.1 U/mg at 10.9 mM FM.

4.3.3 Mediator binding

Molecular docking experiments were performed in order to elucidate the effect of substitutions in position 414 on the activity in the mediator assays. There is no previous prove of the mediator binding in the active site of the GOx or elsewhere. It is known that GOx can also interact with mediators of a size that the mediator cannot fit into the active site pocket and the electrons have to take long-range transfer routes through the enzyme [116, 117] [118]. Such electron transfer routes through GOx have been proposed [57] and therefore a simulation box of 50x50x50 Å, enclosing the complete GOx surface, has been employed in the first molecular docking stage with respect to all possible binding modes on the surface and the inner cavities of the enzyme. The mediator force field preparation and docking performance is described elsewhere [112]. The best binding energies for the applied mediators (QDM-1 and QDM2 as the corresponding quinone diimines) were found in the active site cavity. Additional dockings were performed for all variants with a simulation box of 25x25x25 Å centered in the active site. Figure 4-2 shows the considered binding mode on the examples of QDM-1 in V7 and QDM-2 in V7 I141Y.

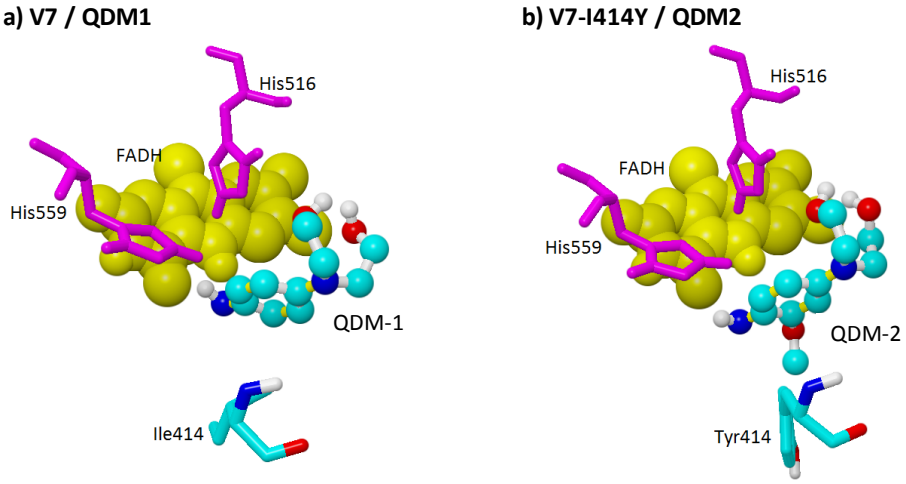

Figure 4-2: Docking poses of QD-mediators in the active site of GOx. a) Active site setup of V7 in combination with QDM-1; b) V7 –I414Y in combination with QDM-2 (ball and stick representation). Figure after A. Bălăceanu 2013 [112].

Figure 4-2 shows that the QM-mediators bind in the active site in distances of approximately 3.5 Å from the N5 atom of the FAD and in a very close vicinity to the residue of interest in position 414. The GOx-mediator complexes were neutralized, solvated in water and energy minimized [112]. These starting structures were subjected to molecular dynamics simulations over 5 ns. Table 4-2 shows the average force field energies of the mediators in the active site obtained from the MD-simulations.

Table 4-2: Average energies of QDM-1 and 2 in GOx WT, V7 and V7-I414Y over 5 ns [112].

	QDM-1			QDM2		
	WT	V7	V7-I414Y	WT	V7	V7-I414Y
Energy [kJ/mol]	104.7	105,2	109.3	161.7	165.3	153.0

The average energy of the QDM-2 is with 153 kJ/mol for V7-I414Y significant lower than for WT and V7, what is in qualitative accordance with the experimental results. For QDM-1 an opposite trend is observed, WT and V7 perform equally and V7-I414Y shows a bad energy. In the experimental results V7 shows significant higher catalytic activities with the QDM-1 than with the QDM-2. Since the differences in the catalysis cannot be explained quantitatively by assessing only the mediator energies, theoretical electron transfer rates (ETR) using the Markus theory were calculated.

The ETR calculations estimate the reorganization energy upon instantaneous electron transfer dependent on the distance and coupling to $FADH^-$. Tab. 4-3 summarizes the calculated ETR's for WT, V7 and V7-I414Y in combination with QDM-1 and QDM-2.

Table 4-3: Calculated electron transfer rates for WT, V7 and V7-I414Y in combination with QDM-1 and QDM-2 [112].

	QDM-1			QDM2		
	WT	V7	V7-I414Y	WT	V7	V7-I414Y
ETR	0.15	0.32	0.28	0.04	0.13	0.25

As expected, the WT shows the lowest ETR for both of the mediators. For V7 the ETR is significantly higher for QDM-1 than for QDM-2 what is also in good accordance with data from the catalysis. Similar ETR were recorded for V7-I414Y for both mediators, what is also going hand in hand with experimental data with respect to specific activities (see chapter 4.3.2).

4.4 Discussion

The electrochemical communication between the redox center of GOx and electrode systems are of high interest not only for glucose sensing but also for bio-fuel cells. While the electron transfer in biofuel cells does not necessarily need to be very specific. However, in glucose sensing a highly specific electron shuttling between the redox center and the transducer of the sensor is absolutely mandatory to ensure an accurate glucose determination. For GOx it has been shown that electrons can be accepted by large mediators like polymers or multi-walled carbon nanotubes (which cannot enter the active site) and by small water soluble compounds like ferrocene or quinone diimine derivates (which can enter the active site) [64] [3] [116, 117] [118]. There are proposals for electron travel routes through the enzyme (from the active site to the surface) and there is a report in which surface substitutions over the whole enzyme showed an increase of a direct electron transfer [57] [96]. However, a specific binding mode of a mediator component in the redox center or on the surface of GOx was never shown. Furthermore, it has never been shown that the mediated electron shuttling can be adjusted for a specific mediator by single amino acid substitutions.

In the previous chapter of this thesis it was shown that substitutions of reside 414 allow the improvement of the mediator activity employing a quinone diimine mediator which is based on the nitrosoaniline N,N-bis[2-hydroxyethyl]-4-nitrosoaniline (see Tab. 3-1). In the extension of the study we could even show that a change in the chemistry of the residue 414 led to a change in the preference of polarity and size of the mediator. So was the activity for the more polar QDM-2 improved through the substitutions I414Y, I414M, I414L and I414V in V7 (see Tab. 4-1). Interestingly, the same substitutions caused drastic decrease in the mediator activity with the less polar QDM-1. Ferrocenemethanol (FM) was employed as control for a small molecular weight mediator and the substitutions I414M, I414L, I414V also significantly decreased the mediator activity, similar to the results of the QDM-1 (see Tab. 4-1). The results indicate that the mediator activity is directly influenced by residue 414.

Since the biggest difference was found between QDM-1 and QDM-2 though the substitution I414Y, the variant V7-I414Y was produced in a 10 L fermentation scale, purified and subsequently subjected to a characterization by kinetic analysis. The specific activities showed that the highest turnovers are still reached by V7 in combination with the QDM-1. However the activity of V7 was increased by 4.8 fold for QDM-2 through the substitution I414Y. This variant V7-I414Y shows a drop in activity for the QDM-1 from 56 to 33 U/mg. The enzymatic kinetic clearly indicates a loss in affinity for the mediator QDM-1 through the substitution I414Y. In this specific case it seems that the more polar mediator QDM-2 prefers the more polar residue tyrosine rather than the aliphatic, non-polar isoleucine. However, the effect by residue 414 cannot be narrowed down to polarity since the aliphatic methionine and leucine and valine show similar effects than thyrosine. Conformational changes need therefore also be considered.

Molecular docking studies elucidated that the QDM-1 and the QDM-2 bind preferable directly in the active site of GOx 3.5 Å away from the N5 atom of the FAD and in direct vicinity to residue 414. A clear distinction between the mediators and the different variants was not possible but it was first time shown that small molecular weight mediators bind directly in the active site. The direct vicinity of the mediator binding site to the residue 414 allows the conclusion, that the substitutions in position 414 influence directly the mediator binding.

The theoretical electron transfer rates were calculated according to the Marcus-Theorie and were in good accordance with the catalytic data received during variant characterization (see Tab. 4-3). A. Bălăceanu 2013 [112] concluded that small fluctuations in the reorganizational energy term lied to significant changes of the reaction rates. The reorganizational energy term describes in the Marcus theory the re-structuring of the molecules and the surrounding environment ahead of the actual electron transfer. Substitutions of the residue 414 could reorganize the active site to minimize molecular reorganization during charge transfer and ensure thereby a more effective electron transfer with QDM mediators.

5. Bio-process development

5.1 Purpose

A prerequisite for a successful directed evolution campaign is the availability of suitable up- and downstream protocols for the respective protein in order to characterize and compare variants in detail. The bioprocess development often turns out to be a challenge in directed protein evolution due to altered protein properties such as surface chemistry, structural properties or functional properties.

GOx is widely used in industry and several host organisms are described for recombinant GOx production [119-124]. Within the present directed evolution campaign the glyco-engineered *S. cerevisae* strain *ngd29* (see chapter 1.6) was selected in order to ensure the production of homogeneous GOx molecules by the reduction of the high-mannose N-glycosylation of $[Man]_n[GlcNac]_2$ to a uniform structure of $[Man]_8[GlcNAC_2]$. The *ngd29* mutant in fact leads to a uniform N-glycosylation pattern but the cells also suffer from a changed cell wall morphology combined with slow growth rates. Furthermore, no fermentation protocols are published for the *S. cerevisiae ngd29* strain and no purification protocols for hypo-glycosylated GOx are available.

An establishment and an optimization of up- and downstream protocols took place in order to produce GOx in a sufficient quantity and quality for detailed enzyme characterizations. Parts of the process establishment were accomplished and published within the master thesis of Meena Reit [125].

5.2 Strategy

For the production of several GOx-variants and controls simple and fast protocols should be established. To reach the goal in a certain time frame existing protocols were consulted and supportively used to meet predefined objectives. The strategy for the development of the up-stream protocol can roughly be divided in the three following activities:

- Media screening
- Investigations for possible feeding strategies

- Process characterization

The establishment of the downstream process was based on the process described in the dissertation of Ziwei Zhu [43]. The process development included the following steps:

- Establishment of an primary separation step by Cross-Flow-Filtration (micro-filtration)
- Establishment of an ultra- / dia-filtration step by Cross-Flow-Filtration (ultra-filtration)
- Investigation of hydroxyapatite as potential chromatography resin (data not shown) [125]
- Optimization of a Anion-exchange chromatography as the major purification step

5.3 Results

5.3.1 Up-stream processing

5.3.1.1 Media-screening

Three yeast cultivation media were selected for comparison. The complex YPD-media, the semi-synthetic SC-U media and a full synthetic media called SynY (for media compositions see material and methods). The YPD media is probably one of the most common yeast media used in molecular biology and also finds its application in industrial processes [126]. SC-U media is based on the yeast nitrogen base media and was described to be suitable for the *S. cerevisiae* strain from Invitogen (*SC*. INV) [127]. The SynY media is fully synthetic and was established based on a published protocol [128].

For the comparison of the selected media *S. cerevisiae* was cultivated in small-scale batch fermentations and the produced bio-mass (OD_{600}) and the GOx-activity (ΔE/h, QDM-1detection system) were used for the assessment of the different media (Figure 5-1). The GOx activity was thereby a measure for the GOx expression.

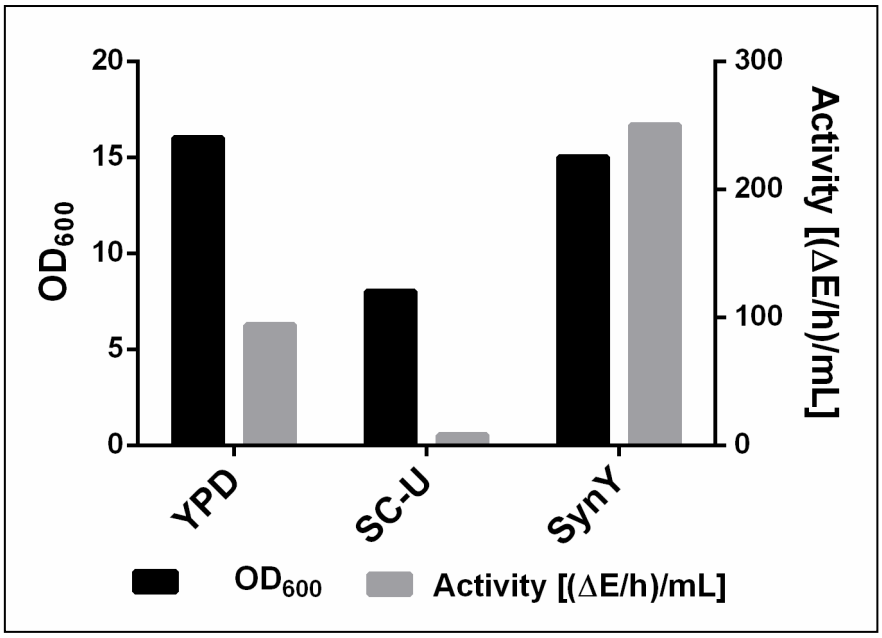

Figure 5- 1: Media comparison in respect to cell growth and GOx-expression. Sc. ngd29/pYES-GOx V7 was cultivated in small scale bioreactors for 48 h in YPD-, SC-U- and SynY-media. The optical density of the cell broth was determined and clarified supernatants were subjected for GOx-activity determination employing the QDM-1 assay. YPD media: yeast extract, peptone, dextrose media; SC-U media: *Saccharomyces cerevisiae* without uracil media; SynY media: synthetic yeast media.

Moderate cell growth was observed with the complex YPD-media (OD600~16) combined with an easy media preparation. Unfortunately the YPD-media exhibits a brownish color which becomes strengthened after cell harvest and which strongly impairs the GOx mediator assay and the ABTS assay (data not shown). The SC-U media does not impair the activity assays but the cell growth was approximately 50 % less (OD600~8) and the GOx expression was significant lower (YPD: 94 (ΔE/h)/mL; SC-U: 8 (ΔE/h)/mL). However, a good cell mass formation and the best GOx expression was observed for the SynY media (OD600~15; 250 (ΔE/h)/mL), which also does not show any brown stain. The SynY media was selected for further investigations accordingly.

5.3.1.2 Feeding strategy

In the selected expression system, the expression of the heterologous GOx gen is controlled by the *GAL1*-promoter which is repressed in the present of β-D-glucose [129]. It is assumed that the gene transcription is induced in case of β-D-glucose limitation and in the present of galactose [113, 114]. For the assessment of the galactose feed two different fermentations were compared. Fermentation one took

place in SynY-media (1% β-D-glucose) without galactose (Fermentation A). Fermentation two took place in YPD-media (1% β-D-glucose) and D(+)-galactose was added after 22 h (3% w/v) and 49 h (1% w/v) (Fermentation B). Figure 5-2 shows the GOx-activity (ΔE/h, QDM-1 assay) as an indicator for the GOx expression for both fermentations.

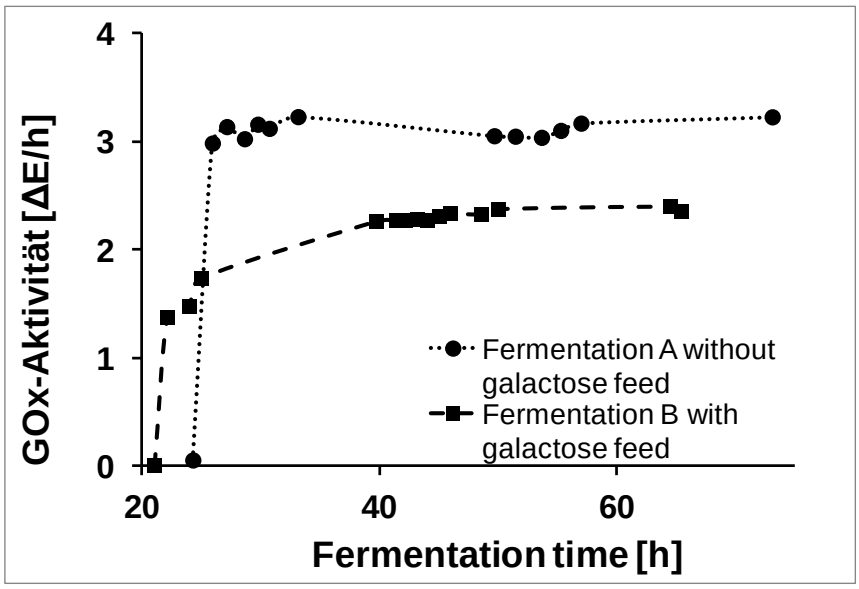

Figure 5-2: GOx expression with and without D(+)-galactose. Sc. *ngd29*/pYES-GOx V7 was cultivated in small scale bioreactors in SynY-media (Fermentation A) and YPD-media (Fermentation B). Fermentation B was supplemented with D(+)-galactose after 22 h (3 % w/v) and after 49 h (1 % w/w). The GOx activity was determined as an indication for the GOx expression (QDM-1 assay).

After 17 h (fermentation without D(+)-galactose) and after 19 h (fermentation with D(+)-galactose) no β-D-glucose was detectable anymore in cell supernatants. As figure 5-2 shows, a strong increase in GOx-activity can be observed in both fermentations (up to 3.2 ΔE/h Fermentation A; up to 2.4 ΔE/h Fermantation B). After a strong initial expression in Fermentation A between fermentation hour 20 and 25 the expression stagnated almost completely. In Fermentation B a slight increase in GOx-activity was observed after the initial expression phase. However, the expression in Fermentation B seems to be independent of from the D(+)-galactose since the initial expression takes place before the first feed and also no significant increase in GOx-activity could be observed after the second D(+)-galactose feed.

β-D-glucose represents the major substrate of GOx. The presence of β-D-glucose in cultivation media which also contains GOx leads to production of hydrogen peroxide what may influence cell growth. Furthermore, β-D-glucose represses the *GAL*1-

ptomotor which controls the expression of GOx in the selected expression system. For those two reasons glycerol was selected to implement an alternative carbon source. The glycerol feeding approach was based on a previous study [130]. To assess the glycerol utilization of *Sc ngd29* two fermentations in SynY-media were executed. 1 % β-D-glucose was present in both fermentations as a growth initiator. In Fermentation-1 glycerol was added controlled by the pH. Therefore, a mixture of 80 % glycerol / 1.5 % ammonia was used as base-feed for regulating the pH in Fermenter-1. In Fermentation-2 the glycerol was replaced by water. Figure 5-3 shows the quantitative glycerol progression as function of the fermentation time (The determination of the glycerol concentration was executed by the "Lehrstuhl für Bioverfahrenstechik" - RWTH AachenUniversity, the method is described elsewhere [125])

.

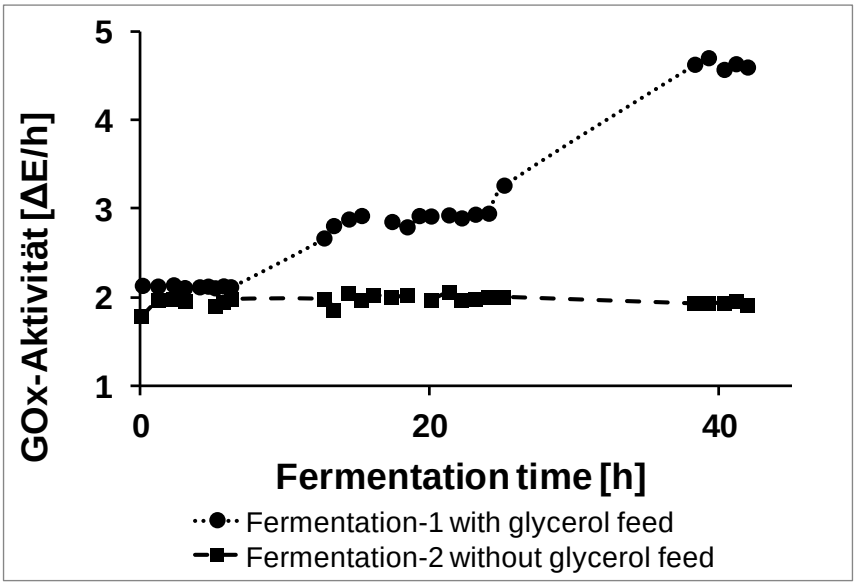

Figure 5-3: Glycerol consumption during fermentation of *Sc ngd29*/pYES-GOx V7. The cultivations took place in small scale bioreactors for 48 h in SynY-media 2% glycerol. The base-feed in Fermentation-1 was supplemented with glycerol (80 % glycerol / 1.5 % ammonia) for a pH controlled glycerol addition. The glycerol concentration was monitored applying HPLC as an indication for the glycerol consumption.

The glycerol concentration in Fermentation-2 remained at approximately 2 % during the entire fermentation, which indicates that no glycerol was metabolized by *Sc* ngd29. In Fermentation-1 an increase of glycerol was observed during fermentation. The observed glycerol concentrations during Fermentation-1 corresponded to the

added amount of glycerol during pH control, which also indicated that *Sc* ngd29 did not metabolize glycerol in the selected fermentation setup.

5.3.1.3 Process characterization

Based on the previous results a final fermentation protocol was implemented. The protocol describes a fermentation process in SynY-media with 1% β-D-glucose and 2 % glycerol over 42 h, the protocol details are described in chapter 2.2.13. For better understanding of the fermentation process a 2 L-characterization run was executed using exhaust gas analysis. The following parameters were used for the fermentation assessment:

- β-D-glucose concentration
- acetate content[1)]
- pO2
- optical density (indicator for cell growth)
- growth rate
- GOx activity (indicator for GOx expression)
- Respiratory quotient (RQ) (indicator for metabolic activity)

1) The determination of the acetate concentration was executed by the "Lehrstuhl für Bioverfahrenstechik" (RWTH AachenUniversity), the method is described elsewhere [125].

The growth rate was calculated based on cell dry mass and the fermentation time according to the following equation:

$$growth\ rate\ \mu = \frac{(\ln X - \ln X_0)}{(t - t_0)}$$

X: *cell dry weight [g/mL] at fermentation time t*

X_0: *cell dry weight [g/mL] at fermentation time t_0*

t: *fermentation time [h], end of the growth phase*

t_0: *fermentation time [h], beginning of the growth phase*

The RQ was calculated based on the O_2 and CO_2 content of the exhaust gas according to the following equation:

$$RQ = \frac{produced\ CO_2}{consumed\ O_2}$$

Figure 5-4 shows the progression of selected fermentation parameters as functions of the fermentation time.

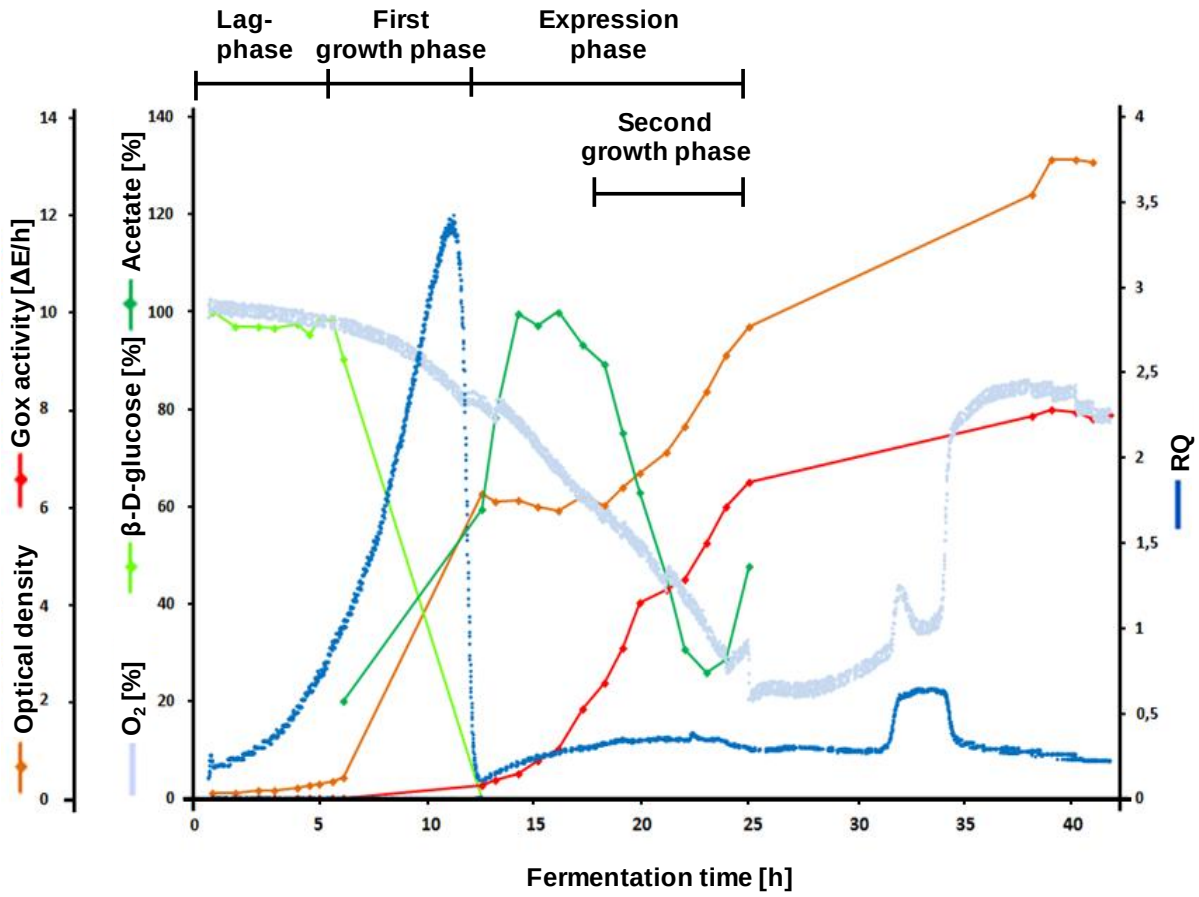

Figure 5-4: Batch-fermentation of the expression system *Sc* ngd29/pYES-GOx V7. The cultivations took place in a small scale bioreactor (2 L) for 48 h in SynY-media 2% glycerol. The fermenter was inoculated by a shaking flask culture (SynY-media) with 5% of the total fermentation volume. The whole cultivation procedure is described in chapter 2.2.13. Online monitoring: pH, pO_2, exhaust gas analysis (O_2 / CO_2); Offline monitoring: GOx activity, optical density, β-D-glucose, acetate, cell dry weight.

As indicated on the top of figure 5-4 the fermentation can be divided in four different phases which will be individually described in the following.

Lag-phase:

During the lag-phase the cells adapted to the new environment, no metabolic activity was detected. During this phase, the GOx expression was repressed by the presence of β-D-glucose.

First growth phase:

Between fermentation hour 6 and 12 the cells consumed the available β-D-glucose and the pO_2 of the fermentation broth dropped significantly. The RQ reached a value of 3.4 which indicates a higher CO_2 production than O_2 consumption, before it dropped to values smaller 1 (after 11 h). In this phase the cells show a typical exponential growth phase with μ=0.4 h^{-1}. The GOs-activity increased only slightly and the cells started to produce acetate.

Expression phase:

Between fermentation hour 12 and 25 a strong increase in the GOx activity was observed reaching a value of 6.5 ΔE/h (QDM-assay). Also the acetate metabolism took place in this phase. The acetate value reached its maximum with 0.33 g/L at around 16 h and started to decrease again afterwards. At acetate concentrations higher than 0.2 g/L the formation of cell mass stopped almost completely (12.7h – 13.4 h). The RQ remained at values smaller 1.

Second growth phase:

After the acetate concentration reached values smaller 0.2 g/L a second cell growth phase with μ=0.07 h^{-1} was observed.

After the second growth phase the cell growth and the product formation stagnated. The metabolic activity also decreased after fermentation hour 25, indicated by an increase of the oxygen content of the fermentation broth.

5.3.2 Down-stream processing

5.3.2.1 Primary separation and ultra / dia-filtration

Initially, the downstream process was adopted for the handling of larger volumes after 10 – 20 L fermentations. Therefore a tangential flow filtration system (TFF) was introduced for concentration of the intermediated after cell harvest and for the buffer exchange before purification (for the principle of TFF and for implementations see materials and methods chapter). A Hydrosart® ultra-filtration cassette (sartorius

stedim biotech) with a membrane area of 0.1 m^2 and a cut-off of 10 kDa was ued. A dia-filtration set up was chosen in which first a concentration step took place, followed by the buffer exchange.

A GOx specific TFF performance optimization took place under the professional supervision of an application specialist (sartorius stedim biotech). Therefore, the permeate flow was optimized dependent on the transmembrane pressure (TMB) (data not shown). In the final setup a TMB of 1.5 bar (1 bar feed pressure, 2 bar retentate pressure) was employed and seven dia-filtration volumes were performed for the buffer exchange.

In the further development the TFF system was also applied for cell harvest (before ultrafiltration) Therefore the cells were retained in the retentate and the GOx containing cell supernatant was collected in the permeate. A microfiltration membrane with a maximum pore size of 0.45 µM and a membrane area of 0.1 m^2 was applied (Hydrosart® 0.45 µm, sartorius stedim siotech).

5.3.2.2 Anion-Exchange Chromatography (AEC)

In Zhu 2006 Anion-Exchange Chromatography (AEC) and Hydrophobic-Interaction Chromatography (HIC) were applied as purification steps after cell separation and buffer exchange. Both separation steps were in a first trial also applied for the purification of GOx-V7 expressed in *Sc ngd29*. The AEC was carried out using a 50 mM sodium phosphate buffer (pH6) for equilibration and washing and 1 M sodium chloride for elution. The GOx-elution fraction from the AEC was complemented with ammonium sulfate (1.5 M) before loading the HIC column. The HIC was carried out with a 50 mM potassium phosphate- / 1.5 M ammonium sulfate buffer (pH 6) for washing and a 1 mM potassium phosphate buffer (pH7) for elution. A linear gradient was applied for elution in both chromatography steps. The execution of the AEC (after optimization) is described in detail in the material and method section. The initial protocol for the AEC and the protocol for the HIC are described elsewhere [43]. Figure 5-5 shows the respective SDS-PAGE's of the collected elution fractions. The fractions for SDS-PAGE analysis were selected by the GOx activity (QDM-1 detection system).

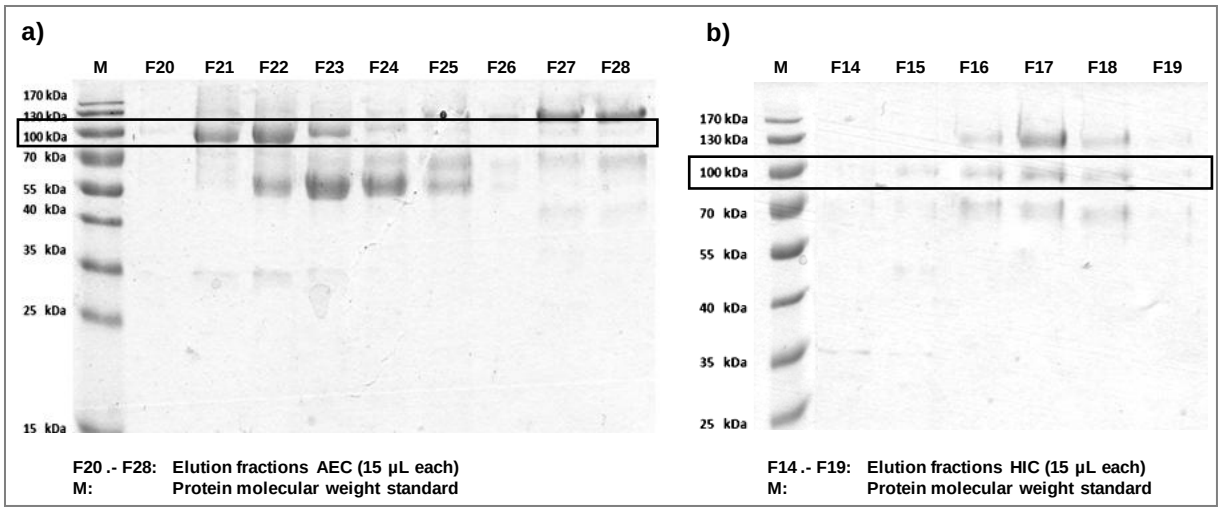

Figure 5-5: SDS-PAGE analysis of GOx containing fractions after AEC and HIC. The GOx containing elution fractions after column chromatography were subjected to SDS-PAGE analysis. The SDS-PAGE was carried out under reducing conditions on a 10% acryl amid gel. The GOx content of the fractions was determined employing the QDM-1 assay (data not shown). a) Elution fractions of the AEC. b) Elution fractions of the HIC. The GOx-band was expected at approximately 100 kDa, black box.

Figure 5-5 a) shows that an enrichment of GOx-V7 took place during AEC (at 100 kDa, black box). However, also a high content of impurities was detected. A significant enrichment of proteins at around 55 kDa and 130 kDa is shown in figure 5-5 a). All fractions (F20 – F28) contained GOx according to the GOx activity assay and were polled for further processing by HIC. The content of the impurities at 55- and 130 kDa were used for the assessment of the HIC performance. As figure 5-5 b) shows, the impurity at 55 kDa could be depleted during HIC. However the unspecific protein at 130 kDa was even more enriched and showed after HIC higher quantities than the GOx fractions. Furthermore a 70 kDa protein band was enriched after HIC.

In order to achieve pure GOx and to establish an efficient and simple purification process, the AEC was optimized with respect to the elution conditions. The AEC was thereby executed like described above since the GOx binding was proven, only the linear elution gradient was replaced by a step gradient. The purpose of this optimization was the determination of the exact wash buffer / elution buffer ratio for a specific GOx elution. In a first approach the design of the elution gradient defined a step wise increase of the elution buffer content by 0.5 % beginning from 0 % until the GOx elution took place. Each step was performed for 1.5 column volumes (CV) (data not shown). In a second approach an optimized step gradient for specific GOx elution was established. Table 5-1 summarizes the elution gradient after optimization.

Table 5-1: GOx elution profile after AEC optimization. The elution gradient of the AEC was optimized towards a specific GOx elution. Wash 1: elution of unspecific proteins; Wash 2: elution of unspecific proteins; Elution of GOx: elution buffer concentration for specific GOx elution; Regeneration: first column regeneration before NaOH treatment.

Amount NaCl (eluition buffer) [%]	Step length (CV)	Purpose
1	1.5	Wash 1
5	3	Wash 2
7.5	1.5	Elution GOx
7.5 - 100	1	Regeneration

Figure 5-6 shows a typical elution profile of the optimized AEC. The chromatogram also includes the GOx activities determined in the respective elution fractions (gray bars). The marked starting points of the gradient step are theoretical calculated considering the death volume from the gradient valve to the column exit.

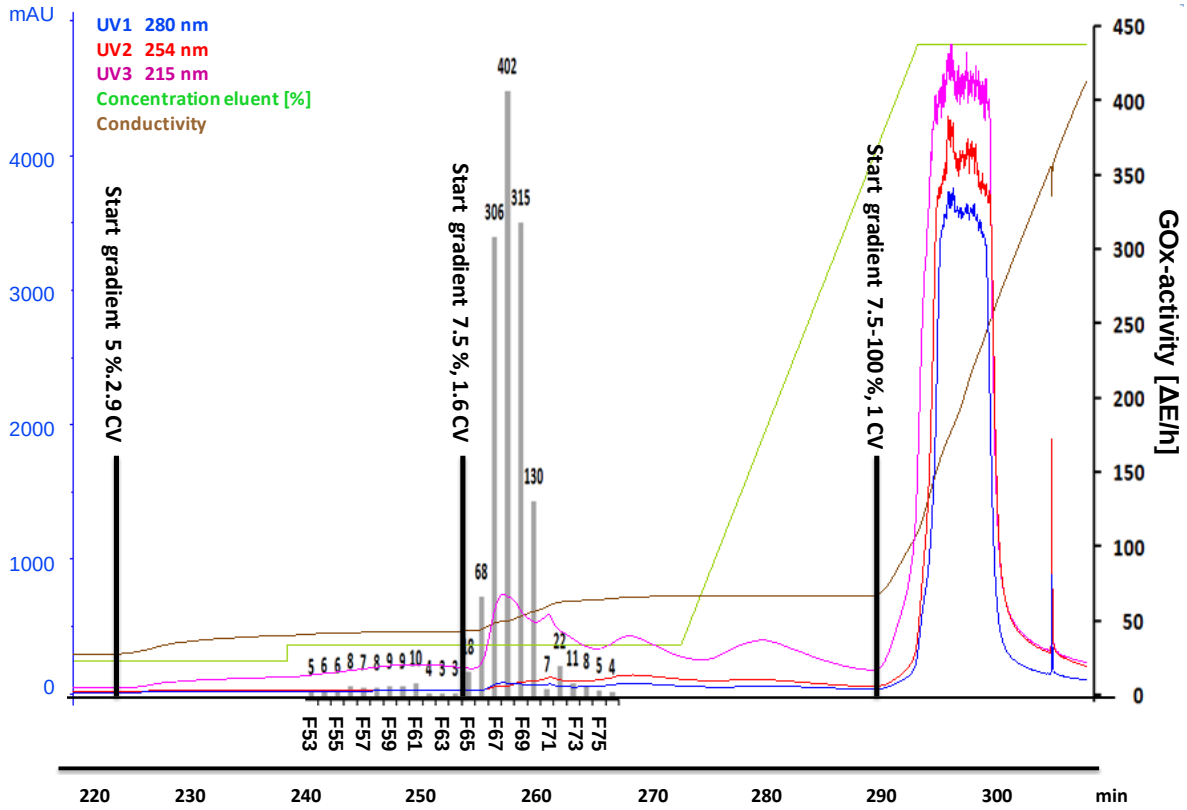

Figure 5-6: AEC elution chromatogram after optimization. The AEC elution gradient was optimized towards a specific GOx elution. The absorbance was monitored at three different wavelengths (215-, 254-, 280 nm). The different gradient steps are marked in the chromatogram (black bars). The GOx activity was determined for all collected fractions and indicated in the graph in [ΔE/h] (gray bars).The final AEC method is described in detail in the material and method section.

Figure 5-6 represents the chromatogram after the first column wash. The absorption at 215 nm started to increase slightly between 220 min and 253 min after the 5% 1 M NaCl gradient reached the column. In these phase mostly impurities were eluted from the column. Between 255min and 265 min the absorption signal shows a double peak with two maximums, one with 900 mAu and one with 800 mAu. The double peak was followed by two broad single peaks. The double peak and the two broad peaks corresponded to the 7.5% 1 M NaCl gradient step. The fractions in which GOx activity was detectable are marked in the chromatogram (grey bars). The fractions of the first maximum of the double showed the highest GOx activity. The fractions with the highest activity were first analyzed by SDS-page (Figure 5-7 a) and afterwards pooled. The pool was concentrated and re-buffered (50 mM K_xPO4, pH7) by ultracentrifugation. The purity of the pool after the optimized AEC step was compared to the purity of the pool after AEC and HIC of the old protocol (Figure 5-7 b).

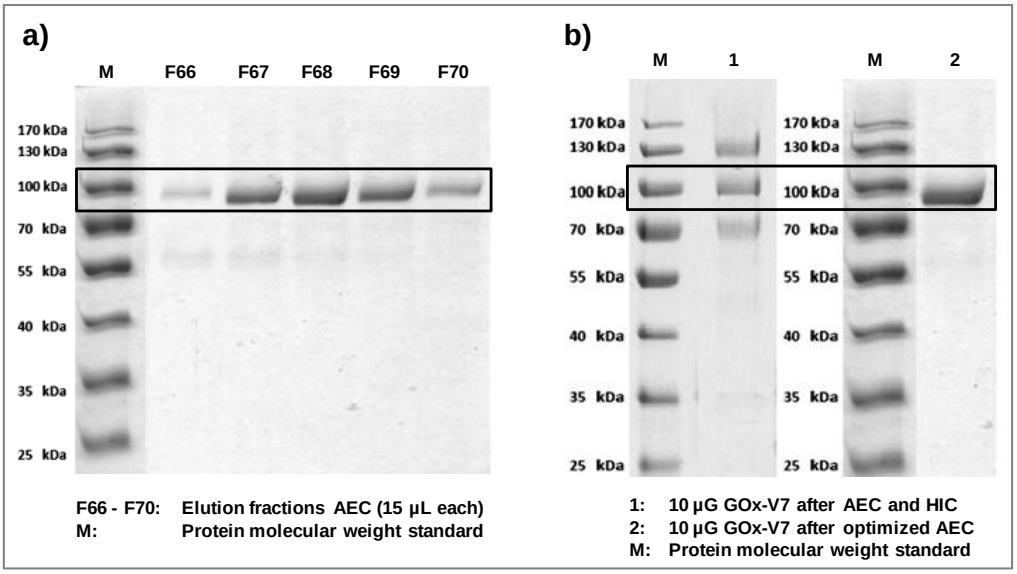

Figure 5-7: SDS-PAGE analysis of GOx containing samples. a) Elution fractions after the optimized AEC with the highest GOx content. b) Pooled elution fractions after the AEC /HIC sequence (old protocol) and after the optimized AEC. The SDS-PAGE was carried out under reducing conditions on a 10% acryl amid gel. The GOx activity of the fractions was determined employing the QDM-1 assay. The GOx content was determined employing a GOx specific ELISA.

Elution fractions 66 - 70 of the optimized AEC exhibit a dominant protein band at around 100 kDa, which are identified as GOx-V7 (Figure 5-7 a, black box). The strongest GOx bands are the ones from fractions 67- 69 what is in accordance with the results presented in the chromatogram (Figure 5-6). Only slight impurities could be identified at around 70- and 55 kDa. To assess the improvement of the AEC in

compare to the two chromatography-step process (AEC / HIC), pooled fractions from both processes were compared (Figure 5-7 b). While the pool of the old two-step process shows significant impurities at 70- and 130 kDa, the pool of the optimized one chromatography-step process exhibits only the GOx as a dominant band and very weak bands at 70- and 55 kDa.

5.4 Discussion

5.4.1 Media screening and feeding strategy

Three different media were tested for the cultivation of the expression strain Sc ngd29/pYES2-GOx, the complex YPD-media, the minimal SC-U media and a synthetic media called SynY. The SynY media is fully synthetic and was established based on a published protocol [128]. The YPD-media showed the best bio-mass formation, followed by the SynY- and the SC-U media in small scale fermentations over 48 h. However, the best product formation was achieved employing the SynY-media (SynY: 250 (ΔE/h)/mL; YPD: 94 (ΔE/h)/mL; SC-U: 8 (ΔE/h)/mL; (ΔE/h)/mL: enzymatic activity as a measure of the product formation). Furthermore, the activity assay for GOx was not influenced by media components after enzyme purification in case of the SynY but in case of the YPD (due to the formation of a dark brown dye – unidentified). The synthetic SynY-media was selected for the further investigations. The media properties regarding the better formation of bio-mass and product might be traced back to the defined composition of the media in which the nutrient composition and concentration is adjusted to the needs of the host organism. Furthermore, the components of the media are available in a pure form and do not need to be cleaved from macro-molecules, what accelerates and simplifies the metabolism of the host organism.

The expression of the GOx gen was under control of the *GAL*1-promoter and the influence of a galactose induction was investigated. The comparison of two different fermentations showed that the addition of galactose to the cell culture does not show a clear influence on the GOx expression. Accordingly, no galactose feed was applied in further fermentations. The *GAL*1 promoter is repressed in the presence of glucose and induced by the presence of galoactose [113, 114]. However, a model for the induction in the absence of galactose was already reported [131]. In the latter report

a model was proposed in which activation by high levels of the GAL1 protein or GAL3 protein does not involve galactose.

Since the *GAL*1 promoter is repressed in the presence of glucose the GOx expression during the cultivation only starts after the initial glucose in the media is almost complete metabolized. Therefore, no additional glucose was added to the culture to ensure the GOx expression after the initial growth phase. To improve the formation of biomass after the initial growth phase and also to increase the GOx yield, glycerol was added to the media as additional carbon source. Glycerol was chosen as a carbon source which does not repress the *GAL*1 promoter and which was already successfully applied for the cultivation of *S. cerevisiae* [130]. With two fermentations over 48 h it was shown that no glycerol was utilized by Sc. *ngd29* under selected conditions (see chapter 5.3.1.2). A diauxic growth was observed during fermentations under the selected conditions employing the host *Sc. ngd29* (see chapter 5.3.1.3). In a diauxic growth the cells always metabolize first the energy richest carbon source, which is glucose. After the utilization of the glucose the cells might prefer ethanol instead of glycerol since it was shown that the achieved growth rates of a *S. cerevisia* strain are higher on ethanol than on glycerol (ethanol: μ_{max}=0.2 h^{-1}; glycerol: μ_{max}=0.01 h^{-1}) [132, 133].

5.4.2 Fermentation analysis

A 2 L fermentation was executed for the assessment of the upstream process. The process could be divided in the four different phases; the lag-phase, the initial growth phase, the expression phase and the second growth phase. Almost no metabolic activity was observed during the lag phase in which the cells adopt to the environment and the GOx expression is repressed through the presence of glucose.

A typical exponential growth was observed between fermentation hour 6 and 12 with μ=0.4 h^{-1}. During this first growth phase an increase of the RQ value up to 3.4 were observed what indicated the formation of components like ethanol and acetate. It is very likely that this phenomenon appeared due to the Crabtree-Effect in which anaerobe metabolism is observed, next to the respiratory [134]. The Crabtree-Effect

would also explain the formation of acetate which started in the first growth phase and reached its maximum with 0.33 g/L after 14 h during the expression phase.

The expression phase started after 12 h initiated by an almost complete utilization of the glucose. Accordingly to the glucose repression of the *GAL*1 promoter, the GOx expression started after glucose utilization and remained constant until fermentation hour 25 was reached. With the complete utilization of the glucose the oxygen value showed a diauxic shift that indicates that the cells switched to an alternative carbon source, which could be acetate or ethanol. The sudden drop down of the RQ to values smaller 1 supports this theory since high amounts of oxygen are necessary for the utilization of reduced substrates. As already mentioned a formation of acetate took place during the first growth phase and the expression phase. While the acetate concentration exceeded a value of 0.3 g/L the biomass formation stagnated, what resulted in the separation between the first and the second growth phase. The cell growth was most likely inhibited by the high acetate concentration during growth phase 1 and 2. In literature it was shown that acetate concentrations from 0.05 to 0.1 % w/v act as a stress factor for yeast cells [135]. After the acetate concentration went below 0.2 g/L a diauxic shift was observed and the formation of biomass continued with μ=0.07 h^{-1} until fermentation hour 25, after which another diauxic shift was monitored. A possible explanation could be the switch to ethanol as the carbon source, assuming the previous carbon source was acetate. After 25 h, the biomass formation as well as the GOx expression stagnated probably due to the switch to a less favorable carbon source.
A simple batch-fermentation protocol was successfully established based on the glyco-engineered strain *Sc.* ngd29, for which not fermentation protocol was reported. The obtained GOx yield was sufficient for the executed GOx characterization studies. Anyhow, a further optimization of the process would be necessary with respect to the GOx yield in order to produce sufficient quantities for instance for electrochemical GOx characterizations and for diabetes test stripe experiments.

5.4.3 GOx purification

The introduction and optimization of A TFF system made the production of the GOx at pilot scale feasible. The TFF system replaced the cell harvest by centrifugation in

several batches and the product concentration and the buffer exchange by death-end filtration and/or dialyses. The implemented TFF unit operations allowed a primary separation of up to 20 L cell culture within one day, including cell separation, volume reduction (≥30-times) and buffer exchange. Furthermore, the volume reduction and buffer exchange can be performed under aseptic conditions employing a closed TFF-system.

The intermediate after primary separation was subjected to column chromatography for the actual product purification. A two chromatography step process was applied including anion exchange chromatography (AEC) and hydrophobic interaction chromatography (HIC). The protocol was successfully applied in the directed evolution experiment by Zuh 2006 [43]. The SDS-page analysis showed that three different protein fractions were enriched after the AEC (first step), one at 55 kDa, one at 100 kDa and the third one at 130 kDa. Activity analysis of the different fractions showed that only the 100 kDa band belongs to GOx. Both impurities (55 kDa, 130 kDa) were also enriched after the HIC. The analysis clearly shows that the available protocol is not applicable for the GOx expressed in *Sc*. ngd29. A possible explanation might be the altered glycosylation pattern by the *Sc.* ngd29 strain. Especially the interaction with the resin of the AEC can be significantly changed due to the less carbohydrate content. The high carbohydrate content of the GOx expressed in the *Sc*. INV strain probably covers a certain portion or the surface charge what would lead to a weaker interaction with the AEC resin.

The SDS-page analysis of the collected chromatography fractions showed the GOx band and the bands of the impurities eluate time-displaced from the AEC column, what is not the case for the HIC in which all three proteins eluate at the same time (Fig. 5-5). The optimization of the AEC resulted in two washing steps, one with 1 % elution buffer (1 M NaCl), one with 5 % elutionbuffer and a subsequent elution step with 7.5 % elution buffer. The comparison of optimized AEC with the the old protocol (AEC + HIC) shows that the single AEC (optimized) is able to deplete the impurities at 55- and 130 kDa, what was not possible with the old two step protocol. The purity reached with the optimized AEC was estimated to be higher than 90 % and sufficient for the characterization of GOx variants. The purity with only the AEC step was reached by stepwise determination of the exact elution point of hypo-glycosylated GOx (with respect to the ratio wash to eleution buffer). Most likely, the impurities eluate from the column during the first and the second wash step, while the GOx is

still retained by the resin. In the final protocol the AEC was only followed by an additional concentration- and buffer exchange step (depth filtration in spin-columns). Figure 5-8 shows an overview of the established downstream process for hypo-glycosylated GOx.

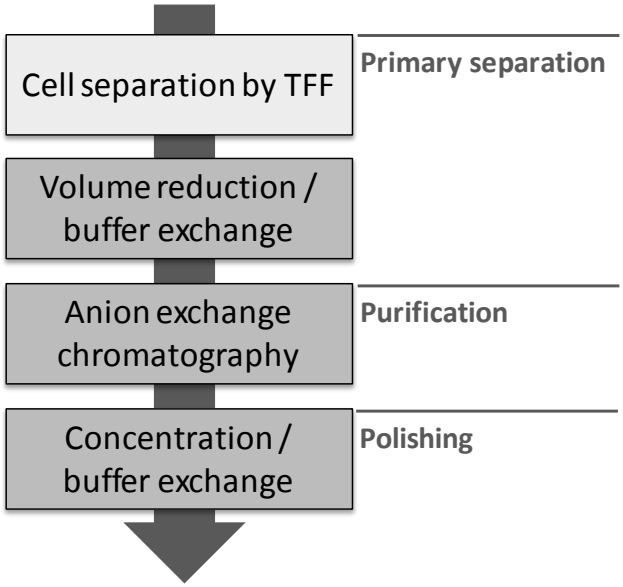

Figure 5-8: Overview of the GOx downstream process after optimization. The process comprises of four unit operations and can be divided in the three parts primary separation, purification and polishing.

A simple and fast downstream process was successfully implemented comprising the four unit operations cell separation, volume reduction / buffer exchange, AEC and final concentration / buffer exchange. The process delivers samples with a GOx content higher than 90 % and can be executed within two days. The latter two attributes make the established downstream process ideal for the characterization of GOx variants.

6. Summary and Conclusion

The present study was divided in three parts: 1) the engineering of GOx for less oxygen sensitivity and improved mediator activity; 2) Investigations for the mediator binding and further improvement of GOx towards the employment of different mediator systems and 3) the establishment of a bio process for the fast and reproducible production of pure GOx.

In the first project part a mircrotiter-plate screening system was established, suitable for the employment of *p*-nitrosoaniline based mediators. The screening system was successfully used for the screening of eleven mutagenesis libraries. The four novel positions 173, 332, 414 and 560 were identified in random mutagenesis libraries. Site saturation studies revealed that position 560 is a key residue for oxygen sensitivity, that positions 173 and 332 increase mediator and oxygen activity, and that position 414 influences mediator activity and increases or reduces oxygen activity depending on the substitution. Simultaneous site saturation by OmniChange allowed the consideration of cooperative effects between the four identified positions and resulted in GOx V7. V7 showed a 37-fold reduced oxygen dependency by maintained β-D-glucose specificity and thermal resistance. Computational investigations revealed that the access to an oxygen stabilizing pocket in the WT can be triggered by substitutions in position 560 and that the access is blocked in V7. Furthermore, MD-simulations showed that the placed oxygen is leaving not only the reactive position in the active site of V7 but the enzyme completely. V7 was successfully evolved to operate oxygen independent with a diabetes relevant mediator system (quinone diimine/phenylendiamine). The main challenge in diabetes analytics is the development of a glucose sensor which operates free from any interference by clinical relevant sugars or by oxygen. V7 gives the opportunity to accomplish that challenge by the combination of the glucose specificity with a significant reduced oxygen dependency. The combination of V7 with well established quinone diimine based mediator systems allow an accurate glucose determination in the presence of clinical relevant sugars and at high oxygen levels with only one sensor. These insights will inspire protein engineers, biofuel cell scientists, clinical researchers and bio-process engineers to redesign other GOxs and oxidoreductases to develop

implantable biofuel cells (GOx in anodic compartment) and to design more robust and accurate glucose monitoring systems.

In the second project part, the influence of residue 414 on the interaction of small soluble mediator compounds and GOx were investigated. A site saturation experiment revealed a subset of amino acids (Y, M, L, V) which changed the preference of GOx from the QDM-1 to the more polar and sterically more demanding QDM-2. The substitution I414Y resulted in a 4.8-fold increased activity of V7 employing the QDM-2 system, what was traced back to a higher affinity through the change to a more polar residue and to structural reorganization. Furthermore, it was shown that substitutions of residue 414 also influence the activity employing ferrocenemethanol, a prominent mediator example for GOx. Molecular docking studies first time showed that small water soluble mediator compounds bind directly in the active site of GOx in close vicinity to residue 414. Theoretical calculated electron transfer rates (according to the Marcus-Theory) [112] were in good accordance with the catalytic data. The analysis of the Marcus-Theory indicated that substitutions of residue 414 might change the mediator activity by minimizing the molecular reorganization during charge transfer. The mediator study revealed a mediator binding model for GOx employing small water soluble mediators. It was found that residue 414 is in direct vicinity to the mediator binding site and substitutions allow modulating the efficiency of the electron transfer rate. The study first time showed the adaption of an enzyme to a specific mediator by protein engineering. Furthermore, it reveals the opportunity to combine protein engineering with mediator engineering to not only screen for suitable mediators but to adopt enzymes to optimal mediator systems for a defined application. This novel approach might not only play an important role in diagnostics but also in the field of bio-fuel cells in order to adopt electron donor or acceptor enzymes to optimized bio-fuel cell setups.

In the last project part a bio-process was established in order to ensure a fast and efficient production of GOx for characterization studies. Media screening and investigations of the feeding strategy revealed a batch fermentation process with a process time of 48 h. The fermentation process was characterized with respect to bio-mass formation, glucose consumption, respiratory properties (RQ, pO2), acetate formation and GOx formation. The fermentation process was divided in four phases, a lag-phase, two growth phases and an expression phase. Thereby, the best

biomass formation was reached in growth phase one with μ=0.4 h^{-1}. The downstream process was scaled-up for the handling of 10 to 20 L of cell broth. Tangential flow filtration was introduced for the cell harvest (mico-filtration) and product isolation (ultra-filtration) in order to handle the respective volumes. The optimization of an anion-exchange chromatography step resulted in a downstream process with only one purification step. Samples with a GOx-content higher 90 % could be reached. The establishment of GOx production protocols resulted in a fast and reproducible process, which was successfully employed within characterization studies of GOx variants (project part one and two).

7. References

1. Whiting DR, Guariguata L, Weil C, Shaw J. IDF diabetes atlas: global estimates of the prevalence of diabetes for 2011 and 2030. *Diabetes Res Clin Pract* 2011,**94**:311-321.
2. Ferri S, Kojima K, Sode K. Review of glucose oxidases and glucose dehydrogenases: a bird's eye view of glucose sensing enzymes. *J Diabetes Sci Technol* 2011,**5**:1068-1076.
3. HOENES J, MUELLER P, SURRIDGE N. The Technology Behind Glucose Meters: Test Strips. *DIABETES TECHNOLOGY & THERAPEUTICS* 2008,**10**:10-26.
4. Jin S, Veetil JV, Garrett JR, Ye K. Construction of a panel of glucose indicator proteins for continuous glucose monitoring. *Biosens Bioelectron* 2011,**26**:3427-3431.
5. Lee YJ, Kim JD, Park JY. FLEXIBLE ENZYME FREE GLUCOSE MICRO-SENSOR FOR CONTINUOUS MONITORING APPLICATIONS. *Transducers 2009, Denver, CO, USA, June* 2009:21-25.
6. Veetil JV, Jin S, Ye K. A glucose sensor protein for continuous glucose monitoring. *Biosens Bioelectron* 2010,**26**:1650-1655.
7. Ye K, Schultz JS. Genetic engineering of an allosterically based glucose indicator protein for continuous glucose monitoring by fluorescence resonance energy transfer. *Anal Chem* 2003,**75**:3451-3459.
8. Park S, Boo H, Chung TD. Electrochemical non-enzymatic glucose sensors. *Anal Chim Acta* 2006,**556**:46-57.
9. Freckmann G, Schmid C, Baumstark A, Pleus S, Link M, Haug C. System accuracy evaluation of 43 blood glucose monitoring systems for self-monitoring of blood glucose according to DIN EN ISO 15197. *J Diabetes Sci Technol* 2012,**6**:1060-1075.
10. Adams EC, Jr., Mast RL, Free AH. Specificity of glucose oxidase. *Arch Biochem Biophys* 1960,**91**:230-234.
11. Raba J, Mottola H. Glucose Oxidase as an Analytical Reagent. *Critical Reviews in Analytical Chemistry* 1995,**25**:1-42.
12. Bankar SB, Bule MV, Singhal RS, Ananthanarayan L. Glucose oxidase--an overview. *Biotechnology Advances* 2009,**27**:489-501.
13. Bentley R, Neuberger A. The mechanism of the action of notation. *Biochem J* 1949,**45**:584-590.
14. Gibson QH, Swoboda BE, Massey V. Kinetics and Mechanism of Action of Glucose Oxidase. *THE JOURNAL OF BIOLOGICAL CHEMISTRY* 1964,**239**:3927-3934.
15. Pazur JH, Kleppe K. The Oxidation of Glucose and Related Compounds by Glucose Oxidase from Aspergillus Niger. *Biochemistry* 1964,**3**:578-583.
16. Ginsberg BH. Factors affecting blood glucose monitoring: sources of errors in measurement. *J Diabetes Sci Technol* 2009,**3**:903-913.
17. Oberg D, Ostenson CG. Performance of glucose dehydrogenase-and glucose oxidase-based blood glucose meters at high altitude and low temperature. *Diabetes Care* 2005,**28**:1261.
18. Dungan K, Chapman J, Braithwaite SS, Buse J. Glucose measurement: confounding issues in setting targets for inpatient management. *Diabetes Care* 2007,**30**:403-409.
19. Kost GJ, Vu HT, Lee JH, Bourgeois P, Kiechle FL, Martin C*, et al.* Multicenter study of oxygen-insensitive handheld glucose point-of-care testing in critical care/hospital/ambulatory patients in the United States and Canada. *Crit Care Med* 1998,**26**:581-590.
20. Tang Z, Louie RF, Lee JH, Lee DM, Miller EE, Kost GJ. Oxygen effects on glucose meter measurements with glucose dehydrogenase- and oxidase-based test strips for point-of-care testing. *Crit Care Med* 2001,**29**:1062-1070.
21. Hauge JG. Kinetics and specificity of glucose dehydrogenase from Bacterium anitratum. *Biochim Biophys Acta* 1960,**45**:263-269.
22. Olsthoorn AJ, Duine JA. On the mechanism and specificity of soluble, quinoprotein glucose dehydrogenase in the oxidation of aldose sugars. *Biochemistry* 1998,**37**:13854-13861.

23. Mistery C, Gokal R. The use of glucose polymer (icodextrin) in peritoneal dialysis: an overview. *JOURNAL OF THE INTERNATIONAL SOCIETY FOR PERITONEAL DIALYSIS* 1994,**14**:158-161.
24. Alsop R. History, chemical and pharmaceutical development of icodextrin. *Perit Dial Int* 1993,**14(Suppl 2)**:5-12.
25. Davies D. Kinetics of icodextrin. *Perit Dial Int* 1993,**14(Suppl 2)**:45-50.
26. Flore KM, Delanghe JR. Analytical interferences in point-of-care testing glucometers by icodextrin and its metabolites: an overview. *Perit Dial Int* 2009,**29**:377-383.
27. Garcia-Lopez E, Lindholm B. Icodextrin metabolites in peritoneal dialysis. *Perit Dial Int* 2009,**29**:370-376.
28. Moberly JB, Mujais S, Gehr T, Hamburger R, Sprague S, Kucharski A*, et al.* Pharmacokinetics of icodextrin in peritoneal dialysis patients. *Kidney Int Suppl* 2002:S23-33.
29. Tsai CY, Lee SC, Hung CC, Lee JJ, Kuo MC, Hwang SJ*, et al.* False elevation of blood glucose levels measured by GDH-PQQ-based glucometers occurs during all daily dwells in peritoneal dialysis patients using icodextrin. *Perit Dial Int* 2010,**30**:329-335.
30. Boenitz-Dulat M, Laggerbauer J, Schmuck R, Kratzsch P, Knappe W-R. In; 2006.
31. Kratzsch P, Schmuck R, Beck D, Shao Z, Thym D, W-R. K. In: Roche Diagnostics Operations, INc., Indianapolis, IN (US); 2002. pp. 1-29.
32. Sode K, Tsugawa W, Yamazaki T, Watanabe M, Ogasawara N, Tanaka M. A novel thermostable glucose dehydrogenase varying temperature properties by altering its quaternary structures. *Enzyme and Microbial Technology* 1996,**19**:82-85.
33. Tsujimura S, Kojima S, Kano K, Ikeda T, Sato M, Sanada H*, et al.* Novel FAD-dependent glucose dehydrogenase for a dioxygen-insensitive glucose biosensor. *Biosci Biotechnol Biochem* 2006,**70**:654-659.
34. Yamaoka H, Sode K. SPCE based glucose sensor employing novel thermostable glucose dehydrogenase, FADGDH: blood glucose measurement with 150nL sample in one second. *J Diabetes Sci Technol* 2007,**1**:28-35.
35. Zafar MN, Beden N, Leech D, Sygmund C, Ludwig R, Gorton L. Characterization of different FAD-dependent glucose dehydrogenases for possible use in glucose-based biosensors and biofuel cells. *Anal Bioanal Chem* 2012,**402**:2069-2077.
36. Holland JT, Harper JC, Dolan PL, Manginell MM, Arango DC, Rawlings JA*, et al.* Rational redesign of glucose oxidase for improved catalytic function and stability. *PLoS ONE* 2012,**7**:e37924.
37. Prodanovic R, Ostafe R, Blanusa M, Schwaneberg U. Vanadium bromoperoxidase-coupled fluorescent assay for flow cytometry sorting of glucose oxidase gene libraries in double emulsions. *Anal Bioanal Chem* 2012,**404**:1439-1447.
38. Prodanovic R, Ostafe R, Scacioc A, Schwaneberg U. Ultrahigh-Throughput Screening System for Directed Glucose Oxidase Evolution in Yeast Cells. *Combinatorial Chemistry & High Throughput Screening* 2011,**14**.
39. Zhu Z, Momeu C, Zakhartsev M, Schwaneberg U. Making glucose oxidase fit for biofuel cell applications by directed protein evolution. *Biosens Bioelectron* 2006,**21**:2046-2051.
40. Zhu Z, Wang M, Gautam A, Nazor J, Momeu C, R P*, et al.* Directed evolution of glucose oxidase from Aspergillus niger for ferrocenemethanol-mediated electron transfer. *Biotechnology Jounal* 2007,**2**:241-248.
41. Horaguchi Y, Saito S, Kojima K, Tsugawa W, Ferri S, Sode K. Construction of mutant glucose oxidases with increased dye-mediated dehydrogenase activity. *Int J Mol Sci* 2012,**13**:14149-14157.
42. Lehle L, Eiden A, Lehnert K, Haselbeck A, Kopetzki E. Glycoprotein biosynthesis in Saccharomyces cerevisiae: ngd29, an N-glycosylation mutant allelic to och1 having a defect in the initiation of outer chain formation. *FEBS Lett* 1995,**370**:41-45.
43. Zhu Z. Making glucose oxidase fit for biofuel cell applications by directed protein evolution [Dissertation]. Bremen: International University Bremen; 2006:105.

44. Eryomin AN, Drozhdenyuk AP, Zhavnerko GK, Semashko TV, Mikhailova RV. Quartz Sand as an Adsorbent for Purification of Extracellular Glucose Oxidase from Penicillium funiculosum 46.1. *Applied Biochemistry and Microbiology* 2004,**40**:151-157.
45. Hatzinikolaou DG, Hansen OC, Macris BJ, Tingey A, Kekos D, Goodenough P*, et al.* A new glucose oxidase from Aspergillus niger: characterization and regulation studies of enzyme and gene. *Appl Microbiol Biotechnol* 1996,**46**:371-381.
46. Kalisz HM, Hecht HJ, Schomburg D, Schmid RD. Effects of carbohydrate depletion on the structure, stability and activity of glucose oxidase from Aspergillus niger. *Biochim Biophys Acta* 1991,**1080**:138-142.
47. Kalisz HM, Hendle J, Schmid RD. Structural and biochemical properties of glycosylated and deglycosylated glucose oxidase from Penicillium amagasakiense. *Appl Microbiol Biotechnol* 1997,**47**:502-507.
48. Sukhacheva MV, Davydova ME, Netrusov AI. [Isolation and properties of glucose oxidase from Penicillum funiculosum 433]. *Prikl Biokhim Mikrobiol* 2004,**40**:32-36.
49. Swoboda BE, Massey V. Purification and Properties of the Glucose Oxidase from Aspergillus Niger. *J Biol Chem* 1965,**240**:2209-2215.
50. Hayashi S, Nakamura S. Multiple forms of glucose oxidase with different carbohydrate compositions. *Biochim Biophys Acta* 1981,**657**:40-51.
51. Pazur JH, Kleppe K, Cepure A. A glycoprotein structure for glucose oxidase from Aspergillus niger. *Arch Biochem Biophys* 1965,**111**:351-357.
52. Hecht HJ, Kalisz HM, Hendle J, Schmid RD, Schomburg D. Crystal structure of glucose oxidase from Aspergillus niger refined at 2.3 A resolution. *J Mol Biol* 1993,**229**:153-172.
53. Wohlfahrt G, Witt S, Hendle J, Schomburg D, Kalisz HM, Hecht HJ. 1.8 and 1.9 A resolution structures of the Penicillium amagasakiense and Aspergillus niger glucose oxidases as a basis for modelling substrate complexes. *Acta Crystallographica Section D Biological Crystallography* 1999,**55**:969-977.
54. Swoboda BE. The mechanism of binding of flavin-adenine dinucleotide to the apoenzyme of glucose oxidase and evidence for the involvement of multiple bonds. *Biochim Biophys Acta* 1969,**175**:380-387.
55. Accelrys Software I. Discovery Studio Visualizer. In. San Diego: Accelrys Software Inc.; 2007.
56. Bright HJ, Porter DJT. Flavoprotein oxidases. *Enzymes* 1975,**12**:421-505.
57. Leskovac V, Trivic S, Wohlfahrt G, Kandrac J, Pericin D. Glucose oxidase from Aspergillus niger: the mechanism of action with molecular oxygen, quinones, and one-electron acceptors. *Int J Biochem Cell Biol* 2005,**37**:731-750.
58. Bright HJ, Appleby M. The pH dependence of the individual steps in the glucose oxidase reaction. *THE JOURNAL OF BIOLOGICAL CHEMISTRY* 1969,**244**:3625-3634.
59. Bright HJ, Gibson QH. The oxidation of 1-deuterated glucose by glucose oxidase. *THE JOURNAL OF BIOLOGICAL CHEMISTRY* 1967,**242**:994-1003.
60. Weibel MK, Bright HJ. The glucose oxidase mechanism. Interpretation of the pH dependence. *THE JOURNAL OF BIOLOGICAL CHEMISTRY* 1971,**246**:2734-2744.
61. Kunst A, Draeger B, Ziegenhorn J. Colorimetric methods with glucose oxidases and peroxidases. *Methods of Enzymatic Analysis* 1984,**3erd ed**.
62. Swoboda BE, Massey V. Purification and Properties of the Glucose Oxidase from Aspergillus Niger. *THE JOURNAL OF BIOLOGICAL CHEMISTRY* 1965,**240**:2209-2215.
63. Tsuge H, Natsuaki O, Ohashi K. Purification, properties, and molecular features of glucose oxidase from Aspergillus niger. *J Biochem* 1975,**78**:835-843.
64. Harper A, Anderson MR. Electrochemical glucose sensors--developments using electrostatic assembly and carbon nanotubes for biosensor construction. *Sensors (Basel)* 2010,**10**:8248-8274.
65. Stankovich MT, Schopfer LM, Massey V. Determination of glucose oxidase oxidation-reduction potentials and the oxygen reactivity of fully reduced and semiquinoid forms. *THE JOURNAL OF BIOLOGICAL CHEMISTRY* 1978,**253**:4971-4979.

66. Kay CJ, Barber MJ, Solomonson LP. Circular dichroism and potentiometry of FAD, heme and Mo-pterin prosthetic groups of assimilatory nitrate reductase. *Biochemistry* 1988,**27**:6142-6149.
67. Arango Gutierrez. E, Mundhada H, Meier T, Duefel H, Bocola M, Schwaneberg U. Reengineered glucose oxidase for amperometric glucose determination in diabetes analytics. *Biosensors & Bioelectronics* 2013,**50**:84-90.
68. Becker O. [DISSERTATION]. Kaiserslautern: Technische Universität Kaiserslautern; 2005:159.
69. HOENES J. Method for the colorimetric determination of analyte using enzymatic oxydation. Application number 89114143.4. In; 1990. pp. 1-15.
70. Wang J. Electrochemical glucose biosensors. *Chem Rev* 2008,**108**:814-825.
71. Thevenot DR, Toth K, Durst RA, Wilson GS. Electrochemical biosensors: recommended definitions and classification. *Biosens Bioelectron* 2001,**16**:121-131.
72. Gambke B, Young D. Accu-Chek Aviva System Evaluierung. *ROCHE* 2005,**1**:1-20.
73. Bornscheuer UT, Pohl M. Improved biocatalysts by directed evolution and rational protein design. *Curr Opin Chem Biol* 2001,**5**:137-143.
74. Jackel C, Kast P, Hilvert D. Protein design by directed evolution. *Annu Rev Biophys* 2008,**37**:153-173.
75. Jaeger KE, Eggert T. Enantioselective biocatalysis optimized by directed evolution. *Curr Opin Biotechnol* 2004,**15**:305-313.
76. Jakoblinnert A, Wachtmeister J, Schukur L, Shivange AV, Bocola M, Ansorge-Schumacher MB*, et al.* Reengineered carbonyl reductase for reducing methyl-substituted cyclohexanones. *Protein Eng Des Sel* 2013,**26**:291-298.
77. Kurtzman AL, Govindarajan S, Vahle K, Jones JT, Heinrichs V, Patten PA. Advances in directed protein evolution by recursive genetic recombination: applications to therapeutic proteins. *Curr Opin Biotechnol* 2001,**12**:361-370.
78. Martinez R, Jakob F, Tu R, Siegert P, Maurer KH, Schwaneberg U. Increasing activity and thermal resistance of Bacillus gibsonii alkaline protease (BgAP) by directed evolution. *Biotechnol Bioeng* 2013,**110**:711-720.
79. Zhu L, Tee KL, Roccatano D, Sonmez B, Ni Y, Sun ZH*, et al.* Directed evolution of an antitumor drug (arginine deiminase PpADI) for increased activity at physiological pH. *Chembiochem* 2010,**11**:691-697.
80. Güven G, Prodanovic R, Schwaneberg U. Protein Engineering - An Option for Enzymatic Biofuel Cell Design. *Electroanalysis* 2010,**22**:765-775.
81. Chusacultanachai S, Yuthavong Y. Random mutagenesis strategies for construction of large and diverse clone libraries of mutated DNA fragments. *Methods Mol Biol* 2004,**270**:319-334.
82. Stemmer WP. Rapid evolution of a protein in vitro by DNA shuffling. *Nature* 1994,**370**:389-391.
83. Zhao H, Giver L, Shao Z, Affholter JA, Arnold FH. Molecular evolution by staggered extension process (StEP) in vitro recombination. *Nat Biotechnol* 1998,**16**:258-261.
84. Wong TS, Zhurina D, Schwaneberg U. The diversity challenge in directed protein evolution. *Comb Chem High Throughput Screen* 2006,**9**:271-288.
85. Mundhada H, Marienhagen J, Scacioc A, Schenk A, Roccatano D, Schwaneberg U. SeSaM-Tv-II generates a protein sequence space that is unobtainable by epPCR. *Chembiochem* 2011,**12**:1595-1601.
86. Arnold FH, Georgiou G. Directed Evolution Library Creation: Methods and Protocols. *Methods in Molecular Biology* 2003,**231**.
87. Cadwell RC, Joyce GF. Randomization of genes by PCR mutagenesis. *PCR Methods Appl* 1992,**2**:28-33.
88. Wong TS, Tee KL, Hauer B, Schwaneberg U. Sequence saturation mutagenesis (SeSaM): a novel method for directed evolution. *Nucleic Acids Res* 2004,**32**:e26.
89. Tindall KR, Kunkel TA. Fidelity of DNA synthesis by the Thermus aquaticus DNA polymerase. *Biochemistry* 1988,**27**:6008-6013.

90. Eckert KA, Kunkel TA. High fidelity DNA synthesis by the Thermus aquaticus DNA polymerase. *Nucleic Acids Research* 1990,**18**:3739-3744.
91. Patel PH, Kawate H, Adman E, Ashbach M, Loeb LA. A single highly mutable catalytic site amino acid is critical for DNA polymerase fidelity. *THE JOURNAL OF BIOLOGICAL CHEMISTRY* 2001,**276**:5044-5051.
92. Wong TS, Roccatano D, Loakes D, Tee KL, Schenk A, Hauer B*, et al.* Transversion-enriched sequence saturation mutagenesis (SeSaM-Tv+): a random mutagenesis method with consecutive nucleotide exchanges that complements the bias of error-prone PCR. *Biotechnol J* 2008,**3**:74-82.
93. Li Z, Roccatano D, Lorenz M, Schwaneberg U. Directed evolution of subtilisin E into a highly active and guanidinium chloride- and sodium dodecylsulfate-tolerant protease. *Chembiochem* 2012,**13**:691-699.
94. Leemhuis H, Kelly RM, Dijkhuizen L. Directed evolution of enzymes: Library screening strategies. *IUBMB Life* 2009,**61**:222-228.
95. Jakob F, Lehmann C, Martinez R, Schwaneberg U. Increasing protein production by directed vector backbone evolution. *AMB Express* 2013,**3**:39.
96. Holland T, Brozik S, Lau C, Atanassov P, Banta S. Glucose Oxidase Enzymes Rationally Engineered for Direct Electron Transfer.
97. Sun L, Petrounia IP, Yagasaki M, Bandara G, Arnold FH. Expression and stabilization of galactose oxidase in Escherichia coli by directed evolution. *Protein Eng* 2001,**14**:699-704.
98. Demain AL, Vaishnav P. Production of recombinant proteins by microbes and higher organisms. *Biotechnology Advances* 2009,**27**:297-306.
99. Pourmir A, Johannes TW. Directed evolution: selection of the host organism. *Computational and Structural Biotechnology Journal* 2012,**2**.
100. Tanner W, Lehle L. Protein glycosylation in yeast. *Biochim Biophys Acta* 1987,**906**:81-99.
101. Sambrook J, Russel D. *Molecular cloning : a laboratory manual*: Cold Spring Harbor Laboratory Press; 2001.
102. Dennig A, Shivange AV, Marienhagen J, Schwaneberg U. OmniChange: The Sequence Independent Method for Simultaneous Site-Saturation of Five Codons. *PLoS ONE* 2011,**6**:e26222.
103. Oldenburg KR, Vo KT, Michaelis S, Paddon C. Recombination-mediated PCR-directed plasmid construction in vivo in yeast. *Nucleic Acids Research* 1997,**25**:451-452.
104. Gietz RD, Schiestl RH. High-efficiency yeast transformation using the LiAc/SS carrier DNA/PEG method. *Nature Protocols* 2007,**2**:31-34.
105. Witt S, Singh M, Kalisz HM. Structural and kinetic properties of nonglycosylated recombinant Penicillium amagasakiense glucose oxidase expressed in Escherichia coli. *Applied And Environmental Microbiology* 1998,**64**:1405-1411.
106. Bartels PC, Roijers AF. A kinetic study on the influence of the parameters in the determination of inorganic phosphate by the molybdenum blue reaction. *Clin Chim Acta* 1975,**61**:135-144.
107. Feig S, Schmidt LH. Zur Optimierung der Phosphat-Bestimmung im Serum und im Urin. *Zbl. Pharm.* 1980,**Heft 12**:1337-1349.
108. Despotovic D, Vojcic L, Prodanovic R, Martinez R, Maurer KH, Schwaneberg U. Fluorescent assay for directed evolution of perhydrolases. *J Biomol Screen* 2012,**17**:796-805.
109. Tee KL, Schwaneberg U. A screening system for the directed evolution of epoxygenases: importance of position 184 in P450 BM3 for stereoselective styrene epoxidation. *Angew Chem Int Ed Engl* 2006,**45**:5380-5383.
110. Zhu Z, Momeu C, Zakhartsev M, Schwaneberg U. Making glucose oxidase fit for biofuel cell applications by directed protein evolution. *Biosensors and Bioelectronics* 2006,**21**:2046-2051.
111. Firth AE, Patrick WM. Statistics of protein library construction. *Bioinformatics* 2005,**21**:3314-3315.

112. Balaceanu A. Computational studies regarding the optimization of Glucose oxidase from Aspergillus niger for diabetes analytics [Master Thesis]. Cluj-Napoca: BABEŞ-BOLYAI" UNIVERSITY CLUJ-NAPOCA; 2013.
113. Giniger E, Varnum SM, Ptashne M. Specific DNA binding of GAL4, a positive regulatory protein of yeast. *Cell* 1985,**40**:767-774.
114. Johnston M. A model fungal gene regulatory mechanism: the GAL genes of Saccharomyces cerevisiae. *Microbiol Rev* 1987,**51**:458-476.
115. Clark LC, Jr., Lyons C. Electrode systems for continuous monitoring in cardiovascular surgery. *Ann N Y Acad Sci* 1962,**102**:29-45.
116. Pourasl AH, Ahmadi MT, Rahmani M, Chin HC, Lim CS, Ismail R*, et al.* Analytical modeling of glucose biosensors based on carbon nanotubes. *Nanoscale Res Lett* 2014,**9**:33.
117. Zhu Z, Garcia-Gancedo L, Flewitt AJ, Xie H, Moussy F, Milne WI. A critical review of glucose biosensors based on carbon nanomaterials: carbon nanotubes and graphene. *Sensors (Basel)* 2012,**12**:5996-6022.
118. Mano N, Mao F, Heller A. A miniature biofuel cell operating in a physiological buffer. *J Am Chem Soc* 2002,**124**:12962-12963.
119. Guo Y, Lu F, Zhao H, Tang Y, Lu Z. Cloning and heterologous expression of glucose oxidase gene from Aspergillus niger Z-25 in Pichia pastoris. *Applied Biochemistry and Biotechnology* 2009,**162**:498-509.
120. Hellmuth K, Pluschkell S, Jung JK, Ruttkowski E, Rinas U. Optimization of glucose oxidase production by Aspergillus niger using genetic- and process-engineering techniques. *Appl Microbiol Biotechnol* 1995,**43**:978-984.
121. Kapat A, Jung J, Park Y. Improvement of extracellular recombinant glucose oxidase production in fed-batch culture of Saccharomyces cerevisiae: Effect of different feeding strategies. *Biotechnology Letters* 1998,**20**:319-323.
122. Lu T, Peng X, Yang H, Ji L. The prduction of glucose oxidase using the waste mycelium of Aspergillus niger and effects of metal ions on the glucose oxidase. *Enzyme and Microbial Technology* 1996,**19**:339-342.
123. Meng Y, Zhao M, Yang M, Zhang Q, Hao J. Production and characterization of recombinant glucose oxidase from Aspergillus niger expressed in Pichia pastoris. *Lett Appl Microbiol* 2013.
124. Rocha SN, Abrahao-Neto J, Cerdan ME, Gonzalez-Siso MI, Gombert AK. Heterologous expression of glucose oxidase in the yeast Kluyveromyces marxianus. *Microbiell Cell Factories* 2010,**9**.
125. Reit M. Etablierung eines Up- und Downstream-Prozesses für hypoglykosylierte Glucoseoxidase für die Diabetesanalytik [Master Thesis]. Aachen: RWTH Aachen; 2012:79.
126. YPD media *Cold Spring Harbor Protocols* 2010,**doi:10.1101/pdb.rec12315**.
127. pYES2/NT user manual (www.invitrogen.com). *Invitrogen* 2003,**Version E**.
128. Chmiel H. *Bioprozesstechnik*. Heidelberg; 2006.
129. West RW, Jr., Yocum RR, Ptashne M. Saccharomyces cerevisiae GAL1-GAL10 divergent promoter region: location and function of the upstream activating sequence UASG. *Mol Cell Biol* 1984,**4**:2467-2478.
130. Eugene Raj A, Sathish Kumar HS, Umesh Kumar S, Misra MC, Ghildyal NP, Karanth NG. High-cell-density fermentation of recombinant Saccharomyces cerevisiae using glycerol. *Biotechnology Progress* 2002,**18**:1130-1132.
131. Bath PJ, Hopper JE. Overproduction of the GAL1 or GAL3 protein causes galactose-independent activation of the GAL4 protein: evidence for a new model of induction for the yeast GAL/MEL regulon. *MOLECULAR AND CELLULAR BIOLOGY* 1992,**12**:2701-2707.
132. Ochoa-Estopier A, Lesage J, Gorret N, Guillouet SE. Kinetic analysis of a Saccharomyces cerevisiae strain adapted for improved growth on glycerol: Implications for the development of yeast bioprocesses on glycerol. *Bioresour Technol* 2011,**102**:1521-1527.
133. Kompala DS. *Bioprocess Engineering: Fundamentals and Applications*: CRC Press Inc; 2013.

134. De Deken RH. The Crabtree effect: a regulatory system in yeast. *J Gen Microbiol* 1966,**44**:149-156.
135. Narendranath NV, Thomas KC, Ingledew WM. Effects of acetic acid and lactic acid on the growth of Saccharomyces cerevisiae in a minimal medium. *J Ind Microbiol Biotechnol* 2001,**26**:171-177.

8. Abbreviations

aa	Amino acid
ABTS	2,2′-azino-bis(3-ethylbenz-thiazoline-6-sulfonic acid)
AEC	Anion-exchange chromatography
A. niger	*Aspergillus niger*
bp	Base pair
cfu	cell forming unit
DNA	deoxyribonucleic acid
dNTP	deoxynucleoside triphosphate
E. coli	*Escherichia coli*
ELISA	enzyme-linked immunosorbent assay
ETR	electron transfer rate
FM	ferrocenemethanol
epPCR	error prone polymerase chain reaction
FAD	Flavin adenine dinucleotide
FWD	forward
FPLC	fast liquid chromatographie
GDH	Glucose dehydrogenase
GOx	Glucose oxidase
HIC	hydrophobic interaction chromatography
HRP	horseradish peroxidase
INV	Invitrogen
MCS	multiple cloning site
MTP	micro-titer plate
OI-ratio	Residual activity QDM assay / residual activity ABTS assay (Oxygen-Independent GOx ratio)
PAGE	polyacrylamide gel electrophoresis
PCR	polymerase chain reaction
pDNA	plasmid-DNA
PMO	phosphomolybdic acid
pO_2	oxygen partial pressure

PQQ	pyrrolochinolinchinon depending
QDM	chinonediimine based mediator
REV	reverse
RQ	respiratory quotient
RV	Reference variant
Sc	*Saccharomyces cerevisiae*
SC-U	*Saccharomyces cerevisiae* media without uracil
SDS	sodium dodecyl sulfate
SeSaM	sequence saturation mutagenesis
SSM	site saturation mutagenesis
Syn-Y	synthetic yeast media
Taq	*Thermus aquatcus*
TFF	tangential flow filtration
TS	transition
TV	transversion
UV/VIS	ultraviolet / visible
V	variant
WT	wild type
YPD	yeast peptone media